(12) INTERNATIONAL APPLICATION PUBLISHED UNDER THE PATENT COOPERATION TREATY (PCT)

(19) World Intellectual Property Organization
International Bureau

(43) International Publication Date
16 November 2017 (16.11.2017)

WIPO | PCT

(10) International Publication Number
WO 2017/194786 A1

(51) International Patent Classification:
A61K 47/60 (2017.01) *A61K 47/59* (2017.01)

(21) International Application Number:
PCT/EP2017/061593

(22) International Filing Date:
15 May 2017 (15.05.2017)

(25) Filing Language: English

(26) Publication Language: English

(30) Priority Data:
62/335,867 13 May 2016 (13.05.2016) US

(71) Applicant: **TECHNISCHE UNIVERSITEIT EINDHOVEN** [NL/NL]; Den Dolech 2, 5612 AZ Eindhoven (NL).

(72) Inventors: **GOOR, Olga Joseph Gertrudis Maria**; p/a Den Dolech 2, 5612 AZ Eindhoven (NL). **DANKERS, Patricia Yvonne Wilhelmina**; p/a Den Dolech 2, 5612 AZ Helmond (NL). **KEIZER, Henk Martin**; p/a Kranenveld 14, 5612 AP Eindhoven (NL). **JANSSEN, Henricus Marie**; p/a Kranenveld 14, 5612 AP Eindhoven (NL).

(74) Agent: **DELTAPATENTS B.V.**; Fellenoord 370, 5611 ZL Eindhoven (NL).

(81) Designated States *(unless otherwise indicated, for every kind of national protection available)*: AE, AG, AL, AM, AO, AT, AU, AZ, BA, BB, BG, BH, BN, BR, BW, BY, BZ, CA, CH, CL, CN, CO, CR, CU, CZ, DE, DJ, DK, DM, DO, DZ, EC, EE, EG, ES, FI, GB, GD, GE, GH, GM, GT, HN, HR, HU, ID, IL, IN, IR, IS, JP, KE, KG, KH, KN, KP, KR, KW, KZ, LA, LC, LK, LR, LS, LU, LY, MA, MD, ME, MG, MK, MN, MW, MX, MY, MZ, NA, NG, NI, NO, NZ, OM, PA, PE, PG, PH, PL, PT, QA, RO, RS, RU, RW, SA, SC,

(54) Title: POST-FUNCTIONALIZATION OF SUPRAMOLECULAR MATERIALS

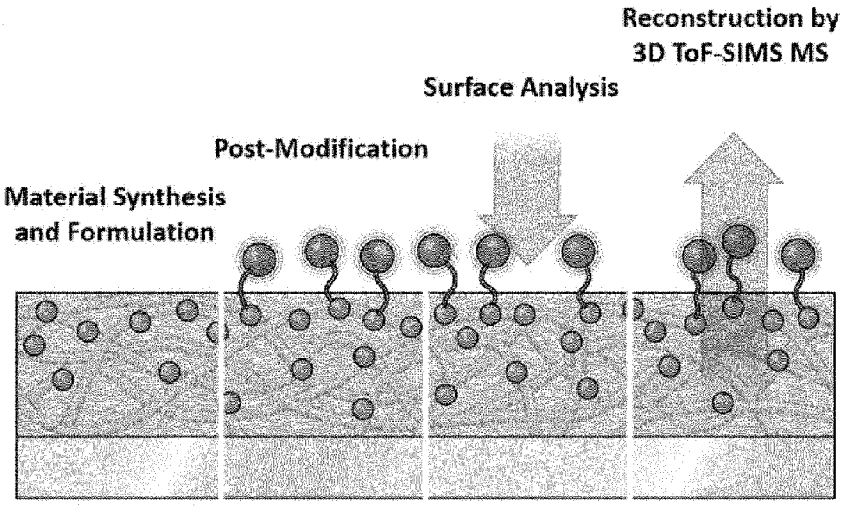

Fig. 1a

(57) Abstract: The present invention relates to a supramolecular material which can be functionalized, in particular surface-functionalized, by an orthogonal reaction with a compound comprising a functionalizing group. The supramolecular material according to the present invention comprises acompound (a) and compound (b), wherein -compound (a) comprises at least two supramolecular subunits S(a) linked by a linker L(a) comprising a polymer P(a), and -compound (b) comprises a supramolecular subunit S(b) and a first orthogonal reaction partner O1 capable of forming a covalent bond to a second orthogonal reaction partner O2. Upon functionalization, the supramolecular material according to the invention, O1 of compound (b) is covalently linked to an O2 in a compound (c), wherein compound (c) comprises an O2 and a functionalizing group F.The invention also relates to a method for the preparation of the supramolecular material and use of the supramolecular material as a biomaterial.

WO 2017/194786 A1

[Continued on next page]

SD, SE, SG, SK, SL, SM, ST, SV, SY, TH, TJ, TM, TN, TR, TT, TZ, UA, UG, US, UZ, VC, VN, ZA, ZM, ZW.

(84) **Designated States** *(unless otherwise indicated, for every kind of regional protection available)*: ARIPO (BW, GH, GM, KE, LR, LS, MW, MZ, NA, RW, SD, SL, ST, SZ, TZ, UG, ZM, ZW), Eurasian (AM, AZ, BY, KG, KZ, RU, TJ, TM), European (AL, AT, BE, BG, CH, CY, CZ, DE, DK, EE, ES, FI, FR, GB, GR, HR, HU, IE, IS, IT, LT, LU, LV, MC, MK, MT, NL, NO, PL, PT, RO, RS, SE, SI, SK, SM, TR), OAPI (BF, BJ, CF, CG, CI, CM, GA, GN, GQ, GW, KM, ML, MR, NE, SN, TD, TG).

Published:

— *with international search report (Art. 21(3))*

— *with sequence listing part of description (Rule 5.2(a))*

POST-FUNCTIONALIZATION OF SUPRAMOLECULAR MATERIALS

FIELD OF THE INVENTION

The present invention lies in the field of supramolecular materials, in particular supramolecular materials that can, be or has been, surface-functionalized after processing, a method for their preparation and their use as biomaterials.

BACKGROUND

Supramolecular polymeric materials are formed by molecular building blocks that are connected through directed non-covalent interactions such as hydrogen bonding, electrostatic, metal-ligand or π-π interactions between the supramolecular subunits of the supramolecular compounds present in the supramolecular material (*1*, *2*). The supramolecular interactions give the materials their dynamic nature, in a similar way as living systems for example control the complex process of extracellular matrix assembly, remodeling and bioactivation (*3*). This dynamic nature results in synthetic supramolecular materials with extraordinary mechanical, processable, responsive, modular and tunable properties that cannot be achieved with conventional macromolecules (*4*). Seminal contributions of supramolecular polymers have been reported, showing applicability as strong thermoplastic elastomers (*5*, *6*), functional biomaterials (*7*, *8*), drug delivery vehicles (*9*), self-healing materials (*10–12*), light-emitting diodes and molecular electronics (*13–15*).

Via a modular approach through co-assembly of several supramolecular constituents, complexity and functionality can be introduced into supramolecular aggregates and polymeric structures (*4*). This modular approach allows for the mixing-and-matching of functional modules with various chemical, physical and/or biological properties. Intrinsically these modified modules influence the assembly, and therefore properties, of the base supramolecular constituents. In soluble assemblies these supramolecular modules have been shown to fulfill plethora of functions (*16– 19*). However, only a few examples are disclosed in which functional modules are incorporated in solid-like supramolecular materials, such as the incorporation of supramolecular reinforcement fillers in supramolecular thermoplastic elastomers (TPE) (*20*).

The present inventors have previously shown that supramolecular TPE can be made using a four-fold hydrogen bonding 2-ureido-4-pyrimidinone (UPy) motif as the supramolecular subunit (*5*, *21–23*). These supramolecular TPE materials could be functionalized via a modular approach by mixing with UPy-functionalized additives, where a UPy-functionalized additive means a compound comprising a supramolecular

subunit and a functionalizing group F (*24*, *25*). Recent developments show applicability of this approach as anti-fouling agents ((*26*)) and bioactive peptides (*27*, *28*). These modules (or functionalized additives) have been simply mixed with the supramolecular TPE to provide the material with functionality, resulting in anti-fouling materials and cell-adhesive scaffolds. In almost all of these materials, the exact distribution of the supramolecular additive as well as specific surface enhancement cannot be fully controlled, whilst in several applications solely surface function is required. Moreover, in biomaterials science, the surface functionality is frequently provided by complex bioactive modules, that are often highly incompatible with the material preparation and processing conditions. Decoupling of processing and functionalization strategies offers flexibility in the choice of processing method, and allows for exclusive surface modification.

It is thus desired to provide a supramolecular material which can be functionalized in a way that overcomes the disadvantages of incorporating the functionalizing group during the assembly of the supramolecular material and which enables control with the distribution of the functionalizing group to be predominantly on the surface of the supramolecular material.

SUMMARY OF THE INVENTION

The present invention relates to a supramolecular material which can be functionalized by incorporation of functionalizing groups on its surface after the supramolecular material has been assembled, and a method for its preparation. The supramolecular material according to the present invention comprises a compound (a) and compound (b), wherein

- compound (a) comprises at least two supramolecular subunits S(a) linked by a linker L(a) comprising a polymer P(a), and
- compound (b) comprises a supramolecular subunit S(b) and a first orthogonal reaction partner O1 capable of forming a covalent bond to a second orthogonal reaction partner O2.

The incorporation of a first orthogonal reaction partner in the supramolecular material allows for a functional group F to be attached to the supramolecular material of the present invention after its assembly. Upon functionalization of the supramolecular material according to the invention, O1 of compound (b) is covalently linked to an O2 in a compound (c), wherein compound (c) comprises an O2 and a functionalizing group F. The present invention thereby overcomes the problems in the prior art of the functionalizing groups being present under the assembly of the supramolecular material which can be disadvantageous for both the functionalizing group, which may

be sensitive to the conditions under which the supramolecular material is assembled, and for the supramolecular material, which may become less uniform and strong by the presence of the functionalizing group throughout the material.

When functionalized, the functionalizing group F is predominantly present on the surface of the functionalized supramolecular material according to the present invention. For example, the present invention provides a supramolecular material, wherein the functionalizing group F is present on the surface of the supramolecular material in a surface:bulk ratio of at least 60:40, such as 65:35, 70:30, 75:25, 80:20, 85:15, 90:10, 95:5, 96:4, 97:3, 98:2 or 99:1. As used herein, the “bulk” of the material is the part of the material not forming part of the surface, i.e. the part of the material that is not directly exposed to the surrounding medium. The control with the incorporation of the functionalizing group predominantly on the surface of the supramolecular material provided by the present invention, is not only advantageous because potential interference of the functionalizing group with the structure of the supramolecular material is avoided, but also because less functionalizing group is needed in order to ensure sufficient exposure of said functionalizing group on the surface.

The present invention also relates to a compound (b) comprising a supramolecular subunit S(b) and a first orthogonal reaction partner O1. Compound (b) is the component of the supramolecular material according to the present invention, which provides for that said supramolecular material can be functionalized after its assembly, i.e. post-functionalized or post-modified.

The present invention also relates to a method for the preparation of the supramolecular material according to the invention and a supramolecular material obtainable from said method.

The present invention also relates to a biomaterial comprising the supramolecular material according to the present invention.

Furthermore, the present invention relates to a supramolecular material according to the invention or a biomaterial according to the invention for use in biomedical applications such as, e.g. for use in tissue engineering, regenerative medicine, implants, prostheses.

BRIEF DESCRIPTION OF THE FIGURES

Figure 1a: Schematic representation of supramolecular material. From the left: Supramolecular material comprising compound (a) and compound (b), Surface-functionalized supramolecular material further comprising compound (c), which is covalently linked to compound (b) via their respective orthogonal reaction partners, surface analysis and reconstruction by 3D ToF-SIMS depth profiling.

Figure 1b: Chemical structures of the molecules used: 1) Compound (a) used herein: telechelically UPy-modified polycaprolactone as base material ($M_{n,PCL}$ = 2 kDa) (PCLdiUPy), 2) Compound (b) as used herein: UPy-OEG_6-tetrazine (UPy-OEG_6-Tz) as reactive additive and 3) Compound (c) as used herein: a TCO-model compound with an I atom for detection with XPS (TCO-I).

Figure 1c: Left: Schematic representation of a pristine supramolecular polymer film (**I**) in which the fibers represent the UPy-dimers that stack upon each other in the lateral direction forming the hard phase of the PCLdiUPy supramolecular thermoplastic elastomer. Right: AFM micrograph of pristine supramolecular polymer film (**I**).

Figure 1d: Left: Schematic representation of a supramolecular film with UPy- OEG_6-Tz additives (compound (b)) incorporated, which are represented by the dots (**II**). Right: AFM micrographs of supramolecular films comprising 5, 10 and 25 mol% UPy-OEG_6-Tz, respectively.

Figure 1e: Left: Schematic representation of a supramolecular film which was surface reacted with TCO-I moieties that are represented by the purple beads (**III**). Right: the corresponding reaction product between UPy-OEG_6-Tz (compound (a)) and TCO-I (compound (b)) (**4**).

Figure 1e: Left: Schematic representation **II** surface reacted with a TCO-model protein (**IV**). Right: the corresponding reaction product between UPy-OEG_6-Tz (compound (a)) and TCO-model protein (compound (b)).

Figure 2a

Figure 2a: Surface analyses of films with UPy-Tz additive. XPS results of the different PCLdiUPy films are shown as intensity (a.u) vs. binding energy (eV). From the bottom, the graphs shown are as follows: 0 mol%, 5 mol%, 10 mol% and 25 mol% compound (b) (UPy-Tz) in the supramolecular material. Increase in F and N peaks are highlighted.

Figure 2b: Surface analyses of films with UPy-Tz additive. XPS zoom of the characteristic F binding energy area for the PCLdiUPy different films is shown as intensity (a.u) vs. binding energy. From the bottom, the graphs shown are as follows: 0 mol%, 5 mol%, 10 mol% and 25 mol% compound (b) (UPy-Tz) in the supramolecular material.

Figure 2c: Surface analyses of films with UPy-Tz additive. XPS zoom of the characteristic N binding energy area for the different PCLdiUPy films is shown as

intensity (a.u) vs. binding energy (eV). From the bottom, the graphs shown are as follows: 0 mol%, 5 mol%, 10 mol% and 25 mol% compound (b) (UPy-Tz) in the supramolecular material.

Figure 2d: Surface analyses of films with UPy-Tz additive. FTIR zoom in of the characteristic C-F vibration stretch for the different PCLdiUPy films is shown as absorbance vs. wavelength (cm^{-1}). From the bottom, the graphs shown are as follows: 0 mol%, 5 mol%, 10 mol% and 25 mol% compound (b) (UPy-Tz) in the supramolecular material.

Figure 3a: Surface analyses of the supramolecular films after post-modification with TCO-I. XPS overview of the different PCLdiUPy films is shown as intensity (a.u) vs. binding energy (eV). Increase in F, I and N peaks are highlighted. From the bottom, the graphs shown are as follows: 0 mol%, 5 mol%, 10 mol% and 25 mol% compound (b) (UPy-Tz) in the supramolecular material.

Figure 3b: Surface analyses of the supramolecular films after post-modification with TCO-I. XPS zoom of the characteristic I binding energy area for the different PCLdiUPy films is shown as intensity (a.u) vs. binding energy (eV). From the bottom, the graphs shown are as follows: 0 mol%, 5 mol%, 10 mol% and 25 mol% compound (b) (UPy-Tz) in the supramolecular material.

Figure 3c: Surface analyses of the supramolecular films after post-modification with TCO-I. XPS zoom of the characteristic F binding energy area for the different PCLdiUPy films is shown as intensity (a.u) vs. binding energy (eV). From the bottom, the graphs shown are as follows: 0 mol%, 5 mol%, 10 mol% and 25 mol% compound (b) (UPy-Tz) in the supramolecular material.

Figure 3d: Surface analyses of the supramolecular films after post-modification with TCO-I. Surface MALDI-ToF MS analysis of the different PCLdiUPy films. From the bottom, the graphs shown are as follows: PCLdiUPy with no UPy-Tz or TCO-I, (bottom line), PCLdiUPy incubated with TCO-I, PCLdiUPy with 10 mol% UPy-Tz and PCLdiUPy with 10 mol% UPy-Tz incubated with TCO-I.

Figure 4: 3D Depth profiling of supramolecular films after post-modification using ToF-SIMS. Relevant mass fragments are depicted in different colors: iodine = purple, fluorine = pink, UPy fragment *m/z* 124 = red, UPy-fragment *m/z* 150 = blue, PCL-fragment = yellow, ITO = green. Dimensions of depth profile area are 100 x 100 µm. Reconstructions were made after 50 sputter cycles of 1 min with 20 keV C60 + sputter beam and subsequent surface analysis of 4 frames (2.13 min) using a 30 keV Bi3 ++ beam. Spatial distribution of I and F ions, and ITO fragment in films of PCLdiUPy with (**A**) 1 mol% UPy-Tz, (**B**) 5 mol% UPy-Tz, (**C**) 10 mol% UPy-Tz, and (**D**) 25 mol% UPy-Tz. Spatial distribution of two UPy-fragments, PCL-fragment, and ITO fragment in films of PCLdiUPy with (**E**) 1 mol% UPy-Tz, (**F**) 5 mol% UPy-Tz, (**G**) 10 mol% UPy-Tz, and

(**H**) 25 mol% UPy-Tz. (**I**) Column diagram showing the total ion count plot of all masses of interest, analyzed for both the surface and the bulk in the different TCO-I modified PCLdiUPy films as measured by ToF-SIMS. The masses measured are shown in each block on in this sequence from the left: Iodine *m/z* 127, Fluorine *m/z* 19, UPy *m/z* 124, UPy *m/z* 150 and PCL *m/z* 113. On the x-axis from the left is shown the following conditions under which the masses were measured: PCLdiUPy + 1 mol% UPy-Tz (surface to the left and bulk to the right), PCLdiUPy + 5 mol% UPy-Tz (surface to the left and bulk to the right), PCLdiUPy + 10 mol% UPy-Tz (surface to the left and bulk to the right) and PCLdiUPy + 25 mol% UPy-Tz (surface to the left and bulk to the right).

Figure 5: Surface analysis of the different PCLdiUPy drop-cast films by XPS. In both figure 5a and 5b the different PCLdiUPy films is shown as intensity (a.u) vs. binding energy (eV) and.

Figure 5a: Survey of PCLdiUPy + 0, 5, 10 and 25 mol% UPy-Tz after 48 h water annealing shown as intensity (a.u) vs. binding energy (eV). From the bottom the graphs shown are as follows: 0 mol%, 5 mol%, 10 mol% and 25 mol% compound (b) (UPy-Tx) in the supramolecular material.

Figure 5b: Atom composition of the air dried and water annealed surfaces.

Figure 5c: Development of PCLdiUPy + 25 mol% UPy-Tz surface survey at different tilt angles (0, 15, 30, 45, 60 and 75 °, respectively).

Figure 5d: F:C ratio at the different tilt angles of the PCLdiUPy + 25 mol% UPy-Tz surface.

Figure 6: Surface analysis of click chemistry with a TCO-iodine at the surface of drop-cast PCLdiUPy films analyzed by MALDI-ToF MS and corresponding chemical structures.

Figure 6a: PCLdiUPy + 5 mol% UPy-Tz (bottom line), PCLdiUPy + 5 mol% UPy-Tz incubated with TCO-iodine (upper line).

Figure 6b: PCLdiUPy + 25 mol% UPy-Tz (bottom line) and PCLdiUPy + 25 mol% UPy-Tz incubated with TCO-iodine (upper line).

Figure 6c: Chemical structure of the UPy-Tz TCO-iodine click product (exemplary compound (d), MW 1936.8 g/mol.

Figure 6d): Chemical structure of the UPy-Tz TCO-iodine click product with UPy-moiety cleaved, MW 1785.8 g/mol.

Figure 6e): UPy-Tz TCO-iodine click product after elimination of the carbamate moiety, MW 1269.7 g/mol.

Figure 6f): UPy-Tz TCO-iodine click product after elimination of the UPy and carbamate moiety, MW 1118.7 g/mol.

Figure 7: Water contact angle measurements of PCLdiUPy, PCLdiUPy + 5 mol% UPy-Tz, PCLdiUPy + 10 mol% UPy-Tz and PCLdiUPy + 25 mol% UPy-Tz drop-cast films

(first column), after post-modification with a TCO-I (second column) and after post-modification with a TCO-Protein (third column).

Figure 8: Pictures of drop-cast films incubated with and without TCO-I compound.

Figure 8a: PCLdiUPy (left, **I**) and PCLdiUPy + 5 mol% UPy-Tz (right, **II**), upper row samples show color change after TCO-I model incubation, lower row samples show unreacted films and PCLdiUPy + 10 mol% UPy-Tz (left, **III**) and PCLdiUPy + 25 mol% UPy-Tz (right, **IV**), upper row samples show color change after TCO-I model incubation, lower row samples show unreacted films.

Figure 8b: reaction mechanism of the iEDDA cycloaddition between tetrazine and TCO.

Figure 9: Protein labeling with TCO-moieties.

Figure 9a: Conjugation scheme of TCO-OEG_4-NHS ester (equatorial isomer) conjugation to peripheral Lysines of the EYFP.

Figure 9b: From left is shown: Q-ToF MS analysis of the conjugated protein (intensity % vs. time (min), total ion count chromatogram, *m/z* spectrum (intensity % vs. *m/z*) as well as the deconvoluted mass spectrum (intensity % vs. mass (Da).

Figure 10: Surface analysis of post-modification with a TCO-EYFP and a non-functionalized control at the surface of drop-cast films of PCLdiUPy with various mol% UPy-Tz by fluorescence spectroscopy, PCLdiUPy (**0**), PCLdiUPy + 1 mol% UPy-Tz (**1**), PCLdiUPy + 5 mol% UPy-Tz (**5**), PCLdiUPy + 10 mol% UPy-Tz (**10**) and PCLdiUPy + 25 mol% UPy-Tz (**25**) incubated with TCO-EYFP (left) or EYFP (right) for 2 hours and subsequent 3 washing steps. Error bars represent standard deviations of triplicate measurements.

Figure11: AFM phase image of spin coated samples, 1 x 1 µm.

Figure 11a: PCLdiUPy.

Figure 11b: PCLdiUPy + 5 mol% UPy-Tz.

Figure 11c: PCLdiUPy + 10 mol% UPy-Tz.

Figure 11d: PCLdiUPy + 25 mol% UPy-Tz.

Figure 12: ToF-SIMS mass spectra of the different surfaces measured in negative mode with Bi3 ++.

Figure 12a: PCLdiUPy.

Figure 12b: PCLdiUPy + 1 mol% UPy-Tz.

Figure 12c: PCLdiUPy + 5 mol% UPy-Tz.

Figure 12d: PCLdiUPy + 10 mol% UPy-Tz.

Figure 12e: PCLdiUPy + 25 mol% UPy-Tz.

Figure 13: 3D ToF-SIMS Principal Component Analysis (PCA) of the first principal component for the first 2 sputter events of the material, 512 x 512 pixels, corresponding to 100 x 100 µm sample area.

Figure 13a-c: a) PCA of the PCLdiUPy with 1 mol% UPy-Tz surface reacted with TCO-iodine, +1 principal component, b) PCA of the PCLdiUPy with 1 mol% UPy-Tz surface reacted with TCO-iodine, -1 principal component, and c) Corresponding loading plot spectrum of the first principal component of PCLdiUPy + 1 mol% UPy-Tz + TCO-iodine, intensity versus *m/z*.

Figure 13d-f: d) PCA of the PCLdiUPy with 5 mol% UPy-Tz surface reacted with TCO-iodine, +1 principal component, e) PCA of the PCLdiUPy with 5 mol% UPy-Tz surface reacted with TCO-iodine, -1 principal component, and f) Corresponding loading plot spectrum of the first principal component of PCLdiUPy + 5 mol% UPy-Tz + TCO-iodine, intensity versus *m/z*.

Figure 13g-i: g) PCA of the PCLdiUPy with 10 mol% UPy-Tz surface reacted with TCO-iodine, +1 principal component, h) PCA of the PCLdiUPy with 10 mol% UPy-Tz surface reacted with TCO-iodine, -1 principal component, and i) Corresponding loading plot spectrum of the first principal component of PCLdiUPy + 10 mol% UPy-Tz + TCO-iodine, intensity versus *m/z*.

Figure 13j-l: j) PCA of the PCLdiUPy with 25 mol% UPy-Tz surface reacted with TCO-iodine, +1 principal component, k) PCA of the PCLdiUPy with 25 mol% UPy-Tz surface reacted with TCO-iodine, -1 principal component and l) Corresponding loading plot spectrum of the first principal component of PCLdiUPy + 25 mol% UPy-Tz + TCO-iodine, intensity versus *m/z*.

Figure 14: Synthesis scheme of the UPy-OEG_6-Tz (**2**), MW 1190.29 g/mol.

Figure 15: Synthesis scheme for TCO-OEG_4-Lys-I **(3)**.

Figure 16: a) Chemical structure of UPy-OEG_0-Tz, b) Chemical structure of UPy-OEG_{12}-Tz, and c) Chemical structure of C5-Tz without a UPy-motif.

Figure 17: a) Chemical structure of Mono-functional-PEG2k-BCN, b) Chemical structure of bi-functional-PEG5k-BCN And c) Chemical structure of Star-PEG10k-BCN.

Figure 18: Quartz crystal microbalance with dissipation monitoring (QCM-D) results after Vroman series adsorption (30 mg/mL BSA, 10 mg/mL γ-Globulin and 3 mg/mL Fibrinogen) onto PCLdiUPy or PCLdiUPy with 10 mol% UPy-Tz surfaces.

Figure 18a: Top: Frequency and Dissipation response at surfaces modified with 0.5 mg/mL mono-functional-PEG-BCN, where the upper three lines correspond to functionalized PCLdiUPy with 10 mol% UPy-Tz surfaces and the deviating lower line corresponds to non-functionalized PCLdiUPy. Bottom: Corresponding graph that plots the mass adsorption (ng/cm^2) on the modified surfaces. All the data represented in the graphs results from visco-elastic modeling using a Voigt-Voinova model. Averages of n =3 measurements are plotted with the corresponding standard deviations.

Figure 18b: Frequency and Dissipation response at surfaces modified with 0.5 mg/mL bi-functional-PEG-BCN, where the upper three lines correspond to functionalized

PCLdiUPy with 10 mol% UPy-Tz surfaces and the deviating lower line corresponds to non-functionalized PCLdiUPy. Bottom: Corresponding graph that plots the mass adsorption (ng/cm^2) on the modified surfaces. All the data represented in the graphs results from visco-elastic modeling using a Voigt-Voinova model. Averages of n =3 measurements are plotted with the corresponding standard deviations.

Figure 18c: Frequency and Dissipation response at surfaces modified with 0.5 mg/mL star-PEG-BCN, where the upper three lines correspond to functionalized PCLdiUPy with 10 mol% UPy-Tz surfaces and the deviating lower line corresponds to non-functionalized PCLdiUPy. Bottom: Corresponding graph that plots the mass adsorption (ng/cm^2) on the modified surfaces. All the data represented in the graphs results from visco-elastic modeling using a Voigt-Voinova model. Averages of n =3 measurements are plotted with the corresponding standard deviations.

DETAILED DESCRIPTION

The present invention relates to a supramolecular material which can be functionalized by incorporation of functional groups on its surface after the supramolecular material has been assembled and a method for its preparation. A key innovation of this invention is the decoupling of material processing on the one hand and the functionalization/modification on the other hand via the incorporation of an additive.

Thereby the present invention provides a way of functionalizing the surface of a supramolecular material which can be performed independently of whether or not a given functionalizing group can withstand the sometimes harsh conditions, e.g. often organic solvent, under which supramolecular materials are assembled. This is advantageous because for some sensitive functional groups the process conditions of the 1-step process (i.e. where the functional groups are present during the assembly of the supramolecular material) is not always compatible. Accordingly, the present invention provides a method to enable the use of a wider range of functional groups, e.g. including functional groups that are sensitive to organic solvent and for which aqueous conditions are preferred. Furthermore, the supramolecular material of the present invention can be functionalized predominantly on the surface thereby overcoming the problem in the art of the functionalizing group affecting the structure of the supramolecular material.

As used herein, the term “supramolecular material” or “supramolecular structure” means a material a comprising a supramolecular base polymer, herein referred to as a compound (a), the supramolecular subunits of which interact with each other so as to form a complex of supramolecular base polymers. Supramolecular material is also sometimes referred to as “supramolecular aggregates”, “supramolecular polymeric

structures" and "supramolecular complexes". In a preferred embodiment, the supramolecular material according to the present invention is a thermoplastic elastomer (TPE). In one embodiment, the supramolecular material is a nano-fiber material.

As used herein, the term "functionalizing group" means the functional group which can be attached to the surface of the supramolecular material of the present invention. It can be a wide variety of different types of groups that would be desired to be present on the surface of the supramolecular material.

The term "assembly" is used herein about the formation of the supramolecular material, i.e. the formation of supramolecular interactions leading to the complexing of enough supramolecular subunits for a supramolecular material to be formed.

The supramolecular material according to the present invention, comprises a first orthogonal reaction partner O1 capable of forming a covalent bond to a complementary orthogonal reaction partner O2, thereby providing a method for modifying the supramolecular material by covalent bonding of functionalizing groups after the formation/assembly of the supramolecular material. Such modification of the supramolecular material after its assembly with functionalizing groups is referred to herein as "post-functionalization" or "post-modification" of the supramolecular material.

Covalent post-modification is an elegant approach to introduce surface functionality on solid materials and has been reported using several chemoselective reaction strategies (*29–32*). However, although functionality can be conveniently introduced on such solid materials, they are not inherently dynamic in comparison to supramolecular materials. In order to benefit both from the dynamic nature of supramolecular polymers, and the advantageous and wide applicability of post-modification strategies on material surfaces, the present invention provides for the first time covalent modification of supramolecular additives (compounds (b)) in supramolecular materials.

Via convenient covalent post-modification of supramolecular reactive additives, in conjunction with advanced depth profiling using 3D ToF-SIMS, selective surface functionalization is shown and the complex supramolecular material composition of both surface and bulk is revealed herein. Elucidation of surface properties and functionalization of supramolecular material surfaces is challenging owing to the inherently dynamic nature of supramolecular structures. To this end, a supramolecular material consisting of ureido-pyrimidinone (UPy) end-functionalized polyesters (which are used as compound (a)) and supramolecular UPy-modified tetrazine additives that

induce reactivity at the surface towards trans-cyclooctene modified molecules (which are used as compound (b)) were developed. High resolution depth profiling by ToF-SIMS clearly shows distinct differences in surface and bulk material composition, which culminates understanding of design criteria and control of supramolecular materials and surfaces. These results provided herein, pave the way for immobilization of bioactive molecules and functional proteins on the surface of supramolecular materials, such as on the surface of supramolecular biomaterials.

The supramolecular material according to the present invention comprises a compound (a) and a compound (b), wherein

- compound (a) comprises at least two supramolecular subunits S(a) linked by a linker L(a) comprising a polymer P(a), and
- compound (b) comprises a supramolecular subunit S(b) and a first orthogonal reaction partner O1 capable of forming a covalent bond to a second orthogonal reaction partner O2.

In a preferred embodiment, the supramolecular material is a solid or semi-solid. The terms “semi-solid” or “solid-like” are used interchangeably herein are intended to mean that although not completely solid the material is highly viscous and has a firm consistency, more or less like a solid. This also means that a semi-solid / solid-like supramolecular material is staying in the position it is put, without flowing away or at least only so slowly that it does not have any practical impact on the application it is intended for.

Supramolecular subunits

As used herein, a “supramolecular subunit” is a functional group of a molecule, which is capable of engaging in supramolecular interactions with another supramolecular subunit either of the same molecule or of another molecule. Usually, supramolecular subunits are capable of engaging in supramolecular interactions with other identical supramolecular subunits. The interaction taking place between supramolecular subunits is referred to herein as supramolecular interactions. The supramolecular interactions can take place between two supramolecular subunits of the same supramolecular compound molecule or between a supramolecular subunits present in different supramolecular compound molecules, where a “supramolecular compound” is a compound comprising at least one supramolecular subunit. Supramolecular compounds are also sometimes referred to herein as supramolecular constituents. The forces involved in supramolecular interactions are non-covalent and include one or more of the of the non-covalent interactions selected from the group consisting of

hydrogen bonding, metal coordination, hydrophobic forces, van der Waals forces, pi-pi interactions and electrostatic effects.

Important concepts that are indicative of supramolecular chemistry include molecular self-assembly, folding, molecular recognition, host-guest chemistry, mechanically interlocked molecular architectures, multiple hydrogen bonding interactions, and dynamic covalent chemistry. In a preferred embodiment of the present invention, the supramolecular base polymers form a supramolecular complex by self-assembly and the forces holding the supramolecular subunits together are preferably hydrogen bonding.

Each of compounds (a) and (b) are supramolecular compounds as defined herein and their respective supramolecular subunits S(a) and S(b) can interact with each other via supramolecular interactions. An individual supramolecular subunit S(a) of compound (a) molecule may interact with other supramolecular subunits S(a) present in the same compound (a) molecule but may also interact with other supramolecular subunits S(a) present in another compound (a) molecule and/or a supramolecular subunit S(b) present in a compound (b) molecule. An individual supramolecular subunit S(b) of a compound (b) molecule may interact with a supramolecular subunit S(a) of a compound (a) molecule and/or a supramolecular subunit S(b) of another compound (b) molecule. However, for a compound (b) to be embedded in the supramolecular material, its supramolecular subunit S(b) should interact with at least one supramolecular subunit S(a) present in a compound (a). Accordingly, in a supramolecular material of the present invention, a supramolecular subunit S(b) of compound (b) interacts with a supramolecular subunit S(a) of compound (a) via supramolecular interactions. Preferably, the supramolecular subunits S(a) and S(b) are of the same type, i.e. have the same hydrogen bonding array or chemical structure, but may vary on the substituents.

Examples of known supramolecular subunits include ureido-pyrimidinone (referred to herein as UPy), bisurea, triazines, H-bond interactions in (poly)urethanes and H-bond interactions in (poly)amides. All of these supramolecular subunits can suitably be used as supramolecular subunits S(a) and S(b) in the present invention.

In a preferred embodiment of the present invention, supramolecular subunits S(a) and S(b) are capable of forming at least 4 hydrogen bridges and have a formula selected from the group consisting of (1') and (2'):

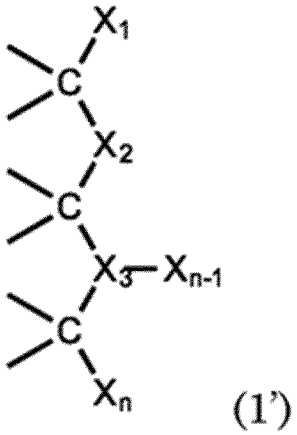

(1')

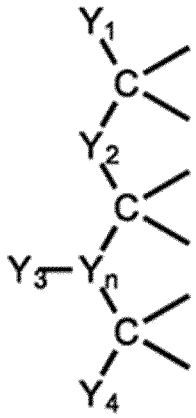

(2')

wherein,

- $C\text{-}X_i$ and $C\text{-}Y_i$ linkages are independently a single or a double bond,
- n is 4 or more, and
- X_i is a hydrogen bridge donor or acceptor capable of forming a hydrogen bridge with the corresponding hydrogen bridge donor or acceptor, Y_i, present in another supramolecular subunit.

If the supramolecular subunits S(a) and S(b) are capable of forming four hydrogen bridges which is preferred according to the invention, they preferably have a formula selected from the group consisting of (1) or (2):

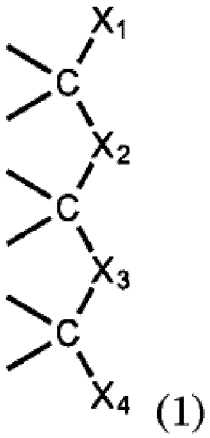

(1)

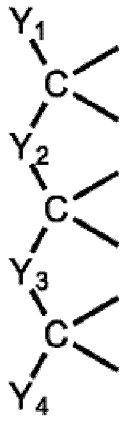

(2)

wherein,

- $C\text{-}X_i$ and $C\text{-}Y_i$ linkages are independently a single or a double bond,
- n is 4 or more, and

- X_i is a hydrogen bridge donor or acceptor capable of forming a hydrogen bridge with the corresponding hydrogen bridge donor or acceptor, Y_i, present in another supramolecular subunit.
-

Properties of and methods for preparing supramolecular subunits having the formula (1'), (2'), (1) or (2) are disclosed in US 6,320,018, which is incorporated herein by reference.

In a highly preferred embodiment of the present invention, supramolecular subunits S(a) and S(b) have a formula selected from the group consisting of (3) and (4):

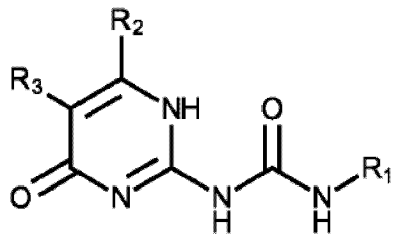

(3)

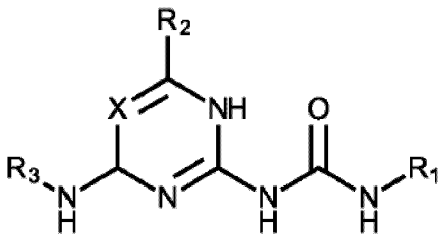

(4)

wherein, R1 is a direct bond connecting the supramolecular subunit to the remainder of compound (a) or compound (b); R2, R3 and R4 are independently selected from the group consisting of hydrogen, C_{1-24} alkyl, C_{6-12} aryl, C_{1-24} alkyl ether; and X in formula (4) is a nitrogen atom or a carbon atom with attached R4-group. The supramolecular subunits with formula (3) and (4) have been described in more detail in WO2007058539, which also discloses methods for their preparation. In a highly preferred embodiment, the supramolecular subunits S(a) and S(b) are both an ureido-pyrimidinone (UPy) with formula (3).

Compound (b)

Compound (b) of the supramolecular material according to the present invention comprises a supramolecular subunit S(b) and a first orthogonal reaction partner O1 capable of forming a covalent bond to a second orthogonal reaction partner O2. This compound is also referred to as the "additive" as it is not the core component of the supramolecular material, but rather added to the polymer solution from which the supramolecular material is formed in order to provide a way of later functionalization the supramolecular material. The function of compound (b) is to provide the supramolecular material with an orthogonal reaction partner enabling orthogonal ligation to another molecule, herein referred to as compound (c), comprising an

orthogonal reaction partner capable of forming a covalent bond to the orthogonal reaction partner of compound (b).

The supramolecular subunit S(b) is capable of interacting with at least one supramolecular subunit S(a) present in compound (a), thereby allowing compound (b) to form part of the supramolecular material. This means that compound (b) will be dispersed throughout the supramolecular material. It is in other words not only present at the surface of the supramolecular material. In a preferred embodiment, the supramolecular subunits S(a) and S(b) are the same, i.e. have the same chemical structure.

Preferably, compound (b) does not form the major constituent of the supramolecular material but is only present in an amount of from about 0.5 mol% to about 30 mol%, such as from about 1 mol% to about 25 mol%, from about 1.5 mol% to about 10 mol%, from about 2 to about 9 mol%, from about 2.5 to about 8 mol%, from about 3 to about 7 mol%, from about 3.5 to about 6.5 mol%, from about 4 to about 6 mol% or at about 5 mol% of the total amount of compound (a) and compound (b) in the supramolecular material. The mol% is here the % of the number of compound (b) in moles, compared to the total number of moles of compound (a) and compound (b).

The orthogonal reaction partner 1 is capable of forming a covalent bond with a second orthogonal reaction partner 2. A combination of a first orthogonal reaction partner O1 and second orthogonal reaction partner O2 capable of forming a covalent bond between them is sometimes referred to herein as an “orthogonal pair” or as “corresponding orthogonal reaction partners”. The incorporation of compound (b) in the supramolecular material results in that the supramolecular material comprises a first orthogonal reaction partner O1, which can be allowed to react with a compound (c) comprising the corresponding second orthogonal reaction partner O2. In other words, orthogonal reaction partners 1 and 2 constitute the reactants of a chemical reaction leading to the establishment of a covalent bond between them. This covalent attachment can be used to post-modify the surface of a supramolecular material according to the present invention.

In a preferred embodiment, the first orthogonal reaction partner O1 forms part of an orthogonal pair selected from the group consisting of *trans*-cyclooctene/azide, *trans*-cyclooctene/tetrazine and *trans*-cyclooctene/tetrazole, bicyclononyne/tetrazine and cyclopropene/tetrazine. The orthogonal pairs are here indicated as orthogonal reaction partner 1 / orthogonal reaction partner 2. By way of example, *trans*-

cyclooctene/tetrazine is an orthogonal pair. It should be understood that any of the two orthogonal reaction partners of an orthogonal pair can the orthogonal reaction partner comprised in compound (b), i.e. orthogonal reaction partner O1. In the example of the *trans*-cyclooctene/tetrazine, orthogonal reaction partner O1 can be either *trans*-cyclooctene or tetrazine. In a preferred embodiment of the present invention, the orthogonal pairs are bio-orthogonal pairs. Bio-orthogonal pairs are orthogonal pairs, wherein the covalent attachment between the orthogonal reaction partner 1 and 2 is established under physiological conditions, i.e. in water and neutral pH, and does not lead to the formation of toxic by-products. It is also preferred that the reaction between orthogonal reaction partner 1 and 2 is a fast reaction. Preferably, the orthogonal reaction should take place in less than two hours, such as less than 1.5 hours, less than 1 hour or less than 0.5 hour. Even more preferred the orthogonal reaction takes place in less than 25 minutes, such as less than 20 minutes, less than 15 minutes or less than 10 minutes.

Orthogonal, and in particular bio-orthogonal, ligation strategies to post-functionalize material surfaces in order to immobilize compounds have gained interest in recent years due to versatile applications in biomedical engineering and materials science (49-52). In particular, the catalyst-free inverse electron demanding Diels- Alder (iEDDA) reaction between 1,2,4,5-tetrazines as electron deficient dienes and trans-cyclooctenes (TCO) as strained electron rich dienophiles has emerged as a compelling advancement in the field (33, 35, 53-56).

The inverse electron demand Diels-Alder (iEDDA) cycloaddition (*33–37*) reaction was used as the orthogonal ligation reaction to prove the concept of the present invention. This reaction has been reported to be the fastest orthogonal reaction in aqueous environment (*38*, *39*) as post-modification strategy. A supramolecular TPE material in which a reactive UPy-modified tetrazine (UPy-Tz) additive was incorporated as a handle for selective surface post-modification via iEDDA, was designed. Using *trans*-cyclooctene moieties, functionalities were introduced at this supramolecular TPE material surface (Fig. 1a). In conjunction with advanced analysis techniques, the UPy-modified additive distribution and concomitant surface modification is shown herein. Although beautiful examples have been reported where materials were analyzed providing detailed chemical analysis in 2D (*40*) and 3D (*41–43*), the present inventors were able for the first time to resolve in detail the surface and bulk composition of a supramolecular material using secondary ion mass spectrometry with depth profiling (3D ToF-SIMS).

In a preferred embodiment, the first orthogonal reaction partner O1 is selected such that it is capable of forming a covalent bond with a second reaction partner O2 by a reaction selected from the group consisting of:

- Copper(I)-Catalyzed Azide-Alkyne Cycloaddition (CuAAC);
- Strain-promoted Azide-Alkyne Cycloaddition (SPAAC);
- Strain-promoted Alkyne-Nitrone Cycloaddition (SPANC);
- Staudinger ligation;
- Native chemical ligation; and
- Oxime ligation.

These types of reactions are the most typical reactions used in the field of "click" chemistry and are therefore known for being useful for performing specific reactions between two reaction partners without affecting the surrounding components of a system or a material.

In a preferred embodiment, the first orthogonal reaction partner O1 is selected such that it is capable of forming a covalent bond with a second orthogonal reaction partner O2 by an inverse electron demand Diels-Alder (iEDDA) cycloaddition reaction. This type of reaction has been proven both very fast and specific in aqueous media at neutral pH. The inverse electron demand Diels-Alder (iEDDA) cycloaddition reaction is very suitable for reacting *trans*-cycloalkenes, such as e.g., *trans*-cyclooctenes, oxanobornadienes or bicyclononyne (BCN), with either azides, tetrazines or tetrazoles. In a preferred embodiment, the first orthogonal reaction partner O1 is therefore selected from the group consisting of *trans*-cycloalkenes, azides, tetrazines and tetrazoles. Preferred *trans*-cycloalkenes are selected from the group consisting of trans-cyclooctenes or oxanobornadienes. In a preferred embodiment, the first orthogonal reaction partner O1 is tetrazine.

In a further preferred embodiment, the first orthogonal reaction partner O1 is selected such that it forms part of a bio-orthogonal pair. Bio-orthogonal pairs are orthogonal pairs, wherein the covalent attachment between the first orthogonal reaction partner O1 and the second orthogonal reaction partner O2 is established under physiological conditions, i.e. in water and neutral pH, and does not lead to the formation of toxic by-products. It is also preferred that the reaction between the first and the second orthogonal reaction partners, O1 and O2, is a fast reaction. Preferably, the first and second orthogonal reaction partners, O1 and O2 are bio-orthogonal reaction partners. More preferably, first orthogonal reaction partner O1 is selected such that it is capable of forming a covalent bond to the second orthogonal reaction partner O2 in less than 2

hours, such as less than 1.5 hour, less than 1 hour, less than 20 minutes, less than 10 minutes or less than 5 minutes.

Compound (b) according to the present invention preferably has a formula selected from the group consisting of S(b)-O1 and S(b)-L(b)-O1, wherein L(b) is a linker. Preferably compound (b) comprises linker L(b), which preferably comprises at least one aliphatic subunit and/or a polymer P(b). In one embodiment, linker L(b) comprises at least two aliphatic subunits, such as, at least three aliphatic subunits. As used herein, the term “aliphatic subunit” means a subunit of a linker, which subunit is aliphatic. For example such aliphatic subunits may be present in linkers L(a), L(b) and L(c) described herein. Suitable aliphatic subunits comprises less than 26 carbon atoms, such as less than 25, less than 24, less than 23, less than 22, less than 21, less than 20, less than 19, less than 18, less than 17, less than 16, less than 15, less than 14, less than 13, less than 12 or less than 11 carbon atoms. In a preferred embodiment, the aliphatic subunits comprises 1-10 carbon atoms, such as, 2-9, 3-8, 4-7 or 5-6 carbon atoms. Preferably, the at least one aliphatic subunits is an alkyl or an alkenyl subunit. It should be understood that when linker L(b) comprises more than one aliphatic subunit, such as at least two or at least three, these can be the same or different. That means that they can independently have different lengths and/or have different chemical structure.

In a preferred embodiment of the present invention, linker L(b) further comprises at least one hydrogen bonding group, such at least two, at least three or at least four hydrogen bonding groups. Preferably, the at least one hydrogen bonding group is selected from the group consisting of a urea functional group, a urethane, a carbonyl group, an amide, a carbamate, a carbonate, an ester and an ether. When linker L(b) comprises at least two aliphatic subunits, the at least one hydrogen bonding group is preferably positioned between two of the at least two aliphatic subunits.

If present, polymer P(b) may be any type of polymer may be any type of polymer, which can suitably be selected from the group consisting of polyethers, polyesters, polyurethanes, polyamides, polyacrylates, polymethacrylates, polyacrylamides, (hydrogenated) polyolefins, polysiloxanes, polycarbamate, polycarbonates, polyorthoesters, polysaccharides, poly(N- vinylcapro lactam), polyvinylpyrrolidone, polyvinylpyrrolidone/vinylacetate copolymer and polyvinylalcohols (preferably partly esterified) and copolymers of these polymers. In a preferred embodiment of the invention, polymer P(b) is selected from the group consisting of polyethers, polyesters, such as e.g. aliphatic polyesters, polycarbonates, polysiloxanes, polyorthoesters, polycarbamate and polycarbonates. More preferably, polymer P(b) is selected from the

group consisting of polyether and polyester. Even more preferably, polymer P(b) is an aliphatic polyether. In a highly preferred embodiment, polymer P(b) is an oligoethylene glycol (OEG) or a polyethylene glycol (PEG).

The nature of the polymer P(b) affects the availability of the orthogonal reaction partner O1 also comprised in compound (b) to the surrounding medium. If the surrounding medium is an aqueous medium, it is preferred that polymer P(b) is a hydrophilic polymer. OEG and PEG are particularly useful as hydrophilic polymers P(b).

The length of polymer P(b) affects the nature of the supramolecular material comprising compound (b). If for instance polymer P(a) is a hydrophobic polymer and an the supramolecular material is a solid or semi-solid, a hydrophilic polymer P(b) is envisaged to be capable of interfering with the structure of the supramolecular material. In order to avoid such potential interference, polymer P(b) is preferably relatively short. Preferably, polymer P(b) comprises from about 1 to about 20 repeating units, such as from about 1 to about 11, from about 2 to about 10, from about 3 to about 9, from about 4 to about 8, from about 5 to about 7, such as 6 repeating units. In a preferred embodiment, Polymer P(b) is an oligomer O(b). In a highly preferred embodiment, polymer P(b) is monodispersed.

When linker L(b) comprises a polymer P(b), linker L(b) comprises the formula -D(b)-P(b)-E(b)-, wherein D(b) and E(b) are independently a direct bond or a connecting group. If D(b) is a direct bond to the supramolecular subunit S(b) and E(b) is a direct bond to the first orthogonal reaction partner O1, the formula of compound (b) is simply S(b)-P(b)-O1. However, linker L(b) may comprise one or more further subunits than the polymer P(b), in which case, D(b) and E(b) are either direct bonds to such further subunits or are connecting groups between the polymer P(b) and the one or more further subunits. As used herein, the term “connecting group” means the moiety of a molecule used for the reaction required in order to incorporate a further subunit in a linker. In this particular case the connection group would have been incorporated upon linking polymer P(a) to a further subunit of linker L(a). Usually, such connecting groups are selected from a group consisting of a urea functional group, urethane, a carbonyl group, amide, carbamate, carbonate, ester, ether and alkyl.

When the linker L(b) comprises at least one further subunit than the polymer P(b), linker L(b) comprises the formula -C(b)-D(b)-P(b)-E(b)-F(b)-, wherein C(b) and F(b) are aliphatic subunits.

C(b) may be directly connected to the supramolecular subunit S(b) or it may be connected to a hydrogen bonding group B(b). F(b) may be directly connected to the first orthogonal reaction partner O1 or it may be connected to a connecting group G(b). When C(b) is directly connected to the supramolecular subunit S(b) and F(b) is directly connected to the first orthogonal reaction partner O1 compound (b) has the formula S(b)-C(b)-D(b)-P(b)-E(b)-F(b)-O1.

In one embodiment, linker L(b) comprises the formula -B(b)-C(b)-D(b)-P(b)-E(b)-F(b)-G(b)-, wherein B(b) is a hydrogen bonding group and G(b) is a connecting group.

Linker L(b) may comprise a further subunit between the hydrogen bonding group B(b) and the supramolecular subunit S(b). In that case, linker L(b) comprises the formula -A(b)-B(b)-C(b)-D(b)-P(b)-E(b)-F(b)-G(b)-, wherein A(b) is an aliphatic subunit.

In a preferred embodiment of the present invention, compound (b) comprises a formula selected from the group consisting of:

i)

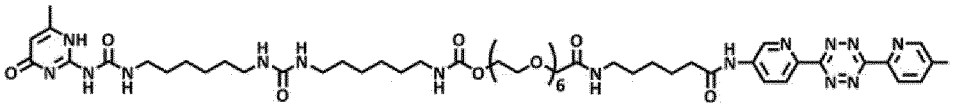

ii)

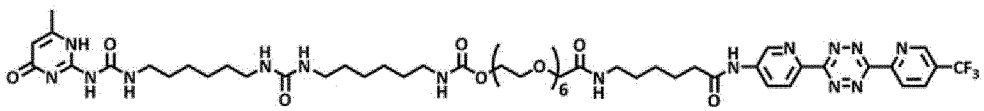

iii)

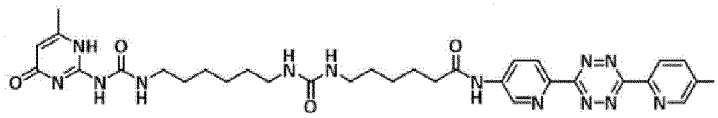

iv)

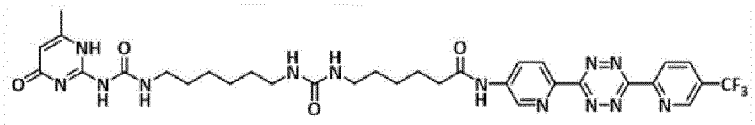

v)

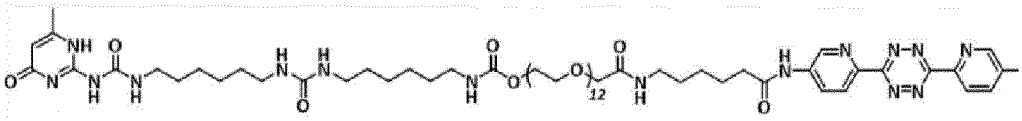

and vi)

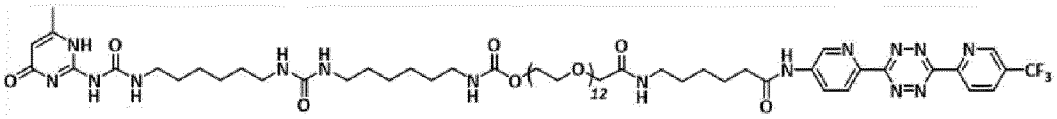

The present invention also relates to the compound (b) per se as defined herein, i.e. a compound comprising a supramolecular subunit S(b) and a first orthogonal reaction partner O1 capable of forming a covalent bond to a second orthogonal reaction partner O2. The various options described in the above for compound (b) and, if present, for linker L(b) shall apply mutatis mutandis for this embodiment of the invention. In one embodiment, compound (b) comprises a structure selected from the group consisting of the structures i, ii, iii, iv, v and vi outlined in the above.

Compound (a)

Compound (a) of the supramolecular material according to the present invention, comprises at least two supramolecular subunits S(a) linked by a linker L(a) comprising a polymer P(a). This compound is also referred to as the "supramolecular base polymer" as it constitutes the major part of the supramolecular material and as it is the properties of this compound that enable the formation of a supramolecular material. In one embodiment of the present invention, compound (a) comprises two supramolecular subunits and has the formula S(a)-L(a)-S(a), wherein L(a) is a linker comprising P(a).

Polymer P(a) may be any type of polymer, e.g. of synthetic origin or of natural origin, such as chitosan, collagen, fibrin, or proteoglycans. However, it is preferred that polymer P(a), is selected from the group consisting of polyethers, polyesters, polyurethanes, polyamides, polyacrylates, polymethacrylates, polyacrylamides, (hydrogenated) polyolefins, polysiloxanes, polycarbamate, polycarbonates, polyorthoesters, polysaccharides, poly(N- vinylcapro lactam), polyvinylpyrrolidone, polyvinylpyrrolidone/vinylacetate copolymer and polyvinylalcohols (preferably partly esterified) and copolymers of these polymers. According to a more preferred embodiment of the invention, polymer P(a) is selected from the group consisting of polyethers, polyesters, such as e.g. aliphatic polyesters, polycarbonates, polysiloxanes, polyorthoesters, polycarbamate and polycarbonates. Even more preferably, polymer P(a) is selected from the group consisting of polyether and polyester. Even more preferably, polymer P(a) is an aliphatic polyester. In a preferred embodiment, polymer P(a) is a hydrophobic polymer. In a highly preferred embodiment, polymer P(a) is polycaprolactone (PCL).

The nature of the polymer P(a) affects the nature of the supramolecular material obtained based on a compound (a). Supramolecular materials can be in the form of particles, hydrogels, solids and semi-solids. If a solid or semi-solid supramolecular material is desired, the polymer P(a) should preferably be a hydrophobic polymer. Polycaprolactone is particularly useful as hydrophobic polymer P(a).

When polymer P(a) is PCL, the PCL prepolymer may be initiated in a ring opening polymerization from a diethyleneglycol moiety as an initiator resulting in a ethyleneglycol spacer within the PCL polymer P(a).

The length of polymer P(a) also affects the nature of the supramolecular material based on a compound (a). In a preferred embodiment of the present invention, polymer P(a) therefor has an Mn from about 100 to 100,000 Dalton, such as from about 100 to 60,000, from about 800 to about 40,000 or from about 2,000 to about 35,000 Dalton. Mn is defined in the art as "total weight of all the polymer molecules in a sample, divided by the total number of polymer molecules in a sample". In a preferred embodiment, the polymer P(a) is a polycaprolactone of about 2,000 Da.

In one embodiment, linker L(a) further comprises at least one aliphatic subunit, such as at least two aliphatic subunits, such as, at least three or at least four aliphatic subunits. The various options described in the above for the aliphatic subunits of linker L(b) shall apply mutatis mutandis for the aliphatic subunits of linker L(a). It should be understood that when linker L(a) comprises more than one aliphatic subunit, such as at least two, at least three or at least four subunits, these can be the same or different. That means that they can independently have different lengths and/or have different chemical structure.

In a preferred embodiment of the present invention, linker L(a) further comprises at least one hydrogen bonding group, such at least two, at least three or at least four hydrogen bonding groups. The various options described in the above for the at least one hydrogen bonding group of linker L(b) shall apply mutatis mutandis for the at least one hydrogen bonding group of linker L(a). It should be understood that when linker L(a) comprises more than one hydrogen bonding group, these can be the same or different. That means that they can independently have different chemical structure. When linker L(a) comprises at least two aliphatic subunits, the at least one hydrogen bonding group is preferably positioned between two of the at least two aliphatic subunits.

Linker L(a) comprises or consists of a polymer P(a) as described herein. In one embodiment, linker L(a) comprises the formula -A(a)-P(a)-A(a)'-, wherein A(a) and A(a)' are independently a direct bond or a connecting group. If A(a) and A(a)' are both a direct bond to the supramolecular subunits S(a), the formula of compound (a) is simply S(a)-P(a)-S(a). However, linker L(a) may comprise, in addition to the polymer P(a), one

or more further subunits, in which case, A(a) and A(a)' are either direct bonds to such further subunits or are connecting groups between the polymer P(a) and the one or more further subunits. The various options described in the above for connecting groups in linker L(b) shall apply mutatis mutandis for the connecting groups in linker L(a).

When the linker L(a) comprises, in addition to the polymer P(a), at least one further subunit, it comprises the formula -B(a)-A(a)-P(a)-A(a)'-B(a)'-, wherein B(a) and B(a)' are such further subunits. B(a) and B(a)' may independently be an aliphatic subunit as described in the above. B(a) and B(a)' may be independently connected by a direct bond to the supramolecular subunits S(a) or may be independently connected to a hydrogen bonding group. When B(a) and B(a)' are connected by a direct bond to the supramolecular subunits S(a), compound (a) has the formula S(a)-B(a)-A(a)-P(a)-A(a)'-B(a)'-S(a).

When B(a) and B(a)' are connected to hydrogen bonding groups, linker L(a) comprises the formula -C(a)-B(a)-A(a)-P(a)-A(a)'-B(a)'-C(a)'-, wherein C(a) and C(a)' are hydrogen bonding groups.

The hydrogen bonding groups C(a) and C(a)' may either be directly bonded to the supramolecular subunits S(a), in which case compound (a) has the formula: S(a)-C(a)-B(a)-A(a)-P(a)-A(a)'-B(a)'-C(a)'-S(a). However, C(a) and C(a)' may also be connected to yet another subunit D(a) and D(a)', respectively, in which case linker L(a) comprises the formula -D(a)-C(a)-B(a)-A(a)-P(a)-A(a)'-B(a)'-C(a)'-D(a)'-, wherein, D(a) and D(a)' are aliphatic subunits. When present, D(a) and D(a)' are preferably directly linked to the supramolecular subunits S(a) resulting in a compound (a) with the formula S(a)-D(a)-C(a)-B(a)-A(a)-P(a)-A(a)'-B(a)'-C(a)'-D(a)'-S(a).

Functionalized supramolecular material

In one embodiment of the present invention, the supramolecular material has been functionalized. As used herein, the term "functionalized" means that the supramolecular material has been modified such that it comprises a functionalizing group F. In a preferred embodiment, the functionalized supramolecular material according to the present invention is surface-functionalized. As used herein, the term "surface-functionalized" means that the functionalizing group F is predominantly present on the surface of the supramolecular material.

The supramolecular material according to the present invention comprising compounds (a) and (b) as described herein, may be functionalized by an orthogonal reaction between the first orthogonal reaction partner O1 forming part of compound (b) with a second orthogonal reaction partner O2 forming part of a compound (c), wherein compound (c) comprises the second orthogonal reaction partner O2 and a functionalizing group F. Once the first orthogonal reaction partner O1 comprised in compound (b) has formed a covalent bond to the second orthogonal reaction partner O2 comprised in compound (c), the supramolecular material of the present invention has been functionalized.

A functionalized supramolecular material according to the present invention is a supramolecular material comprising the compounds (a) and (b), wherein the first orthogonal reaction partner O1 comprised in compound (b) is covalently linked to a second orthogonal reaction partner O2 comprised in compound (c). The reaction product between compound (b) and compound (c) upon the orthogonal reaction between their orthogonal reaction partners O1 and O2, respectively, is called compound (d). In other words, compound (d) is the reaction product of the compounds (b) and (c), the first orthogonal reaction partner O1 comprised in compound (b) has formed a covalent bond to the second orthogonal reaction partner O2 comprised in compound (c). Thus, compound (d) comprises a supramolecular subunit (b) linked to a first orthogonal reaction partner O1, which is linked to a second orthogonal reaction partner O2 which is again linked to a functionalizing group F. Accordingly, a functionalization supramolecular material according to the present invention comprises the compound (a) and a compound (d), wherein compound (d) comprises compound (b) and compound (c) covalently linked to one another via the first orthogonal reaction partner O1 of compound (b) and the second orthogonal reaction partner O2 of compound (c).

Compound (c)

In a preferred embodiment, compound (c) comprises the formula O2-L(c)-F, wherein O2 is the second orthogonal reaction partner O2, L(c) is a direct bond or a linker and F is a functionalizing group. When L(c) is a linker it comprises at least one aliphatic subunit and/or a polymer P(c). The various options described in the above for the aliphatic subunits of linker L(b) shall apply mutatis mutandis for the aliphatic subunits of linker L(c).

In a preferred embodiment of the present invention, linker L(c) further comprises at least one hydrogen bonding group. The various options described in the above for the

at least one hydrogen bonding group of linker L(b) shall apply mutatis mutandis for the at least one hydrogen bonding group of linker L(c). It should be understood that when linker L(c) comprises more than one hydrogen bonding group, these can be the same or different. That means that they can independently have different chemical structure. When linker L(c) comprises at least two aliphatic subunits, the at least one hydrogen bonding group is preferably positioned between two of the at least two aliphatic subunits.

If present, polymer P(c) may be any type of polymer, which can suitably be selected from the group consisting of polyethers, polyesters, polyurethanes, polyamides, polyacrylates, polymethacrylates, polyacrylamides, (hydrogenated) polyolefins, polysiloxanes, polycarbamate, polycarbonates, polyorthoesters, polysaccharides, poly(N- vinylcapro lactam), polyvinylpyrrolidone, polyvinylpyrrolidone/vinylacetate copolymer and polyvinylalcohols (preferably partly esterified) and copolymers of these polymers. Polymer P(c) may be a short polymer, such as on oligomer.

In a preferred embodiment of the invention, polymer P(c) is selected from the group consisting of polyethers, polyesters, such as e.g. aliphatic polyesters, polycarbonates, polysiloxanes, polyorthoesters, polycarbamate and polycarbonates. More preferably, polymer P(c) is selected from the group consisting of polyether and polyester. Even more preferably, polymer P(c) is an aliphatic polyether. In a preferred embodiment, linker P(c) is a hydrophilic polymer. In a highly preferred embodiment, polymer P(c) is an oligoethylene glycol (OEG) or a polyethylene glycol (PEG).

The nature and length of the polymer P(c) affects the availability of the functionalizing group F to the surrounding medium. In a preferred embodiment, polymer P(c) comprises from about 1 to about 20 repeating units, such as from about 1 to about 8, from about 2 to about 7, from about 3 to about 5, such as 4 repeating units. If the surrounding medium is an aqueous medium, it is preferred that polymer P(c) is a hydrophilic polymer. OEG and PEG are particularly useful as hydrophilic polymer P(c).

The functionalizing group F attached to the supramolecular material of the present invention upon functionalization can be any functionalizing group. Examples of functionalizing groups are imaging agents, therapeutical agents, bioactive molecules, proteins, peptides and antifouling agents.

Since the functionalization is taking place after the formation of the supramolecular material, the functionalizing groups F are primarily present on the surface of the

supramolecular material. The supramolecular material according to the present invention is then said to be “surface-functionalized”. In a preferred embodiment of the present invention, the functionalizing group F is present on the surface of the supramolecular material in a surface:bulk ratio of at least 60:40, such as 65:35, 70:30, 75:25, 80:20, 85:15, 90:10, 95:5, 96:4, 97:3, 98:2 or 99:1.

In a preferred embodiment of the present invention, the combination of the first orthogonal reaction partner O1 and the second orthogonal reaction partner O2 is selected such that a covalent bond is formed or can be formed between O1 and O2 by a reaction selected from the group consisting of:

- Copper(I)-Catalyzed Azide-Alkyne Cycloaddition (CuAAC);
- Strain-promoted Azide-Alkyne Cycloaddition (SPAAC);
- Strain-promoted Alkyne-Nitrone Cycloaddition (SPANC);
- Staudinger ligation;
- Native chemical ligation; and
- Oxime ligation.

.

Preferably, the combination of the first orthogonal reaction partner O1 and the second orthogonal reaction partner O2 is selected such that a covalent bond is formed or can be formed between O1 and O2 by an inverse electron demand Diels-Alder (iEDDA) cycloaddition reaction. Even more preferred, one of the first and the second orthogonal reaction partners O1 or O2 is a trans-cycloalkene, such as e.g., a *trans*-cyclooctene or a oxanobornadiene, and the other of O1 or O2 is selected from the group consisting of an azide, a tetrazine and a tetrazole. And even more preferably, one of O1 or O2 is a *trans*-cyclooctene and the other of O1 or O2 is a tetrazine. In yet another preferred embodiment, the first and second orthogonal reaction partners O1 and O2 are bio-orthogonal reaction partners.

Method of preparation

The present invention also relates to a method for the preparation of a supramolecular material according to the present invention. In the below the main method steps for the preparation of a supramolecular material capable of being functionalized and the further step of functionalizing the material are described. The various options described in the above for the components of the supramolecular materials according to the present invention shall apply mutatis mutandis for the components used in the methods of preparation. In one embodiment, the method for the preparation of a supramolecular material according to the present invention comprises the steps of:

1. Mixing the compounds (a) and (b) in a solvent to obtain a polymer solution, and
2. Subjecting the polymer solution obtained in step 1) to any of the following steps:
   a) Evaporating at least 70% (v/v) of the solvent off from from the polymer solution obtained in step 1) to obtain supramolecular material, or
   b) Decreasing the pH in the polymer solution obtained in step 1) to obtain a hydrogel supramolecular material.

Step 1) is performed in a solvent, wherein compounds (a) and (b) are dissolved. The solvent may be an aqueous solvent or an organic solvent, wherein the organic solvent may comprise one or more organic solvents. Preferably, the one or more organic solvents are selected from the group consisting of chloroform, DCM, methyl ethyl ketone, THF, DMSO, NMP, scCO2, aliphatic alcohols and Hexafluoroisopropanol (HFIP). In a preferred embodiment of the present invention, the solvent is Hexafluoroisopropanol. What is important for the choice of solvent is that compounds (a) and (b) are both dissolved in the solvent.

Compound (a) is preferably dispersed or dissolved in the one or more solvents used in step 1) in an amount of from about 5 to about 100 mg/ml, such as from about 10 to about 80 mg/ml, from about 15 to about 65 mg/ml, from about 20 to about 50 mg/ml.

Compound (b) is preferably dispersed or dissolved in the one or more solvents used in step 1) in an amount from about 0.5 mol% to about 30 mol%, such as from about 1 mol% to about 25 mol%, from about 1.5 mol% to about 10 mol%, from about 2 to about 9 mol%, from about 2.5 to about 8 mol%, from about 3 to about 7 mol%, from about 3.5 to about 6.5 mol%, from about 4 to about 6 mol% or at about 5 mol% of the total amount of compound (a) and compound (b) in the polymer solution. The mol% is here the % of the number of compound (b) in moles, compared to the total number of moles of compound (a) and compound (b).

In one embodiment, further ingredients intended for incorporation in the supramolecular material may added to the polymer solution in step 1). Such further ingredients may for example be excipients, anti-oxidants and pH-buffers.

The polymer solution obtained in step 1) is processed by subjecting it to either of steps 2a) or 2b). Preferably, step 2a) is performed. If step 2a) is performed, it is preferred that at least 75% (v/v), such as at least 80% (v/v), 85% (v/v), 90% (v/v), 95% (v/v), 96% (v/v), 96% (v/v), 96% (v/v) or 96% (v/v) of the solvent is evaporated off from the

polymer solution obtained in step 1). Preferably, the evaporation is completed such that all the solvent, or essentially all of the solvent, is evaporated off from the polymer solution obtained in step 1).

In a preferred embodiment, the evaporation performed in step 2a) may suitably be performed by a technique selected from the group consisting of solvent casting, drop-casting, dip- coating, freeze-drying, precipitation casting, spray coating, painting, roll-coating, foaming, solvent spinning, wet spinning, electro-spinning, spin coating, micro-contact printing, ink jet printing, particulate-leaching techniques, phase-separation techniques and emulsion processes. Preferably, the isolation in step 2a) is performed by drop-casting and spin coating.

In a preferred embodiment, the supramolecular material obtained in step 2a) is a solid or a semi-solid supramolecular material.

If step 2b) is performed, pH is decreased from a pH of above the pH of gelation in the polymer solution to the pH of gelation or less. In one embodiment, compound (a) comprises a hydrophilic polymer P(a), step 1) is performed in an aqueous solvent at a pH higher than the pH of gelation and the polymer solution obtained in step 1) is subjected to step 2b) wherein pH is decreased to a pH lower than the pH of gelation. As used herein, “pH of gelation” means the pH at which the polymer solutions forms a hydrogel, also sometimes referred to in the art as the pH of the sol-to-gel switch. In a preferred embodiment, the pH of gelation of the supramolecular material is between pH 6 and 8 or about 7.

An alternative method for the preparation of a supramolecular material involves melting compounds (a) and (b) with no solvent present and afterwards subjecting the material to e.g. spinning or casting.

A supramolecular material according to the present invention can be functionalized by orthogonal ligation between the first orthogonal reaction partner O1 of the compound (b) described herein and the second orthogonal reaction partner O2 of compound (c) described herein. Accordingly, the present invention also relates to a method for obtaining a supramolecular material according to the present invention, the method further comprising a post-functionalizing step 3:

3. subjecting the supramolecular material obtained in any of steps 2a) or 2b) to a reaction with the compound (c) to obtain the covalent bond between the first

orthogonal reaction partner O1 of compound (b) and the second orthogonal reaction partner O2 of compound (c).

In a preferred embodiment, O1 and O2 are selected such that the reaction in step 3 is selected from the group consisting of:

- Copper(I)-Catalyzed Azide-Alkyne Cycloaddition (CuAAC);
- Strain-promoted Azide-Alkyne Cycloaddition (SPAAC);
- Strain-promoted Alkyne-Nitrone Cycloaddition (SPANC);
- Staudinger ligation;
- Native chemical ligation; and
- Oxime ligation.

In a more preferred embodiment, O1 and O2 are selected such that the reaction in step 3 is an inverse electron demand Diels-Alder (iEDDA) cycloaddition reaction.

In a preferred embodiment, the reaction in step 3 is a reaction that can take place in an aqueous solution. It is also preferred that the reaction in step 3 can take place at pH 6-8, such as 6.5-7.5 or at about 7. Furthermore, it is also preferred that the reaction in step 3 is a fast reaction and accordingly, that step 3 can be performed in less than 2 hours, such as less than 1.5 hour, less than 1 hour, less than 20 minutes, less than 10 minutes or less than 5 minutes. The inverse electron demand Diels-Alder (iEDDA) cycloaddition reaction between tetrazine as O1 and *trans*-cyclooctene as O2, is an example of such a reaction.

In a highly preferred embodiment, the method for the preparation of the functionalized supramolecular material according to the present invention, i.e. the method comprising step 3, involves that:

- The first orthogonal reaction partner O1 of compound (b) is a tetrazine;
- The second orthogonal reaction partner O2 of compound (c) is a *trans*-cyclooctene; and
- The reaction in step 3 is performed in an aqueous solution at pH 6-8 for less than 0.5 hours, such as less than 20 minutes, less than 10 minutes or less than 5 minutes.

The present invention also relates to a supramolecular material obtainable from any of steps 2a), 2b) or 3. In a preferred embodiment, the present invention relates to a supramolecular material obtainable from step 2a). In a further preferred embodiment, the present invention relates to a supramolecular material obtainable from step 2a). I

yet a further preferred embodiment, the present invention relates to a supramolecular material obtainable from a combination of step 2a) and 3, i.e. where the supramolecular material obtained in step 2a) is further subjected to step 3.

Applications

The supramolecular material according to the present invention can suitably be used as a biomaterial. As used herein, the term "biomaterial" means a material engineered to interact with biological systems for a medical purpose, e.g. to treat, augment, repair or replace a tissue or a tissue function of the body. Accordingly, the present invention also relates to a biomaterial comprising the supramolecular material according to the present invention. The supramolecular material according to the invention and the biomaterial according to the invention are preferably suitable for applications related to biomedical applications, such as in regenerative medicine including tissue-engineering, or as materials for the manufacture of a prosthesis or an implant. The supramolecular material according to the present invention and the biomaterial according to the invention can also be applied as a coating on prostheses, implants, stents, catheters, or other medical devices that come in contact with living tissue.

When used as a biomaterial, polymers (a) and (b) are preferably biocompatible. Known examples of biocompatible polymers include, but are not limited to, polyester polycaprolactone (PCL) and the polyether polyethylene glycol (PEG). Accordingly, PCL is highly suitable as polymer P(a) and PEG is highly suitable as polymer P(b) when the supramolecular material of the present invention is used as a biomaterial.

In summary, the present invention provides a novel, elegant and successful strategy to functionalize supramolecular material surfaces via an orthogonal click reaction between a UPy-Tz moiety/additive, modularly incorporated into our supramolecular polymer, and a TCO-modified model compound. The strategy presented here is a prove of concept of that it is possible to incorporate the compound (b) in a supramolecular material comprising compound (a) thereby providing a way of post-functionalization of the supramolecular material according to the invention.

XPS measurements showed that a model compound (b) (UPy-Tz) is preferentially present at the surface of the supramolecular films. Moreover, upon click reaction with a model compound (c) (TCO-model compound equipped with an iodine atom), a significant increase in iodine signal is observed in films consisting of PCLdiUPy with UPy-Tz as compared to PCLdiUPy films without UPy-Tz. Fluorescence spectroscopy

showed that upon incorporating increasing amounts of UPy-Tz in the material, higher fluorescence signals originating from TCO-modified fluorescent protein were observed. Surface MALDI-TOF-Ms experiments revealed presence of the UPy-Tz – TCO-modified model compound click product (exemplary compound (d)), a direct proof of the success of this novel strategy. 3D TOF-SIMS experiments allowed to reconstruct a density map of the different compounds incorporated in our materials and provided useful insights in their spatial distribution.

Here we show that selective modification reactions can be performed on additives that are supramolecularly incorporated into supramolecular materials. Careful design and synthesis of the additive facilitates control on the assembly process within the material and allows for selective surface post-modification in aqueous environment. Importantly, in this way processing of the material, that regularly requires harsh processing conditions (i.e. the use of organic solvents and/or high temperatures), and functionalization can be decoupled. Along these lines, this approach endorses various material preparation methods (i.e. 3D-printing, melt spinning, electrospinning), whereby bulk material properties can easily be tuned and yet the material surfaces can be functionalized via covalent post-modification. In conjunction with advanced ToF-SIMS depth profiling of bulk and surface we are now able to reveal the distribution of additive and reactant. At a supramolecular chemistry level these results allow for further exploration of these selective reactions on inherently more dynamic systems, such as aggregates in solution and supramolecular hydrogels, yielding complex assemblies with various functionalities. This post-modification strategy of supramolecular systems might accommodate for better control on the assembled structure, when specific functionality is introduced after assembly. Additionally, the accurate depth resolution of ToF-SIMS is proposed to aid in elucidating the complex structures of such hierarchical assemblies. Finally, this functionalization and characterization strategy holds great promise in the field of regenerative medicine, in which design and detailed analysis of bioactive, functional biomaterials is important for the ultimate interaction with cells and tissues, and the essential performance.

EXAMPLES

All reagents and chemicals used in the examples were obtained from commercial sources at the highest purity available and used without further purification unless stated otherwise. Water was purified on an EMD Millipore Milli-Q Integral Water

Purification System. Data processing and analysis was performed in Excel 2010 and Origin 2015. Where reported SD the standard deviation of the sample is given.

Example 1. Materials and Methods used in examples 1-19.

Synthesis of compounds and materials

PCLdiUPy was synthesized by SyMO-Chem BV (Eindhoven, The Netherlands) (*27*). 1, 1, 1, 3, 3, 3-Hexafluoroisopropanol (HFIP) was obtained from Sigma-Aldrich (Zwijndrecht, The Netherlands). TCO-OEG_4-NHS ester (equatorial isomer) used in the synthesis of the model functionalization compounds TCO-I and TCO-EYFP in examples 7 and 8, respectively, was obtained from Kerafast (Boston, MA, USA). Water was deionized prior to use. 2(6- Isocyanatohexylaminocarbony-lamino)-6-methyl-4[1H]pyrimidinone (UPy-C_6-NCO) was synthesized as described(*5*). The synthesis of UPy-Tz (**2**) and TCO-I (**3**) are described in examples 3 and 7, respectively (see also Fig. 14 and Fig. 15, respectively).

Instrumentation

^{1}H NMR and ^{13}C NMR spectra were recorded on a 400 MHz NMR (Varian Mercury Vx or Varian 400MR) operating at 400 MHz for ^{1}H NMR and 100 MHz for ^{13}C NMR. Proton chemical shifts are reported in ppm downfield from tetramethylsilane (TMS) and carbon chemical shifts in ppm downfield from TMS using the resonance of the deuterated solvent as internal standard. Abbreviations used are s: singlet, d: doublet, t: triplet, q: quartet, m: multiplet. IR spectra were acquired on a Perkin-Elmer spectrum Two equipped with a UATR Two sample stage.

X-ray photoelectron spectroscopy (XPS)

XPS was performed on drop-cast films that were attached to the sample plate by copper clamps and spectra were recorded using a Thermo Scientific K-Alpha spectrometer equipped with a monochromatic, small-spot X-ray source and a 180° double focusing hemispherical analyzer with a 128-channel detector. Spectra were obtained using an aluminum anode (Al Kα, 1486.6 eV) operating at 72 W. Survey scans were measured at a pass energy of 200 eV and region scans at a pass energy of 50 eV. The background pressure was 2 x 10^{-8} mbar and during measurement 3 x 10-7 mbar argon, because of the 3 charge compensating dual beam source. For angle-resolved XPS, the samples were mounted with conducting carbon tape to the sample holder and spectra were measured at 0°, 15°, 30°, 45°, 60° and 75°. Analysis and quantification of the spectra were performed using the CasaXPS software version 2.3.16, using the C 1s, N 1s, O 1s and F 1s regions.

FTIR measurements

IR spectra were recorded using a Varian 670-IR FTIR spectrometer / 610-IR FTIR Microscope setup equipped with a germanium slide-on ATR accessory. Spectra were recorded with a resolution of 2 cm^{-1} with 50 scans per spectrum for the samples and 100 scans per spectrum for the background. Spectra were analyzed using Spekwin32 version 1.71.6.1.

Atomic force microscopy (AFM)

AFM images were recorded at room temperature in air using a Digital Instrument Multimode Nanoscope IV operating in tapping regime mode using silicon cantilever tips (PPP-NCH-50, 204-497 kHz, 10-130 N/m). Surface roughness has been measured and images have been processed using Gwyddion software (version 2.39, hhtp://www.gwyddion.net).

Water contact angle measurements

Water contact angles were measured at room temperature on an OCA30 (DataPhysics). Water droplets (5 µL) were applied on the drop-cast films on glass and the angle at the polymer-air-water interface was determined after 5 seconds using an automatic fitting routine (SCA20 software). The mean and the standard deviation of three to five samples are reported.

Surface fluorescence experiments

Fluorescence assays were performed on a Thermo Scientific Fluoroskan Ascent Microplate Fluorometer and analyzed with Ascent Software for Fluoroskan Ascent FL. Surfaces were excited at 488 nm and emission was recorded at 538 nm. Samples were prepared by 25 µL dropcast of 50 mg/mL PCLdiUPy + 0, 1, 5, 10 or 25 mol% UPy-Tz in HFIP into a 96-wells plate. After overnight drying of the surface, wells were incubated with 200 µg/mL TCO-EYFP or 200 µg/mL EYFP for 2 hours. Fluorescence was measured directly after 2 hour incubation. Supernatant was removed and surface fluorescence was measured. Subsequently, surfaces were washed 3 times with milli-Q water and after each washing step, surface fluorescence was measured.

Surface MALDI-ToF MS measurements

Matrix-assisted laser desorption ionization time-of-flight mass spectrometry (MALDI-ToF MS) was performed on an Autoflex Speed MALDI-MS (Bruker) using an α-cyano-4-hydroxycinnamic acid (CHCA) matrix. Surface MALDI-ToF MS experiments were performed on drop-cast samples on a MTP 384 target plate polished steel TF. Dropcast were prepared by 5 µL 50 mg/mL PCLdiUPy + 0, 5, 10 or 25 mol% UPy-Tz and directly

deposited on the MALDI plate. Next, drop-cast spots were incubated with 4µL 1 µM TCO-iodine solution for 70 minutes, after which the reaction solution was discarded from the MALDI plate and the spots were washed 3 times with 5 µL milli-Q water. 4 Subsequently 1 µL CHCA in 49.5/49.5/1 acetonitrile/water/TFA (v/v/v) was spotted on each surface and allowed to dry for 30 minutes. MALDI-ToF Ms measurements were performed in positive linear mode (method: 700-2000 Da), 1500 shots per spot and a laser power of 50%.

3D ToF-SIMS measurements

The in depth ToF-SIMS experiments were performed using a PHI *nanoToF* II TRIFT mass spectrometer (Physical Electronics, Minnesota, USA) equipped with a 30 kV bismuth liquid metal ion gun (LMIG) and a 20 kV C60 ion gun (Ionoptika, Hampshire, UK). A pulsed Bi3 ++ cluster ion beam was used for analysis and a continuous C60 + cluster ion beam was used for sputtering in the described depth profiling measurements. 50 cycles of alternating between sputtering and analyzing were executed, each cycle consisted of 4 frames (512x512 pixel density, 2.13 minutes) LMIG analysis and 1 minute of sputtering with the C60 ion beam (1.47 x 1017 ions/cm2) while the sample is kept at ground potential. The analytical area was 100x100 µm, the sputter area was 400x400 µm. On each sample, an in depth experiment was performed in both positive and negative ion mode, with a mass range of *m/z* 0-1850. All raw data was produced using PHI SmartSoft-ToF and was subsequently processed into 3D visualizations of ion distributions and spectra with PHI ToF-DR (both Physical Electronics, Minnesota, USA).

Principal Component Analysis (PCA)

PCA is a statistical tool that is often used to inspect large mass spectrometry imaging data sets. PCA optimizes the variance that is described in each principal component (PC) in descending order of magnitude. The first PC contains the maximum variance direction, the second one the next maximum, etcetera. Therefore, each PC will contain different percentages of the variance originating from multiple analytes and the PC score images reveal the distribution and relative concentrations of this mixture. A PCA was done on the first two analysis layers from each depth profiling ToF-SIMS data set. The analyses were performed using the ChemomeTricks toolbox for MATLAB version R2014a (The Math-Works, Natick, MA, USA) developed at the FOM Institute AMOLF.

HPLC-ESI-MS analysis

Purity and exact mass of the proteins were determined using a Waters Xevo G2 Quadrupole Time of Flight (Q-ToF) Liquid Chromatography – Mass Spectrometry

equipped with an Agilent Polaris C18A reverse phase column (ID 2.0 mm, length 100 mm). Proteins were flowed (0.3 ml/min) over the column using a 15% to 75% water/acetonitrile gradient with 0.1% formic acid prior to analysis in positive mode in the mass spectrometer. Deconvolution of the m/z spectra was done using the MaxENT1 algorithm in the MassLynx software. 6

Example 2. Synthesis of the supramolecular base polymer (compound (a)), PCLdiUPy

As base supramolecular TPE polycaprolactone (Mn=2 kDa) telechelically modified with UPy-units was used (PCLdiUPy, Fig. 1b). PCLdiUPy was synthesized by SyMO-Chem BV (Eindhoven, The Netherlands) (*27*).

Example 3. Synthesis of the additive, UPy-OEG_6-Tz

In order to achieve selective surface reaction, analysis and detailed depth profiling, we carefully designed and synthesized a supramolecular UPy- OEG_6-Tz additive (Fig. 1b, Fig. 14), that provides supramolecular intercalation into the TPE (*44*). The UPy-Tz additive consists of a hydrophilic oligo (ethylene glycol) (OEG) spacer which is proposed to facilitate surface exposure via extension into water. Furthermore, the UPy-Tz molecule is equipped with a CF_3 group that allows for detection.

The synthesis scheme of the synthesis of UPy- OEG_6-Tz is shown in Figure 14. In the below, the reaction is outlined step for step. References to compounds made in parenthesis after the chemical name of a compound refers to the number indicated for that compound in Figure 14:

Step 1: Synthesis of tert-Butyl (6-((6-cyanopyridin-3-yl)amino)-6-oxohexyl)carbamate (16)

6-((Tert-butoxycarbonyl)amino)hexanoic acid (5.18 g, 22.39 mmol), EDC (6.44 g, 33.6 mmol), DMAP (4.10 g, 33.6 mmol), and PPTS (0.56 g, 2.24 mmol) were dissolved in 50 mL DCM. After stirring for 30 minutes 5-aminopicolinonitrile (4.0 g, 33.6 mmol) was added. The reaction mixture was stirred for 1 h, after which 50 mL chloroform was added. The organic phase was washed twice with 40 mL 0.5 M citric acid, saturated sodium hydrogen carbonate, and brine, followed by drying with Na_2SO_4 and evaporating to dryness yielding 7.5 g of the crude product. Eluting over silica with chloroform containing 2.5% methanol afforded 5.9 g (79 %) of the pure product.

^{1}H NMR of the *tert*-Butyl (6-((6-cyanopyridin-3-yl)amino)-6-oxohexyl)carbamate (16) obtained in step I:

^{1}H NMR (399 MHz, $CDCl_3$) δ 8.90 (s, 1H), 8.68 (s, 1H), 8.46 (d, 1H), 7.65 (d, *J* = 8.6 Hz, 1H), 4.74 (t, *J* = 6.1 Hz, 1H), 3.10 (q, *J* = 6.7 Hz, 2H), 2.42 (t, *J* = 7.5 Hz, 2H), 1.74 (p, *J* = 7.5 Hz, 2H), 1.59 – 1.29 (m, ^{13}H). ^{13}C NMR (100 MHz, $CDCl_3$) δ 172.69, 156.43, 141.94, 138.51, 129.14, 127.17, 126.08, 117.44, 79.48, 40.13, 37.15, 29.61, 28.40, 26.10, 24.67. LC-MS(ESI) Rt= 6.52 min *m/z* calcd ($C_{17}H_{24}N_4O_3$) 332.4; found 233.3 [M-*t*Bu (degraded on MS) + H+]$^+$,277.2 [M-*t*Bu +HCOOH]$^+$, 355.3 [M+Na]$^+$, 687.2 [2M+Na]$^+$.

Step 2: Synthesis of *tert*-Butyl (6-oxo-6-((6-(6-(5-(trifluoromethyl)pyridin-2-yl)-1,2-dihydro-1,2,4,5-tetrazin-3-yl)pyridin-3-yl)amino)hexyl)carbamate (17)

5-(Trifluoromethyl)picolinonitrile (0.93 g, 5.42 mmol) and the *tert*-Butyl (6-((6-cyanopyridin-3-yl)amino)-6-oxohexyl)carbamate (16) obtained in step I (1.5 g, 4.51 mmol) were dissolved in EtOH (3 mL) and heated to 70˚C. Hydrazine hydrate (50-60% sol, 0.89 mL, ~18 mmol) was added and this solution was stirred overnight at 70˚C under argon. To the yellow/brown precipitate water (30 mL was added) and the suspension was centrifuged. The yellow solution was decanted off and water 50 mL was added. This was repeated until the filtrate was colorless. The yellow/brown residue was redissolved in chloroform/ MeOH 1:1, which was removed in vacuo yielding 2.2 g of the crude product. Eluting over silica with chloroform containing 5-20% acetone afforded 0.4 g (17 %) of the pure product. The obtained *tert*-Butyl (6-oxo-6-((6-(6-(5-(trifluoromethyl)pyridin-2-yl)-1,2-dihydro-1,2,4,5-tetrazin-3-yl)pyridin-3-yl)amino)hexyl)carbamate (17) is also sometimes referred to herein as "Dihydrotetrazine (17)".

^{1}H NMR of the *tert*-Butyl (6-oxo-6-((6-(6-(5-(trifluoromethyl)pyridin-2-yl)-1,2-dihydro-1,2,4,5-tetrazin-3-yl)pyridin-3-yl)amino)hexyl)carbamate (17) obtained in step II:

^{1}H NMR (399 MHz, $CDCl_3$) δ 8.78 (s, 1H), 8.66 (s, 1H), 8.57 (s, 1H), 8.39 (s, 1H), 8.18 – 8.07 (m, 2H), 8.01 – 7.81 (m, 2H), 5.00 (s, 1H), 3.32 (s, 1H), 3.03 (q, *J* = 6.7 Hz, 2H), 2.33 (t, *J* = 7.5 Hz, 2H), 1.67 (t, *J* = 7.5 Hz, 2H), 1.53 – 1.22 (m, ^{13}H). ^{13}C NMR (100 MHz, $CDCl_3$) δ 173.05, 156.61, 150.48, 146.30, 145.73, 145.37, 141.45, 139.46, 137.06, 133.89, 127.50, 127.13, 124.52, 121.60, 120.99, 79.36, 77.38, 77.26, 77.06, 76.74, 39.96, 36.75, 29.33, 28.20, 25.97, 24.83. LC-MS (ESI) Rt= 8.31 min, *m/z* calcd ($C_{24}H_{29}F_3N_8O_3$) 534.5; found 535.2 [M+H]$^+$. MS (MALDI-ToF, *m/z*): Calcd for $C_{24}H_{29}F_3N_8O_3Na$+, ([M+Na]$^+$): 557.2207, Found: 557.2384. FT-IR (ATR): υ (cm^{-1}) = 3372, 3330, 3297, 2985, 2941, 2857, 1685, 1667, 1603, 1573, 1528, 1466, 1414, 1389,

1368, 1330, 1279, 1249, 1237, 1160, 1132, 1087, 1049, 1016, 990, 958, 942, 914, 899, 862, 777, 758, 707, 662, 651, 636, 623, 577, 516, 472.

Step III: Synthesis of *tert*-Butyl(6-oxo-6-((6-(6-(5-(trifluoromethyl)pyridin-2-yl)-1,2,4,5-tetrazin-3-yl)pyridin-3-yl)amino)hexyl)carbamate (18)

Dihydrotetrazine (17) (0.4 g, 0.75 mmol) was dissolved in 6 mL THF and cooled to 0˚C, followed by the addition of AcOH (6 mL). A solution of $NaNO_2$ (0.21 g, 3.0 mmol in 6 mL water) was added dropwise over 10 min, a clear color change was observed from orange/brown to purple. This solution was stirred for another 5 min. Then it was poured in a separation funnel containing 30 mL water, 10 mL MeOH and chloroform 40 mL, subsequently the organic phase was washed with saturated sodium hydrogen carbonate (twice), water and brine. The organic phase was dried in vacuo, yielding a purple powder (0.39 g, 98%). The obtained *tert*-Butyl(6-oxo-6-((6-(6-(5-(trifluoromethyl)pyridin-2-yl)-1,2,4,5-tetrazin-3-yl)pyridin-3-yl)amino)hexyl)carbamate (18) is also sometimes referred to herein as “Tetrazine (18)”.

^{1}H NMR of the *tert*-Butyl(6-oxo-6-((6-(6-(5-(trifluoromethyl)pyridin-2-yl)-1,2,4,5-tetrazin-3-yl)pyridin-3-yl)amino)hexyl)carbamate (18) obtained in step III:

^{1}H NMR (400 MHz, $CDCl_3/CD_3OD$) δ 9.14 (d, J = 2.2 Hz, 1H), 8.85 (d, J = 8.2 Hz, 1H), 8.79 (s, 1H), 8.72 (dd, J = 8.7, 0.7 Hz, 1H), 8.63 (d, J = 9.0 Hz, 1H), 8.26 (dd, J = 8.5, 2.3 Hz, 1H), 3.04 (t, J = 6.8 Hz, 2H), 2.41 (t, J = 7.5 Hz, 2H), 1.71 (p, J = 7.6 Hz, 2H), 1.49 (p, J = 7.0 Hz, 2H), 1.38 (s, ^{13}H). ^{13}C NMR (100 MHz, $CDCl_3/CD_3OD$) δ 173.45, 163.16, 162.71, 153.02, 147.51, 143.05, 141.67, 139.07, 135.02, 126.88, 125.52, 123.82, 120.58, 79.35, 40.02, 36.86, 29.57, 29.40, 28.22, 27.85, 26.07, 24.87, 24.79. LC-MS (ESI) Rt= 6.72 min, *m/z* calcd ($C_{24}H_{27}F_3N_8O_3$) 532.5; found 533.0 $[M+H]^+$.]$^+$. MS (MALDI-ToF, *m/z*): Calcd for $C_{24}H_{27}F_3N_8O_3Na+$, ($[M+Na]^+$): 555.2050, Found: 555.2412. FT-IR (ATR): υ (cm^{-1}) = 3351, 3320, 3099, 3082, 3048, 3001, 2941, 2865, 2490, 1676, 1661 1596, 1575, 1542, 1522, 1483, 1466, 1449, 1429, 1403, 1381, 1370, 1330, 1283, 1257, 1231, 1161, 1131, 1081, 1052, 1013 982, 942, 924, 882, 862, 801, 776, 728, 706, 665, 649, 620, 583, 533, 490, 473.

Step IV: Synthesis of 6-Amino-N-(6-(6-(5-(trifluoromethyl)pyridin-2-yl)-1,2,4,5-tetrazin-3-yl)pyridin-3-yl)hexanamide (19)

Tetrazine (18) (0.2 g, 0.374 mmol) was dissolved in 2 mL DCM and 2 mL of TFA was added. The solution was stirred for 1 h at room temperature under Argon. The solvent was removed under reduced pressure and co-evaporated twice with toluene. After

redissolving in MeOH/$CHCl_3$ and precipitating in ether (2x) a solid was filtered off. Drying yielded 6-Amino-N-(6-(6-(5-(trifluoromethyl)pyridin-2-yl)-1,2,4,5-tetrazin-3-yl)pyridin-3-yl)hexanamide (19) as a pink solid (170 mg, quant.). The obtained 6-Amino-N-(6-(6-(5-(trifluoromethyl)pyridin-2-yl)-1,2,4,5-tetrazin-3-yl)pyridin-3-yl)hexanamide (19) is also sometimes referred to herein as "Tetrazine (19)".

^{1}H NMR of the 6-Amino-N-(6-(6-(5-(trifluoromethyl)pyridin-2-yl)-1,2,4,5-tetrazin-3-yl)pyridin-3-yl)hexanamide (19) obtained in step IV: ^{1}H NMR (399 MHz, CD_3OD) δ 9.20 (s, 1H), 9.06 (d, *J* = 2.5 Hz, 1H), 8.94 (d, *J* = 8.4 Hz, 1H), 8.78 (d, *J* = 8.7 Hz, 1H), 8.49 (t, *J* = 9.6 Hz, 2H), 2.96 (t, *J* = 7.6 Hz, 2H), 2.54 (t, *J* = 7.3 Hz, 2H), 1.76 (dp, *J* = 23.4, 7.6 Hz, 4H), 1.52 (q, *J* = 7.9 Hz, 2H). ^{13}C NMR (100 MHz, DMSO-*d6*) δ 172.79, 163.18, 162.86, 154.23, 147.62, 143.96, 141.81, 139.12, 135.93, 126.55, 125.60, 125.24, 124.58, 122.53, 39.19, 36.54, 27.30, 25.91, 24.74. LCMS (ESI) Rt= 6.72 min, *m/z* calcd ($C_{19}H_{19}F_3N_8O$) 432.4; found 433.0 $[M+H]^+$. MS (MALDI-ToF, *m/z*): Calcd for C19H20F3N8O +, ($[M+H]^+$): 433.1707, Found: 433.2352. FT-IR (ATR): υ (cm^{-1}) = 3263, 3171, 3095, 3048, 2962, 1705, 1672, 1601, 1580, 1541, 1439, 1404, 1329, 1261, 1229, 1202, 1172, 1129, 1082, 1021, 927, 864, 799, 722, 621, 585, 479.

Step V: Synthesis of UPy-C_6-U-C_6-Ut-OEG_6-C_5-Tz-CF_3 (2)

UPy-C_6-U-C_6-Ut-OEG_6-COOH (*48*) **20** (169 mg, 0.22 mmol) was dissolved in DMF (3 mL) and HATU (87 mg, 2.23 mmol) and pyridine (0.11 mL, 2.18 mmol) were added. The solution was stirred for 30 minutes under argon. Thereafter, tetrazine (19) (170 mg, 0.39 mmol) dissolved in 3 mL DMF was added. The reaction mixture was stirred overnight and subsequently poured into 2% FA water solution and centrifuged (2x). Eluting over silica with FA/MeOH/CHCl3 1:5:94 afforded UPy-C_6-U-C_6-Ut-OEG_6-C_5-Tz-CF_3 (2) (230 mg, 88%) as a pink solid.

^{1}H NMR of UPy-C_6-U-C_6-Ut-OEG_6-C5-Tz-CF_3 obtained in step V:

^{1}H NMR (399 MHz, $CDCl_3$/CD_3OD) δ 1.20-1.55 (14H), 1.59 (t, 2H), 2.24 (s, 3H), 3.11 (m, 6H), 3.27 (m, 2H), 3.68 (m, 20H), 4.15 (s, 2H), 4.19 (t, 2H), 5.85 (s, 1H). ^{13}C NMR (100 MHz, $CDCl_3$/CD_3OD) δ 173.68, 173.68, 173.55, 170.76, 163.43, 162.92, 159.43, 157.03, 156.22, 154.48, 153.29, 148.98, 147.68, 143.37, 142.04, 139.26, 135.18, 129.30, 128.96, 126.97, 125.68, 124.55, 124.02, 121.83, 106.48, 70.99, 70.62, 70.55, 70.33, 70.27, 69.70, 63.88, 40.73, 40.08, 40.01, 39.76, 38.70, 37.03, 30.10, 30.00, 29.77, 29.31, 29.16, 26.54, 26.46, 26.40, 26.35, 24.95, 18.84. LC-MS (ESI) Rt= 5.75 min, *m/z* calcd ($C_{53}H_{78}F_3N_{15}O_{13}$) 1189.6; found 595.8 [M+2H]2+,606.7 $[M+Na+H]^+$ 1190.3 $[M+H]^+$, 1212.4 $[M+Na]^+$. MS (MALDI-ToF, *m/z*): Calcd for $C_{53}H_{78}F_3N_{15}O_{13}Na$+,

([M+Na]$^+$): 1212.5748, Found: 1212.6470. FT-IR (ATR): υ (cm^{-1}) = 3299, 2930, 2857, 1701, 1667, 1616, 1580, 1526, 1462, 1440 1405, 1382, 1331, 1257, 1119, 1081, 1014, 941, 923, 878, 854, 768, 741, 621, 602, 583, 526, 481.

Example 4. Preparation of polymer solutions

Solutions of PCLdiUPy were prepared at a concentration of 50 mg/mL in HFIP. For mixtures, 1, 5, 10 or 25 mol% of the UPy-Tz was added to resp. 99, 95, 90 and 75 mol% solution of PCLdiUPy.

Example 5. Preparation of drop-cast surfaces

Samples were prepared by dropcast 30 µL of a solution of 50 mg/mL of the PCLdiUPy + 1, 5, 10 or 25 mol% UPy-Tz from HFIP on glass coverslips with a diameter of 12 mm. Fluorescence assay samples were prepared by dropcast 25 µL of a solution of 50 mg/mL of the PCLdiUPy + 0, 5, 10 or 25 mol% UPy-Tz from HFIP in a well of a 96-wells plate. Subsequent evaporation of the HFIP yielded the drop-cast films.

Example 6. Preparation of spin coated surfaces

Samples were prepared by spin coating 50 µL of a solution of 50 mg/mL of the PCLdiUPy + 1, 5, 10 or 25 mol% UPy-Tz from HFIP at 2000 rpm for 60 seconds on glass coverslips with a diameter of 12 mm. The samples were allowed to dry for 2 h at room temperature before continuing experiments.

Example 7. Synthesis of model functionalizing compound, TCO-I

An iodinated TCO-moiety (TCO-iodine) was synthesized to perform the cycloaddition at the surface-liquid interface of the material (Fig. 1b, 1e, Fig. 15).

The synthesis scheme of the synthesis of TCO-iodine is shown in Figure 15. In the below, the reaction is outlined step for step. References to compounds made in parenthesis after the chemical name of a compound refers to the number indicated for that compound in Figure 15:

Step I: Synthesis of 4-Iodobenzoyl chloride (22)

To a suspension of **21** (0.5 g, 2.02 mmol) in DCM (8 mL) oxalylic chloride (0.31 mL, 3.63 mmol) was added, followed by 2 drops of DMF. The reaction mixture was stirred for 30 minutes. The solvent was removed under reduced pressure and co-evaporated twice with toluene and ether. A light yellow solid **22** (0.52 g, 97%) was obtained, which was used without further purification.

^{1}H NMR of the 4-Iodobenzoyl chloride (22) obtained in step I

^{1}H NMR (200 MHz, $CDCl_3$) δ 7.98 – 7.72 (m, 4H). FT-IR (ATR): υ (cm^{-1}) = 3085, 1765, 1720, 1577, 1560, 1476, 1392, 1199, 1174, 1057, 1008, 865, 826, 713, 690,641, 625, 527, 458.

Step II: Synthesis of 4-Iodobenzamide-Lys(Boc)-NH_2 (24)

H-Lys(Boc)-NH_2 **23** (0.1 g, 0.36 mmol) was suspended in DMF (0.5 mL), triethylamine (0.20 mL, 1.42 mmol) and iodobenzoyl chloride **22** (0.12 g, 0.44 mmol) were added. The suspension was stirred for 2 h. Then, the solvent was removed under reduced pressure and co-evaporated twice with toluene. After dissolving in $CHCl_3$/MeOH 1:0.05 the solution was washed with 0.1 M HCl (2x) and saturated NaHCO3 and dried over Na_2SO_4. Recrystallization from $CHCl_3$ resulted in a slightly yellow crystalline solid 4-Iodobenzamide-Lys(Boc)- NH_2 (24) (110 mg, 65%).

^{1}H NMR of the 4-Iodobenzamide-Lys(Boc)- NH_2 (24) obtained in step II:

^{1}H NMR (399 MHz, $CDCl_3$) δ 7.80 (d, *J* = 8.1 Hz, 2H), 7.58 (d, *J* = 8.0 Hz, 2H), 4.58 (s, 1H), 3.41 (d, *J* = 29.8 Hz, 1H), 3.07 (p, *J* = 6.4 Hz, 2H), 1.83 (d, *J* = 51.5 Hz, 2H), 1.52 (p, *J* = 7.0 Hz, 2H), 1.42 (s, 11H). ^{13}C NMR (100 MHz, $CDCl_3$/CD_3OD) δ 174.99, 167.43, 156.84, 137.91, 133.21, 129.02, 99.02, 79.50, 53.11, 40.01, 32.08, 29.51, 28.43, 22.79. LC-MS (ESI) Rt= 5.84 min, *m/z* calcd ($C_{18}H_{26}IN_3O_4$) 475.3; found 376.1 $[MNBoc]^+$, 419.9 $[M\text{-}tBu]^+$ 475.8 $[M+H]^+$, 498.1 $[M+Na]^+$, 972.5 $[2M+Na]^+$. FT-IR (ATR): υ (cm^{-1}) = 3366, 3302, 2979, 2945, 2928, 2857, 2499, 2383, 1678, 1652, 1631, 1587, 1527, 1479, 1461, 1427, 1389, 1366, 1333, 1296, 1281, 1249, 1167, 1113, 1047, 1007, 990, 975, 880, 838, 754, 707, 673, 666, 625, 585, 474.

Step III: Synthesis of 4-Iodobenzamide-Lys(H)- NH_2 (25)

4-Iodobenzamide-Lys(Boc)- NH_2 **24** (40 mg, 0.084 mmol) was dissolved in 2 mL DCM and 2 mL of TFA was added. The solution was stirred for 2 h at room temperature under Argon. The solvent was removed under reduced pressure and co-evaporated twice with toluene. After redissolving in acetonitrile and precipitating in ether (2x) the solid was centrifuged off. Drying yielded 4-Iodobenzamide-Lys(H)- NH_2 (25) as a light yellow solid (41 mg, quant.)

^{1}H NMR of the 4-Iodobenzamide-Lys(H)-NH_2 (25) obtained in step III:

^{1}H NMR (399 MHz, CD_3OD) δ 7.85 (d, *J* = 8.1 Hz, 2H), 7.63 (d, *J* = 8.1 Hz, 2H), 4.55 (dd, *J* = 9.2, 5.2 Hz, 1H), 3.31 (s, 0H), 2.97 – 2.88 (m, 2H), 2.03 – 1.90 (m, 1H), 1.83 (dtd, *J* = 14.0, 9.2, 5.3 Hz, 1H), 1.78 – 1.62 (m, 2H), 1.52 (th, *J* = 14.6, 7.1 Hz, 2H). ^{13}C NMR (100 MHz, CD_3OD) δ 176.72, 169.43, 138.92, 134.69, 130.23, 99.49, 54.71,

49.28, 40.53, 32.51, 28.12, 24.01. LC-MS (ESI) Rt= 3.53 min, *m/z* calcd ($C_{13}H_{18}IN_3O_2$) 375.0; found 376.0 $[M+H]^+$. FT-IR (ATR): υ (cm^{-1}) = 3288, 3060, 2943, 2866, 2459, 2072, 1666, 1635, 1588, 1535, 1480, 1427, 1390, 1314, 1200, 1180, 1133, 1059, 1025, 978, 838, 799, 752, 722, 683, 667, 625, 592, 555, 517.

Step IV: Synthesis of 4-Iodobenzamide-Lys(OEG_4-TCO)-NH_2 (3)

4-Iodobenzamide-Lys(H)-NH_2 (25) (11.4 mg, 0.023 mmol) was dissolved in DMF (0.5 mL), triethylamine (10.8 µl, 0.078 mmol) and TCO-OEG_4-NHS (equatorial isomer) (14) (10.0 mg, 0.019 mmol) were added. The solution was stirred for 1 h at room temperature under Argon. The solvent was removed under reduced pressure and co-evaporated twice with toluene. Ether was added, stirred and decanted off 2x, then acetonitrile was added, stirred and decanted off 2x. Drying resulted in a slightly yellow solid 4-Iodobenzamide-Lys(OEG_4-TCO)-NH_2 (3) (12 mg, 80%).

^{1}H NMR of the 4-Iodobenzamide-Lys(OEG_4-TCO)-NH_2 (3) obtained in step IV:

^{1}H NMR (399 MHz, $CDCl_3$) δ 7.76 (d, *J* = 8.1 Hz, 2H), 7.61 (d, *J* = 8.0 Hz, 2H), 7.45 (d, *J* = 6.9 Hz, 1H), 6.81 (d, *J* = 33.1 Hz, 2H), 5.95 (s, 1H), 5.64 – 5.34 (m, 3H), 4.58 (q, *J* = 6.9 Hz, 1H), 4.40 – 4.22 (m, 1H), 3.85 – 3.43 (m, 16H), 3.39 – 3.17 (m, 4H), 2.38 (dt, *J* = 38.7, 5.3 Hz, 5H), 2.07 – 1.82 (m, 6H), 1.71 (s, 2H), 1.64 – 1.37 (m, 6H), 1.25 (s, 1H).LC-MS (ESI) Rt= 6.09 min, *m/z* calcd ($C_{33}H_{51}IN_4O_9$) 774.3; found 775.1 $[M+H]^+$, 797.3 $[M+Na]^+$.

Example 8. Synthesis of model functionalizing compound, TCO-EYFP

To show that the approach of cycloaddition modification at the surface-liquid interface of the supramolecular material is generally applicable, a TCO-conjugated fluorescent protein was reacted at the supramolecular TPE surface (Fig. 1f).

Sequence of EYFP

MVSKGEELFTGVVPILVELDGDVNGHKFSVSGEGEGDATYGKLTLKFICTTGKLP
VPWPTLVTTFGYGLQCFARYPDHMKQHDFFKSAMPEGYVQERTIFFKDDGNYK
TRAEVKFEGDTLVNRIELKGIDFKEDGNILGHKLEYNYNSHNVYIMADKQKNGI
KVNFKIRHNIEDGSVQLADHYQQNTPIGDGPVLLPDNHYLSYQSALSKDPNEKR
DHMVLLEFVTAAGITLGMDELYKKAAALELPETGGHHHHHH

Expression of EYFP protein in *E. coli*

The pET29a plasmids were transformed in *E. coli* BL21(DE3) host strain (Novagen). The bacteria were cultured in 2 L LB medium containing 100 µg/mL Kanamycin at 37°C and 180 rpm until an OD600 of ~0.7. Subsequently, protein expression was induced by

adding isopropyl-β-D-thiogalactopyranoside (IPTG) to a final concentration of 0.5 mM. Cells were incubated for 7 hours at 25˚C and 180 rpm before being harvested by centrifugation (8000 g for 10 minutes). Bacterial cells were lysed by resuspending the 5 pellet in Bugbuster Protein Extraction Reagent supplemented with benzonase (Novagen) and incubated for 1 hour at room temperature. The insoluble fraction was removed by centrifugation (40.000 g for 30 minutes). The soluble fraction was further purified by using Ni affinity chromatography. Proteins were concentrated using an Amicon Ultra centrifugal filter device (MWCO: 10 kDa) (Millipore). The purity and correct mass were confirmed by SDS-PAGE electrophoresis and LC-ESI-MS. Finally, ~4 mg per liter culture for EYFP yield was obtained. Concentrations were determined using the Nanodrop ND-1000 spectrophotometer using the reported extinction coefficient ε_{514} 83400 $M^{-1}cm^{-1}$ (*47*). Conjugation of TCO-NHS ester to EYFP TCO-OEG_4-NHS ester was reacted with EYFP in order to functionalize the protein with TCO-moieties via non-specific ligation with lysines. 1.72 µL (MW: 514, 57 Da, 0.086 mg, 3 eq) TCO-OEG_4-NHS ester was added to 100 µL 558 µM of EYFP (MW: 28952.6 Da) (1 eq) and allowed to react at 20˚C and 550 rpm in the dark for 2 hours. Afterwards, the mixture was purified using 500 µL 10,000 MWCO Amicon filters, by diluting the reaction mixture with up to 500 µL NaPi pH 7.4 buffer and spinning down at 13.4 k rpm for 5 minutes, repeated 5 times. The conjugated protein remained in the filter and was obtained by inverted spinning and analyzed using LC-ESI-MS to confirm 0-3 times conjugated protein on average. HPLC-ESI-MS analysis Purity and exact mass of the proteins were determined using a Waters Xevo G2 Quadrupole Time of Flight (Q-ToF) Liquid Chromatography – Mass Spectrometry equipped with an Agilent Polaris C18A reverse phase column (ID 2.0 mm, length 100 mm). Proteins were flowed (0.3 ml/min) over the column using a 15% to 75% water/acetonitrile gradient with 0.1% formic acid prior to analysis in positive mode in the mass spectrometer. Deconvolution of the m/z spectra was done using the MaxENT1 algorithm in the MassLynx software. Bugbuster Protein Extraction Reagent supplemented with benzonase (Novagen) and incubated for 1 hour at room temperature. The insoluble fraction was removed by centrifugation (40.000 g for 30 minutes). The soluble fraction was further purified by using Ni affinity chromatography. Proteins were concentrated using an Amicon Ultra centrifugal filter device (MWCO: 10 kDa) (Millipore). The purity and correct mass were confirmed by SDS-PAGE electrophoresis and LC-ESI-MS. Finally, ~4 mg per liter culture for EYFP yield was obtained. Concentrations were determined using the Nanodrop ND-1000 spectrophotometer using the reported extinction coefficient $_{\varepsilon 514}$ 83400 $M^{-1}cm^{-1}$ (*47*).

Conjugation of TCO-NHS ester to EYFP

TCO-OEG_4-NHS ester was reacted with EYFP in order to functionalize the protein with TCO-moieties via non-specific ligation with lysines. 1.72 µL (MW: 514, 57 Da, 0.086 mg, 3 eq) TCO-OEG_4-NHS ester was added to 100 µL 558 µM of EYFP (MW: 28952.6 Da) (1 eq) and allowed to react at 20˚C and 550 rpm in the dark for 2 hours. Afterwards, the mixture was purified using 500 µL 10,000 MWCO Amicon filters, by diluting the reaction mixture with up to 500 µL NaPi pH 7.4 buffer and spinning down at 13.4 k rpm for 5 minutes, repeated 5 times. The conjugated protein remained in the filter and was obtained by inverted spinning and analyzed using LC-ESI-MS to confirm 0-3 times conjugated protein on average.

Example 9. Preparation of surface-functionalized supramolecular material

As supramolecular base material polycaprolactone telechelically modified with UPy moieties was used (PCLdiUPy as prepared in example 2). UPy-modified tetrazine (UPy-Tz) moieties that can be incorporated into our materials were synthesized as described in example 3. Both a TCO-modified model compound (TCO-I) as well as a TCO-modified protein (TCO-EYFP) were synthesized as described in examples 7 and 8, respectively, and subsequently reacted at the surface-water interface, enabling surface functionalization. Surfaces were characterized using different techniques, including X-ray photoelectron spectroscopy (XPS), Fourier transform infrared spectroscopy (FTIR), atomic force microscopy (AFM), water contact angle measurements, surface matrix assisted laser/desorption ionization time-of-flight mass spectrometry (MALDI-TOF Ms), 3D time-of-flight secondary ion mass spectrometry (3D TOF-SIMS) and fluorescence spectroscopy.

Example 10. Presence of additive at the surface of the supramolecular material

The influence of UPy-Tz addition to PCLdiUPy dropcast films with respect to surface morphology was investigated with AFM (Fig. 1c,d). Fibrous structures were observed up to 5 mol% of UPy-Tz, whereas introduction of 10 mol% UPy-Tz showed the formation of hard domains among the fibrous structures. An increase of the UPy-Tz content to 25 mol% results in a fully covered surface with crystalline domains (Fig. 1d). The presence of fibers in the 5 mol% UPy-Tz phase image indicates the UPy-Tz is completely mixed with the PCLdiUPy (Fig. 1d), while the hard domains are proposed to be phase separated, crystalline domains of the UPy-Tz (Fig. 1d). In contrast, AFM phase images of spin coated material films show fibrous structures up to 10 mol% UPy-Tz incorporation, and phase separation at 25 mol% UPy-Tz incorporation (Fig. 11). Moreover, the fibers are both thinner and shorter in length in the spin coated samples, which is possibly explained by faster solvent drying during spin coating which reduces assembly time. On a macroscopic level, water contact angle measurements on air

dried dropcast films show an increase in hydrophobicity from 68.4±1.1° for PCLdiUPy to 84.4±1.2° for PCLdiUPy with 25 mol% UPy-Tz (Fig. 7). XPS measurements revealed fluorine intensities of 0.49 atom%, 4.07 atom% and 7.43 atom% for PCLdiUPy with 5, 10 and 25 mol% UPy-Tz, respectively. Concomitantly an increase in nitrogen intensities was detected: 4.75 atom% for PCLdiUPy, and 5.14 atom%, 8.92 atom% and 12.9 atom% for 5, 10 and 25 mol% UPy-Tz, respectively (Fig. 2ac, Fig. 5b). These results demonstrate that surfaces of the supramolecular films are gradually enriched in both fluorine and nitrogen upon addition of higher amount of UPy-Tz. In addition, also angle resolved XPS (ARXPS) measurements, with angle increments of 15° to a maximum angle of 75°, pleasingly confirmed an increase in the fluorine to carbon (F:C) ratio from 0.13 to 0.22 upon increasing resolving angle (Fig. 5c and Fig. 5d).

Since the iEDDA cycloaddition post-modification reactions are performed in aqueous solution, it was of interest to investigate the surface composition after water annealing. XPS measurements after 48 hours of water annealing showed an increase in fluorine intensity from 4.36 atom% (PCLdiUPy with 5 mol% UPy-Tz) up to 9.65 atom% (PCLdiUPy with 25 mol% UPy-Tz) as well as nitrogen from 4.82 atom% for PCLdiUPy to 16.2 atom% for PCLdiUPy with 25 mol% UPy-Tz (Fig. 5b) compared to air dried samples. We hypothesize that this enhanced stratification might favor the reaction of the TCO-moiety at the surface-water interface. Subsequent investigation of the dropcast films with FTIR revealed a gradual increase in stretch vibration around 1330 cm^{-1} upon increasing amounts of UPy-Tz incorporation, which is attributed to the typical C-F bond vibration found in the 1400 - 1100 cm^{-1} region (45), confirming the presence of UPy-Tz at the surface of the material film (Fig. 2d). In conclusion, surface analysis both on a macroscopic level as well as on the molecular level revealed UPy-Tz presence at the material surface and moreover demonstrated further enrichment after water annealing. Additionally, we showed that the UPy-Tz module is mixed into the supramolecular TPE, and that the material properties are tunable, i.e. accessibility of UPy-Tz for reaction, based on the amount that was mixed in. Therefore we propose these moieties to be perfectly suitable for selective surface functionalization of supramolecular materials.

Example 11. Selective surface modifications

The presence of the UPy-Tz at the surface of the films, suggests convenient surface modification using a TCO-modified molecule as reagent (Fig. 1b). Upon reaction of the TCO-iodine with the UPy-Tz the pink color of the tetrazine disappears instantaneously. This corresponds to a decrease in the characteristic tetrazine absorption band at 540 nm, after the 1,2-diazine click product has been formed and N2 is released (*46*), indicative for the reaction to have occurred (Fig. 8). Furthermore, after reaction with

TCO-iodine, water contact angle measurements revealed increased surface hydrophobicity upon incorporation of higher amounts of UPy-Tz with angles of 63.4±5.0° for PCLdiUPy up to 75.8±1.1° for PCLdiUPy containing 25 mol% UPy-Tz (Fig. 7).

Importantly, XPS measurements show an increase of an additional iodine peak in line with the increase in fluorine peak intensity upon the addition of higher amounts of UPy-Tz (Fig. 3a-c). The spectrum of the reference surface, i.e. pristine PCLdiUPy, shows a minor iodine signal (0.12 atom%) suggesting slight nonspecific adsorption of the TCO-iodine, which is attributed to the hydrophobic nature of the surface (Fig. 3b). Upon the incorporation of 5 and 10 mol% UPy-Tz, an increase in iodine intensity to 0.34 atom% is observed in both cases, indicative for a successful reaction at the surface. The incorporation of 25 mol% UPy-Tz shows a further increase to 0.72 atom% iodine, indicating more TCO-iodine is reacted at this materials surface. Surface MALDI-ToF MS studies were performed to directly confirm the presence of the reaction product (Fig. 3d). The mass spectrum of the control PCLdiUPy surface without TCO-iodine (Fig. 3d; black spectrum) does not show any signal, which is proposed to result from the matrix solvent (acetonitrile) to suppress polymer signals. PCLdiUPy incubated with TCO-iodine (Fig. 3d; grey spectrum) shows the TCO-iodine mass (*m/z* 798.02) and a cleaved TCO-iodine adduct which corresponds to a fragment from which CO2 is released (*m/z* 624.45). The surface of PCLdiUPy with 10 mol% UPy-Tz incorporated that was not incubated with TCO-iodine (Fig. 3d; blue spectrum) presents a few matrix peaks in the TCO region. Additionally, in the UPy-Tz region the UPy-Tz mass (*m/z* 1190.29) and the corresponding salt adducts are visible. Besides that, a UPy-Tz fragment resulting of cleavage of the urea bond next to the UPy-moiety (*m/z* 1042.59) is present as well. The surface of PCLdiUPy with 10 mol% UPy-Tz incorporated that was incubated with TCO-iodine (Fig. 3d; red spectrum) clearly presents the cycloaddition click product (*m/z* 1937.68) with the corresponding salt adducts. Moreover, the cycloaddition product where the UPy-moiety is cleaved (*m/z* 1787.52) was observed. Furthermore, two additional peaks are present that correspond to the mass of the cycloaddition product after release of CO_2 from the TCO-iodine (left peaks, cleaved UPy, *m/z* 1122.05; right peaks, intact UPy, *m/z* 1272.30), indicating that all UPy-Tz has reacted. Surface MALDI-ToF MS of PCLdiUPy with 5 and 25 mol% UPy-Tz show similar trends (Fig. 6). Accordingly, surface MALDI-ToF MS measurements revealed indisputable evidence for the successful click reaction at the surface of the supramolecular material surface.

Example 12. Surface and bulk depth profiling using 3D ToF-SIMS

To the best of our knowledge, we for the first time report on the spatial characterization of the surface and bulk composition of supramolecular polymer films, using a series of 50 subsequent surface analyses and sputter events in negative ion mode. 3D reconstruction of the 50 sputter cycles convincingly shows a gradual increase in fluorine content throughout the material film upon increasing amounts of UPy-Tz (Fig. 4a-d). For relatively low amounts of UPy-Tz (i.e. 1 and 5 mol%) the fluorine predominantly appears at the surface of the material film, whereas at high amounts (i.e. 10 and 25 mol%) the fluorine is also distributed throughout the bulk of the material. 3D reconstruction concomitantly reveals an increase in iodine content at the material surface (Fig. 4 a-d) demonstrating occurrence of the reaction at the surface. Distribution profiles of UPy-fragments (compound (b)) (*m/z* 124 and 150, respectively) and monomers of the polycaprolactone (PCL) part (compound (a)) (*m/z* 113) showed a homogeneous distribution throughout the films (Fig. 4e-h). Upon detailed total-ion-count analyses of the different conditions (1, 5, 10 and 25 mol% UPy-Tz, respectively) both at the surface and in the bulk (Fig. 4i) we observed that in all cases total ion counts of both fluorine and iodine decreased in bulk as compared to the surface. Additionally, a general trend in the increase of the fluorine and the iodine content at the surface upon higher UPy-Tz amounts was measured, whereas both UPy and PCL ion counts remain constant (Fig. 4i). Interestingly, principal component analysis (PCA) of the surface of PCLdiUPy with 1 and 5 mol% UPy-Tz, respectively, reacted with TCO-iodine showed a correlation between fluorine and iodine (+1 principal component), and between the UPy-fragments and the PCL-fragments (-1 principal component) (Fig. 13a-f).

Pleasingly 3D ToF-SIMS imaging with $C60^+$ depth profiling has provided useful and detailed insight into the chemical composition of our materials, both at the surface and in bulk. Due to the high depth resolution, this technique holds immense promise in a variety of material science developments, where control and understanding of the polymer structures is extremely important for their function. This technique now paves the way for high resolution analysis of materials in 3D and thereby allows for specific molecular design in order to meet material requirements for a variety of applications.

Example 13. Conjugation of proteins

Post-modification of our supramolecular material surfaces with more complex molecules, such as proteins, demonstrates the generality of our approach. Therefore, we investigated the cycloaddition click reaction of enhanced yellow fluorescent protein (EYFP) to UPy-Tz by fluorescence spectroscopy (Fig. 10). EYFP was non-specifically functionalized with TCO-moieties (TCO-EYFP, Fig. 9). Incorporation of 1 and 5 mol% UPy-Tz showed a 9 times increase in surface fluorescence after TCO-EYFP

incubation, whereas for both 10 and 25 mol% UPy-Tz 4 times and 2 times increase, respectively, was observed. This moderate increase for larger mol% of UPy-Tz can be explained by differences in morphology of the different mixtures, i.e. the occurrence of phase separated domains at the surface (Fig. 2a-d). It is proposed that in these cases tetrazine moieties are less available for reaction. An additional explanation might be that a higher amount of protein is reacted on the PCLdiUPy with 10 and 25 mol% UPy-Tz surfaces, thereby inducing quenching of the fluorophores. Surfaces incubated with non-functionalized EYFP did not show any fluorescence indicating the EYFP is washed off. In conclusion, these protein conjugation experiments show the versatility of our strategy towards more complex surface modifications.

Example 14. Atomic Force Microscopy on supramolecular materials with UPy-Tz additives incorporated that comprise oligo(ethylene glycol) spacers of different lengths.

The influence of the incorporation of the different additives on the surface morphology of the dropcast films was investigated with AFM. Via a modular approach, additives are mixed into the supramolecular polymer material, based on PCLdiUPy (1, Figure 1b). Four different additives are investigated, a UPy-Tz additive without an oligo(ethylene glycol) (OEG) spacer, UPy-OEG_0-Tz (Figure 16a), with a OEG-spacer of 6 repeating units, UPt-OEG_6-Tz (2, Figure 1b) and with 12 repeating units, UPy-OEG_{12}-Tz (Figure 16b). Additionally, an additive without a UPy-moiety and without an OEG-spacer is investigated, C5-Tz (Figure 16c). All additives were used in concentrations of 1, 5 and 10 mol%.

Fibrous structures were observed for the pristine PCLdiUPy surfaces and showed that incorporation of the UPy-OEG_0-Tz shows fibrous structures up to 5 mol% incorporation, indicative for complete mixing with the PCLdiUPy, whereas the introduction of 10 mol% showed the formation of phase separated, hard domains to a limited extent. The incorporation of UPy-OEG_6-Tz shows fiber morphology for 1 and 5 mol% and small phase separated domains for the 10 mol% surface. For the UPy-OEG_{12}-Tz, which is equipped with a larger OEG-spacer, the onset of crystalline domain formation was found to start at 5 mol% incorporation and was further increased at 10 mol%, whereas the 1 mol% shows fibrous structures. The incorporation of C5-Tz, which lacks the UPy-motif, showed complete phase separation at the material surface in all cases, for 1, 5 and 10 mol%, indicative for complete demixing.

These results demonstrate that the presence of the UPy-motif facilitates incorporation into the PCLdiUPy polymer material. Moreover, based on the length of the OEG-spacer

the onset of phase separation and crystalline domain formation is different, i.e. the longer the OEG-spacer, the earlier the phase separation behavior starts.

Example 15. Preparation of a supramolecular material that is postmodified at the surface with various poly(ethylene glycol) molecules.

The introduction of anti-fouling functionality at the surface of supramolecular materials via the selective modification of a reactive UPy-modified tetrazine (UPy-Tz) additive (Figure 1b, 2) is in examples 17-19. The supramolecular material used in examples 17-19 is prepared by incorporation of UPy-Tz (Figure 1b, 2) as compound (b) in a supramolecular material based on telechelically UPy-modified polycaprolactone (PCLdiUPy) as compound (a) (Figure 1b, 1). Examples 17-19 show that the UPy-Tz model compound (b) provides a handle for selective surface post-modification via an inverse electron demand Diels-Alder cycloaddition. Three different poly(ethylene glycol) (PEG) polymers modified with bicyclononyne (BCN) moieties, mono-functional-PEG-BCN (Figure 17a), bi-functional-PEG-BCN (Figure 17b) and star-PEG-BCN (Figure 17c), respectively, were synthesized and introduced to facilitate the anti-fouling function.

Solutions of PCLdiUPy were prepared at a concentration of 20 mg/mL in 1,1,1,3,3,3-Hexafluoroisopropanol (HFIP). For the mixtures, 5 mol% UPy-Tz solutions were prepared by adding 10 mol% UPy-Tz solutions were prepared by adding 10 mol% UPy-Tz to 90 mol% PCLdiUPy solutions. PEG solutions were prepared at different concentrations in ultrapure water, obtained using a Milli-Q Advantage A-10 equipped with a Q-Guard T2 purification pack.

Spin coated samples were prepared by spin coating 50 µL of a solution of 20 mg/mL PCLdiUPy or PCLdiUPy with 10 mol% UPy-Tz at 3000 rpm for 30 seconds on glass coverslips (Ø 12mm, thickness 1 mm) or gold-coated sensors (BiolinScientific AB). Samples conjugated with a BCN functionalized PEG polymer were prepared by incubating spin coated samples with 0.5 or 0.1 mg/mL PEG solution for 90 minutes at room temperature. The samples were washed for 10 minutes in Milli-Q water and dried with air before continuing experiments.

Example 16. Protein adsorption on poly(ethylene glycol) modified surfaces using QCM-D measurements.

QCM-D measurements were performed to quantify the amount of proteins adsorbed onto the supramolecular surfaces under physiologically relevant conditions. The Vroman series was applied on the different surfaces, PCLdiUPy and PCLdiUPy with 10 mol% UPy-Tz, that were modified with either mono-functional-PEG-BCN, bi-functional-PEG-BCN or star-PEG-BCN. Both the change in frequency (Δf) and dissipation (ΔD) were monitored over time. After equilibration of the signal, the protein mixture was applied and after 30 minutes the surfaces were rinsed to remove all non-adsorbed proteins.

QCM-D measurements were performed on the Q-Sense E4 instrument (BiolinScientific) using gold-coated AT-cut quartz discs with a fundamental frequency of 4.95 MHZ (QSX 301 Gold, BiolinScientific AB). Before use, sensors were rinsed with piranha solution and subsequently heated for 15 minutes at 70˚C in a 4:1:1 mixture of ultrapure water, ammonia and 30% hydrogen peroxide (base piranha). Subsequently, sensors were rinsed with water and acetone and dried with nitrogen gas. Clean crystals were mounted to record their fundamental frequency in air and subsequently removed for spin coating. All experiments were performed at 37 °C. After equilibration, the frequency and dissipation of the sensors were measured in air for 1 minute. After mounting the sensors with the spincoated material, sensors were again measured in air for 1 minute. The frequency and dissipation changes of the sensor before spincoating and after spincoating were stitched and Sauerbrey was applied to the stitched data to determine the layer thickness. After mounting the PEG-BCN to the sensor surfaces, PBS was passed over the surface at 0.1 mL/min until the signal equilibrated. Subsequently, the protein solution was passed over the surface at 0.1 mL/min. Frequency and dissipation changes were recorded for 30 minutes, and the sensors were rinsed with PBS. Each experiment was repeated in two-fold, and means and standard errors of the mean are reported. After each experiment, the system was cleaned by rinsing with PBS for 10 minutes, followed by 50 mL a 2 wt% solution of Hellmanex III (Hellma) in ultrapure water, followed by rinsing with ultrapure water for 10 minutes. Next, the sensors were removed and the components were dried using nitrogen.

Shifts in frequency and dissipation for overtones 3, 5, 7, 9 and 11 were analyzed using the Voigt-Voinova model and the QTools software (Q-sense). As became evident from the measurements, the viscosity of the protein solutions was higher than the viscosity of PBS. Therefore, the viscosity of the protein solution was accounted in the model by the use of a 1 layer (L1) viscoelastic model with a viscosity of 0.001 Pa s and a fluid density of 1100 kg/m^3. The protein layer density was set to 1145 kg/m^3 for all protein

layers as found in literature. The minimum and maximum estimate for the fitted parameters of L1 viscosity, L1 shear and L1 thickness were set between 0.0001-0.1, 1000 – 1E8 and 1E-11 – 1E-7 respectively. A 2nd order polynomial model was used to estimate the standard deviation. The data was fitted by using a descending incremental fitting mode with a first row to fit grid mode. The model was optimized by decreasing $\chi 2$ by tuning the selection of overtones.

It was hypothesized that the PCLdiUPy surfaces show the largest Δf, indicative for a higher mass adsorption. Concomitantly, the increase in molecular mass of the PEG polymers and the additional BCN moieties that are available for surface reaction of the mono-functional-PEG-BCN, bi-functional-PEG-BCN and star-PEG-BCN, respectively, are envisioned to increase the anti-fouling properties of the surface alongside. Upon mono-functional-PEG-BCN modification, the remaining frequency and dissipation shifts for the PCLdiUPy surface are larger than for the PCLdiUPy with UPy-Tz surfaces (-65 Hz, $5 \cdot 10^{-6}$ and -30 Hz and $2 \cdot 10^{-6}$, respectively), which indicates a reduction in mass adsorption at the surfaces that were covalently modified with mono-functional-PEG-BCN (Figure 18a). For the bi-functional-PEG-BCN a similar trend is observed for the frequency and dissipation values for the PCLdiUPy and PCLdiUPy with UPy-Tz surfaces (-55 Hz, $4 \cdot 10^{-6}$ and -35 Hz and $5 \cdot 10^{-6}$, respectively) (Figure 18b). The dissipation shifts at the modified surfaces are higher compared to the mono-functional-PEG-BCN functionalized surfaces. This might be explained by a different packing of the PEG-BCN polymer coating at the surfaces. The higher dissipation values at the bi-functional-PEG-BCN surfaces indicate a more visco-elastic layer is formed. The results of star-PEG-BCN functionalization are depicted in Figure 18c. Both the frequency and dissipation shifts of the PCLdiUPy surfaces are larger than the PCLdiUPy with UPy-Tz surfaces (-45 Hz, $7 \cdot 10^{-6}$ and -15 Hz and $2 \cdot 10^{-6}$, respectively), which indicates that the star-PEG-BCN coating successfully decreases protein adsorption. Since the dissipation values for all the different experiments are >5-10% of the Δf, a Voigt-Voinova visco-elastic model was applied to analyze the datasets. A summary of all the results is depicted, which shows the areal mass adsorption (ng/cm^2) for the different surfaces (Figure 18d). No significant differences were observed for the PCLdiUPy surfaces that were incubated with the different PEG-BCN polymers. Upon the incorporation of 10 mol% UPy-Tz, a significant reduction in protein adsorption can be appreciated. In addition, the protein adsorption gradually decreases for the mono-functional-PEG-BCN, bi-functional-PEG-BCN and star-PEG-BCN polymers, respectively.

Example 17. Culturing of HK-2 cells on spin coated surfaces comprising different poly(ethylene glycol) molecules.

Transwell inserts were sterilized in 70% ethanol bath and placed in a LAF-cabinet to evaporate the ethanol from the inserts. Spincoated coverslips were placed in the bottom ring of the transwells using sterile forceps. The top of the insert was placed on top of the bottom ring and transferred to a 12-wells plate. The coverslips were sterilized under UV for 30 minutes. Cells were trypsinized and cell concentration was determined via cell counting in a hemocytometer. The cells were diluted untill a concentration of 60.000 cells·mL-1 and 500 µL of cell suspension was added to each transwell insert. Cells were cultured for 24 h, 72 h or one week at 37°C and 5% CO2 in a humidified atmosphere in complete medium (DMEM with 10 v% FBS and 1 v% pencillin-streptomycin solution). Cell medium was changed ones for the 72 h culture and twice for the 1-week culture.

In order to investigate the development of these coatings in time, cell morphology and spreading were studied by fluorescence microscopy graphs of HK-2 cells on spincoated surfaces after 7 days of culture. Surfaces of pristine PCLdiUPy and PCLdiUPy with 10 mol% UPy-Tz were both incubated with either mono-functional-PEG-BCN, bi-functional-PEG-BCN or star-PEG-BCN as compound (c). The actin skeleton was stained with Phalloidin, the nuclei were stained with DAPI. Magnification is 10x and sale bars represent 200 µm before fluorescence microscopy. The pristine PCLdiUPy and PCLdiUPy with UPy-Tz surfaces with no surface-modification (i.e. not incubated with a compound (c)) show a confluent layer at the material surface. For both mono-functional-PEG-BCN and bi-functional-PEG-BCN incubation on the pristine PCLdiUPy surfaces, the cell adhesion and morphology were not affected. However, the star-PEG-BCN incubation on the pristine PCLdiUPy surface shows a reduction in cell adhesion, which suggests the star-PEG-BCN non-specifically interacts with the PCLdiUPy surface. In contrast to the 24h culture period, the mono-functional-PEG-BCN functionalization of the PCLdiUPy with UPy-Tz surface shows a reduction in cell adhesion and spreading at the surface, however no complete anti-fouling effect was observed. The bi-functional-PEG-BCN and star-PEG-BCN modified PCLdiUPy with UPy-Tz surfaces, show complete prevention of cell attachment 7 days after cell seeding, demonstrating the effective introduction of an anti-fouling coating. The covalent functionalization of the supramolecular surfaces via a post-modification reaction demonstrates an elegant approach to introduce a highly effective anti-fouling coating at the material surface, as was demonstrated here.

Example 18. Culturing of HK-2 cells in a competition assay.

Transwell inserts were sterilized in 70% ethanol bath and placed in a LAF-cabinet to evaporate the ethanol from the inserts. Spincoated coverslips were placed in the bottom ring of the transwells using sterile forceps. The top of the insert was placed on top of the bottom ring and transferred to a 12-wells plate. The coverslips were sterilized under UV for 30 minutes. PEG-BCN powder was diluted in complete medium until a concentration of 0.5 mg·mL-1. Cells were trypsinized and cell concentration was determined via cell counting in a hemocytometer. The cells were diluted till a concentration of 60.000 cells/mL. The cells were divided in four 15 mL falcon tubes and centrifuged at 1000 rpm for 5 minutes. The supernatant was aspirated and the cell pellet was resuspended in PEG-BCN solutions in complete medium. 500 µL of cell suspension was added to each transwell insert and cells were cultured for 24 h or 72 h at 37°C and 5% CO2 in a humidified atmosphere. Cell medium was changed ones for the 72 h culture.

Surfaces of pristine PCLdiUPy and PCLdiUPy with 10 mol% UPy-Tz were both incubated with either mono-functional-PEG-BCN, bi-functional-PEG-BCN or star-PEG-BCN as compound (c). The actin skeleton is stained with Phalloidin, the nuclei are stained with DAPI and the focal adhesions were stained with Atto-555. The PCLdiUPy with UPy-Tz surfaces with mono-functional-PEG-BCN, bi-functional-PEG-BCN or star-PEG-BCN present in the culture medium with the cells were hypothesized to display anti-fouling properties due to the effective click reaction between the reactive UPy-Tz additive and the BCN-functionality on the PEG polymers, which was reported to be performed in complex medium and living systems. For PCLdiUPy with UPy-Tz surfaces incubated with mono-functional-PEG-BCN present in the culture medium with the cells, a reduction of cell attachment was observed, hence the surface did not display complete anti-fouling behavior. For the PCLdiUPy with UPy-Tz surfaces that were incubated with bi-functional-PEG-BCN or star-PEG-BCN present in the culture medium with the cells, no cells were observed, indicating that the surfaces were completely anti-fouling and thereby prevent cell adhesion. In conclusion, the presence of the bi-functional-PEG-BCN and the star-PEG-BCN in the culture medium with the cells could completely reduce cell adhesion at the PCLdiUPy with UPy-Tz surfaces, which demonstrate the high efficiency of the reaction between the UPy-Tz and the BCN-modified PEG polymers, even in the presence of complex medium and cells.

Example 19. Decoupling processing and functionalization of electrospun supramolecular polymer materials.

Preparation of the electrospun samples. Two different electrospinning solutions were prepared in glass vials. 20 wt/wt% PCLdiUPy was dissolved in 80 wt/wt% 1,1,1,3,3,3-hexafluoro-2-propanol (HFIP, 147545000, Acros) as a control sample. The solution containing the 5 mol% UPy-Tz for post-modification was composed of 17.5 wt/wt% PCLdiUPy in 82.5 wt/wt% HFIP and 5 mol% UPy-Tz. The solutions were stirred overnight at room temperature and then transferred into separate 2.5 mL glass syringes (Hamilton). Approximately 1 mL of the solution was fed at 0.02 mL/min using a syringe pump (KR analytical) at the outside of the electrospinning cabinet via 35 cm long 1 mm I.D. PTFE tube connected to a flat-tip stainless-steel 23 g needle (Intertronics, United Kingdom). Inside the cabinet, the solution was spun with an in-house built electrospin setup by applying 18.5 kV with a collector distance of 12 cm. Fibers were collected on a 12 x 12 cm grounded collector plate. To enable facile removal of the non-woven electrospun membrane, the collector plate was covered with a thin sheet of polyethylene (PE) film. Round 12 mm Ø cover glasses were placed to collect the fibers. Short electrospinning times of around 1 minute were applied in order to allow electrospinning of a thin layer. The electrospun samples were dried overnight in vacuo at room temperature to remove any residual solvent.

Environmental scanning electron microscopy (ESEM). Environmental scanning electron microscopy (ESEM) imaging was performed using FEI Quanta 600 and Xt Microscope Control software. The fiber samples on the round cover glasses were mounted with fiber side up to a metal stub by using double sided carbon tape. The samples were visualized under low vacuum with an accelerating voltage of 10 kV, a spot size of 4 and a working distance of 10 mm. Images were recorded at a resolution of 2048 x 1768, a dwell time of 10 µs and magnifications between 1000 and 10,000 times. Both backscattering electrons (BSEs) and secondary electrons (SEs) were detected. The fiber diameters were determined from multiple high magnification images using ImageJ software and expressed as average ± standard deviation. Scanning electron microscopy images shows fiber formation for both the PCLdiUPy with 5 mol% UPy-Tz and the PCLdiUPy with fiber diameters of 0.6 ± 0.24 µm and 0.8 ± 0.36 µm, respectively.

Confocal laser scanning microscopy (CLSM). Electrospun samples that were reacted with either the TCO-Cy5 dye or the TCO-EYFP model protein, were mounted between a microscope glass slide and a cover glass using Mowiol. The samples were analyzed with a confocal laser scanning microscope (CLSM), Zeiss LSM510 META NLO and ZEN software. The TCO-Cy5 samples were excited with a Helium-Neon laser at 633 nm, 5% laser power and fluorescence was collected via HFT 488/543/633 mai

dichroics, NFT 545 secondary dichroics and BP 650-710 IR filter. A Plan-Apochromat 63x/1.4 Oil objective was used with 1 AU (132 µm) pinhole. Images were recorded with a master gain of 719, 1024 x 1024 resolution, line average of 8, pixel dwell of 51.2 µs and zoom up to 4.5 times. The TCO-EYFP samples were excited with an Argon laser at 488 nm, 5% laser power and fluorescence was collected via HFT 488/543 main dichroics, NFT 490 secondary dichroics and BP 500-530 IR filter. A Plan-Apochromat 63x/1.4 Oil objective was used with 1 AU (94 µm) pinhole. Images were recorded with a master gain of 808, 1024 x 1024 resolution, line average of 8, pixel dwell of 51.2 µs and zoom up to 2 times.

Electrospun meshes of PCLdiUPy with 5 mol% UPy-Tz were prepared, and PCLdiUPy as control. After electrospinning the materials were incubated with either a TCO-conjugated Cy5 dye or a TCO-EYFP protein. Scanning electron microscopy images shows fiber formation for both the PCLdiUPy with 5 mol% UPy-Tz and the PCLdiUPy with fiber diameters of 0.6 ± 0.24 µm and 0.8 ± 0.36 µm, respectively. Functionalization with the TCO-Cy5 dye showed clear red appearance of the fibers for the PCLdiUPy with 5 mol% UPy-Tz materials whereas the PCLdiUPy materials did not show any fluorescence. A similar trend was observed after incubation with the TCO-EYFP, the PCLdiUPy with 5 mol% UPy-Tz showed green fiber morphology while the PCLdiUPy materials did not yield any fluorescence. This approach shows decoupling of the material processing conditions and subsequent material functionalization via a post-modification approach.

REFERENCES

1. J.-M. Lehn, Supramolecular polymer chemistry—scope and perspectives. *Polym. Int.* **51**, 825–839 (2002).

2. G. M. Whitesides, B. Grzybowski, Self-assembly at all scales. *Science*. **295**, 2418–2421 (2002).

3. R. J. Epstein, *Human Molecular Biology: An Introduction to the Molecular Basis of Health and Disease* (Cambridge University Press, 2003).

4. T. Aida, E. W. Meijer, S. I. Stupp, Functional supramolecular polymers. *Science*. **335**, 813– 817 (2012).

5. B. J. B. Folmer, R. P. Sijbesma, R. M. Versteegen, J. a. J. van der Rijt, E. W. Meijer, Supramolecular Polymer Materials: Chain Extension of Telechelic Polymers Using a Reactive Hydrogen-Bonding Synthon. *Adv. Mater.* **12**, 874–878 (2000).

6. A. W. Bosman, R. P. Sijbesma, E. W. Meijer, Supramolecular polymers at work. *Mater. Today*. **7**, 34–39 (2004).

7. K. Rajangam *et al.*, Heparin binding nanostructures to promote growth of blood vessels. *Nano Lett.* **6**, 2086–2090 (2006).

8. V. M. Tysseling-Mattiace *et al.*, Self-assembling nanofibers inhibit glial scar formation and promote axon elongation after spinal cord injury. *J. Neurosci. Off. J. Soc. Neurosci.* **28**, 3814–3823 (2008).

9. Y. Bae, S. Fukushima, A. Harada, K. Kataoka, Design of Environment-Sensitive Supramolecular Assemblies for Intracellular Drug Delivery: Polymeric Micelles that are Responsive to Intracellular pH Change. *Angew. Chem. Int. Ed.* **42**, 4640–4643 (2003).

10. P. Cordier, F. Tournilhac, C. Soulié-Ziakovic, L. Leibler, Self-healing and thermoreversible rubber from supramolecular assembly. *Nature*. **451**, 977–980 (2008).

11. M. Burnworth *et al.*, Optically healable supramolecular polymers. *Nature*. **472**, 334–337 (2011).

12. Q. Wei *et al.*, Supramolecular Polymers as Surface Coatings: Rapid Fabrication of Healable Superhydrophobic and Slippery Surfaces. *Adv. Mater.* **26**, 7358–7364 (2014).

13. J. P. Hill *et al.*, Self-assembled hexa-peri-hexabenzocoronene graphitic nanotube. *Science*. **304**, 1481–1483 (2004).

14. L. N. Lucas, J. J. D. de Jong, J. H. van Esch, R. M. Kellogg, B. L. Feringa, Syntheses of Dithienylcyclopentene Optical Molecular Switches. *Eur. J. Org. Chem.* **2003**, 155–166 (2003).

15. R. Abbel *et al.*, White-Light Emitting Hydrogen-Bonded Supramolecular Copolymers Based on π-Conjugated Oligomers. *J. Am. Chem. Soc.* **131**, 833–843 (2009).

16. L. Albertazzi *et al.*, Spatiotemporal control and superselectivity in supramolecular polymers using multivalency. *Proc. Natl. Acad. Sci.* **110**, 12203–12208 (2013).

17. J. D. Hartgerink, E. Beniash, S. I. Stupp, Self-assembly and mineralization of peptideamphiphile nanofibers. *Science*. **294**, 1684–1688 (2001).

18. J. D. Hartgerink, E. Beniash, S. I. Stupp, Peptide-amphiphile nanofibers: A versatile scaffold for the preparation of self-assembling materials. *Proc. Natl. Acad. Sci.* **99**, 5133– 5138 (2002).

19. A. R. Hirst *et al.*, Biocatalytic induction of supramolecular order. *Nat. Chem.* **2**, 1089–1094 (2010).

20. E. Wisse, L. E. Govaert, H. E. H. Meijer, E. W. Meijer, Unusual Tuning of Mechanical Properties of Thermoplastic Elastomers Using Supramolecular Fillers. *Macromolecules*. **39**, 7425–7432 (2006).

21. R. P. Sijbesma *et al.*, Reversible polymers formed from self-complementary monomers using quadruple hydrogen bonding. *Science*. **278**, 1601–1604 (1997).

22. F. H. Beijer, R. P. Sijbesma, H. Kooijman, A. L. Spek, E. W. Meijer, Strong Dimerization of Ureidopyrimidones via Quadruple Hydrogen Bonding. *J. Am. Chem. Soc.* **120**, 6761– 6769 (1998).

23. R. E. Kieltyka *et al.*, Mesoscale Modulation of Supramolecular Ureidopyrimidinone-Based Poly(ethylene glycol) Transient Networks in Water. *J. Am. Chem. Soc.* **135**, 11159–11164 (2013).

24. P. Y. W. Dankers, M. C. Harmsen, L. A. Brouwer, M. J. A. Van Luyn, E. W. Meijer, A modular and supramolecular approach to bioactive scaffolds for tissue engineering. *Nat. Mater.* **4**, 568–574 (2005).

25. E. Wisse *et al.*, Multicomponent supramolecular thermoplastic elastomer with peptidemodified nanofibers. *J. Polym. Sci. Part Polym. Chem.* **49**, 1764–1771 (2011).

26. G. C. van Almen *et al.*, Development of Non-Cell Adhesive Vascular Grafts Using Supramolecular Building Blocks. *Macromol. Biosci.* (2015), doi:10.1002/mabi.201500278.

27. B. B. Mollet *et al.*, A modular approach to easily processable supramolecular bilayered scaffolds with tailorable properties. *J. Mater. Chem. B.* **2**, 2483–2493 (2014).

28. D. E. P. Muylaert *et al.*, Early in-situ cellularization of a supramolecular vascular graft is modified by synthetic stromal cell-derived factor-1α derived peptides. *Biomaterials*. **76**, 187–195 (2016).

29. Z. P. Tolstyka *et al.*, Chemoselective Immobilization of Proteins by Microcontact Printing and Bioorthogonal Click Reactions. *Chembiochem Eur. J. Chem. Biol.* **14**, 2464–2471 (2013).

30. J. Zheng, K. Liu, D. H. Reneker, M. L. Becker, Post-Assembly Derivatization of Electrospun Nanofibers via Strain-Promoted Azide Alkyne Cycloaddition. *J. Am. Chem. Soc.* **134**, 17274–17277 (2012).

31. P. M. Imbesi, C. Fidge, J. E. Raymond, S. I. Cauët, K. L. Wooley, Model Diels–Alder Studies for the Creation of Amphiphilic Cross-Linked Networks as Healable, Antibiofouling Coatings. *ACS Macro Lett.* **1**, 473–477 (2012).

32. T. N. Gevrek, T. Bilgic, H.-A. Klok, A. Sanyal, Maleimide-Functionalized Thiol Reactive Copolymer Brushes: Fabrication and Post-Polymerization Modification. *Macromolecules*. **47**, 7842–7851 (2014).

33. R. Huisgen, Kinetics and Mechanism of 1,3-Dipolar Cycloadditions. *Angew. Chem. Int. Ed. Engl.* **2**, 633–645 (1963).

34. R. Huisgen, 1,3-Dipolar Cycloadditions. Past and Future. *Angew. Chem. Int. Ed. Engl.* **2**, 565–598 (1963).

35. H. C. Kolb, M. G. Finn, K. B. Sharpless, Click Chemistry: Diverse Chemical Function from a Few Good Reactions. *Angew. Chem. Int. Ed.* **40**, 2004–2021 (2001).

36. R. Rossin, S. M. J. van Duijnhoven, T. Läppchen, S. M. van den Bosch, M. S. Robillard, Trans-Cyclooctene Tag with Improved Properties for Tumor Pretargeting with the Diels– Alder Reaction. *Mol. Pharm.* **11**, 3090–3096 (2014).

37. M. L. Blackman, M. Royzen, J. M. Fox, Tetrazine Ligation: Fast Bioconjugation Based on Inverse-Electron-Demand Diels−Alder Reactivity. *J. Am. Chem. Soc.* **130**, 13518–13519 (2008).

38. F. Thalhammer, U. Wallfahrer, J. Sauer, Reaktivität einfacher offenkettiger und cyclischer dienophile bei Diels-Alder-reaktionen mit inversem elektronenbedarf. *Tetrahedron Lett.* **31**, 6851–6854 (1990).

39. M. T. Taylor, M. L. Blackman, O. Dmitrenko, J. M. Fox, Design and Synthesis of Highly Reactive Dienophiles for the Tetrazine–trans-Cyclooctene Ligation. *J. Am. Chem. Soc.* **133**, 9646–9649 (2011).

40. F. Yang *et al.*, Nanodomain analysis with cluster-SIMS: application to the characterization of macromolecular brush architecture. *Surf. Interface Anal.* **47**, 1051–1055 (2015).

41. M. Taylor *et al.*, 3D chemical characterization of frozen hydrated hydrogels using ToFSIMS with argon cluster sputter depth profiling. *Biointerphases*. **11**, 02A301 (2016).

42. J. Bailey *et al.*, 3D ToF-SIMS Imaging of Polymer Multilayer Films Using Argon Cluster Sputter Depth Profiling. *ACS Appl. Mater. Interfaces*. **7**, 2654–2659 (2015).

43. T. K. Claus *et al.*, Simultaneous Dual Encoding of Three-Dimensional Structures by Light- Induced Modular Ligation. *Angew. Chem. Int. Ed.* **55**, 3817–3822 (2016).

44. H. Kautz, D. J. M. van Beek, R. P. Sijbesma, E. W. Meijer, Cooperative End-to-End and Lateral Hydrogen-Bonding Motifs in Supramolecular Thermoplastic Elastomers. *Macromolecules*. **39**, 4265–4267 (2006).

45. G. Socrates, *Infrared and Raman Characteristic Group Frequencies: Tables and Charts* (John Wiley & Sons, 2004).

46. W. Chen, D. Wang, C. Dai, D. Hamelberg, B. Wang, Clicking 1,2,4,5-tetrazine and cyclooctynes with tunable reaction rates. *Chem. Commun.* **48**, 1736–1738 (2012).

47. R. H. Newman, M. D. Fosbrink, J. Zhang, Genetically Encodable Fluorescent Biosensors for Tracking Signaling Dynamics in Living Cells. *Chem. Rev.* **111**, 3614–3666 (2011).

48. I. de Feijter *et al.*, Solid-Phase-Based Synthesis of Ureidopyrimidinone–Peptide Conjugates- for Supramolecular Biomaterials. *Synlett*. **26**, 2707–2713 (2015).

49. Somorjai, G. A. & Li, Y. Impact of surface chemistry. *Proc. Natl. Acad. Sci.* **108,** 917–924 (2011).

50. Hasan, A. *et al.* Recent Advances in Application of Biosensors in Tissue Engineering. *BioMed Res. Int.* **2014,** e307519 (2014).

51. Camarero, J. A. Recent developments in the site-specific immobilization of proteins onto solid supports. *Pept. Sci.* **90,** 450–458 (2008).

52. Kuzmin, A., Poloukhtine, A., Wolfert, M. A. & Popik, V. V. Surface Functionalization Using Catalyst-Free Azide−Alkyne Cycloaddition. *Bioconjug. Chem.* **21,** 2076–2085 (2010).

53. Devaraj, N. K., Weissleder, R. & Hilderbrand, S. A. Tetrazine-Based Cycloadditions: Application to Pretargeted Live Cell Imaging. *Bioconjug. Chem.* **19,** 2297–2299 (2008).

54. Devaraj, N. K. & Weissleder, R. Biomedical Applications of Tetrazine Cycloadditions. *Acc. Chem. Res.* **44,** 816–827 (2011).

55. Selvaraj, R. & Fox, J. M. trans-Cyclooctene — a stable, voracious dienophile for bioorthogonal labeling. *Curr. Opin. Chem. Biol.* **17,** 753–760 (2013).

56. Agard, N. J., Prescher, J. A. & Bertozzi, C. R. A Strain-Promoted [3 + 2] Azide−Alkyne Cycloaddition for Covalent Modification of Biomolecules in Living Systems. *J. Am. Chem. Soc.* **126,** 15046–15047 (2004).

CLAIMS

1. A supramolecular material comprising compound (a) and compound (b), wherein
   - compound (a) comprises at least two supramolecular subunits S(a) linked by a linker L(a) comprising a polymer P(a), and
   - compound (b) comprises a supramolecular subunit S(b) and a first orthogonal reaction partner O1 capable of forming a covalent bond to a second orthogonal reaction partner O2.

2. A supramolecular material according to claim 1, wherein O1 is is capable of forming a covalent bond with a second reaction partner O2 by a reaction selected from the group consisting of:
   - Copper(I)-Catalyzed Azide-Alkyne Cycloaddition (CuAAC);
   - Strain-promoted Azide-Alkyne Cycloaddition (SPAAC);
   - Strain-promoted Alkyne-Nitrone Cycloaddition (SPANC);
   - Staudinger ligation;
   - Native chemical ligation; and
   - Oxime ligation.

3. A supramolecular material according to any of claims 1 and 2, wherein O1 is capable of forming a covalent bond with O2 by an inverse electron demand Diels-Alder (iEDDA) cycloaddition reaction.

4. A supramolecular material according to any of the preceding claims, wherein O1 is selected from the group consisting of *trans*-cycloalkenes, azides, tetrazines and tetrazoles.

5. A supramolecular material according to any of the preceding claims, wherein O1 is a tetrazine.

6. A supramolecular material according to any of the preceding claims, wherein O1 and O2 are bio-orthogonal reaction partners.

7. A supramolecular material according to any of the preceding claims, wherein S(a) and S(b) are capable of forming at least 4 hydrogen bridges and have the general formula selected from the group consisting of (1') and (2'):

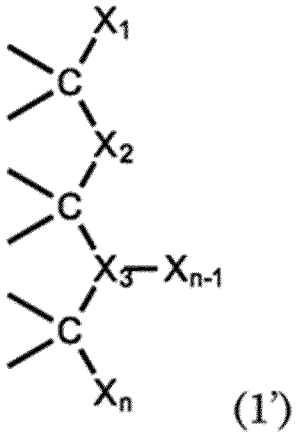

(1')

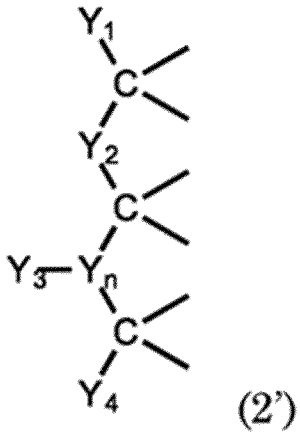

(2')

wherein,

- C-X_i and C-Y_i linkages are independently a single or a double bond,
- n is 4 or more, and
- X_i is a hydrogen bridge donor or acceptor capable of forming a hydrogen bridge with the corresponding hydrogen bridge donor or acceptor, Y_i, present in another supramolecular subunit.

8. A supramolecular material according to any of the preceding claims, wherein S(a) and S(b) are capable of forming 4 hydrogen bridges and have a formula selected from the group consisting of:

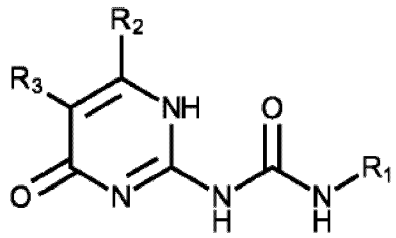

(3)

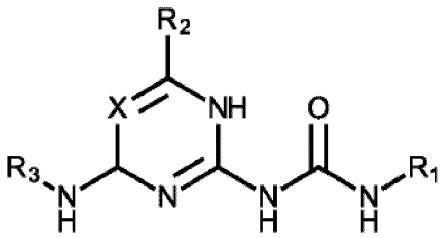

(4)

wherein

- R1 is a direct bond connecting the supramolecular subunit to the remainder of compound (a) or compound (b),
- R2, R3 and R4 are independently selected from the group consisting of hydrogen, C1-24 alkyl, C6-12 aryl, C1-24 alkyl ether; and
- X in formula (4) is a nitrogen atom or a carbon atom with attached R4-group.

9. A supramolecular material according to any of the preceding claims, wherein compound (b) has a formula selected from the group consisting of S(b)-O1 and S(b)-L(b)-O1, wherein L(b) is a linker.

10. A supramolecular material according to claim 9, wherein linker L(b) comprises at least one aliphatic subunit and/or a polymer P(b).

11. A supramolecular material according to claim 10, wherein the at least one aliphatic subunit is at least two aliphatic subunits, such as, at least three aliphatic subunits.

12. A supramolecular material according to any of claims 9-11, wherein linker L(b) further comprises at least one hydrogen bonding group.

13. A supramolecular material according to claim 12, wherein linker L(b) comprises at least two aliphatic subunits and the at least one hydrogen bonding group is positioned between two of the at least two aliphatic subunits.

14. A supramolecular material according to any of claims 10-13, wherein P(b) is a hydrophilic polymer.

15. A supramolecular material according to any of claims 10-14, wherein P(b) is a polyether or a polyester.

16. A supramolecular material according to any of claims 10-15, wherein P(b) is an oligoethylene glycol (OEG) or a polyethylene glycol (PEG).

17. A supramolecular material according to any of claims 10-16, wherein P(b) comprises from about 1 to about 20 repeating units, such as from about 1 to about 11, from about 2 to about 10, from about 3 to about 9, from about 4 to about 8, from about 5 to about 7, such as 6 repeating units.

18. A supramolecular material according to any of the preceding claims, wherein compound (a) comprises two supramolecular subunits and has the formula S(a)-L(a)-S(a), wherein L(a) is a linker comprising polymer P(a).

19. A supramolecular material according to any of the preceding claims, wherein linker L(a) further comprises at least one aliphatic subunit.

20. A supramolecular material according to claim 19, wherein linker L(a) comprises at least two aliphatic subunits, such as, at least three or at least four aliphatic subunits.

21. A supramolecular material according to any of the preceding claims, wherein linker L(a) further comprises at least one hydrogen bonding group.

22. A supramolecular material according to claim 21, wherein linker L(a) comprises at least two aliphatic subunits and the at least one hydrogen bonding group is positioned between two of the at least two aliphatic subunits.

23. A supramolecular material according to any of the preceding claims, wherein P(a) is a hydrophobic polymer.

24. A supramolecular material according to any of the preceding claims, wherein P(a) is a polyether or a polyester.

25. A supramolecular material according to any of the preceding claims, wherein P(a) is polycaprolactone.

26. A supramolecular material according to any of the preceding claims, wherein P(a) has a Mn from about 100 to 100,000 Dalton, such as from about 100 to 60,000, from about 800 to about 40,000 or from about 2,000 to about 35,000 Dalton.

27. A supramolecular material according to any of claims 10-26, wherein each of the at least one aliphatic subunits independently comprise less than 26 carbon atoms, such as less than 25, less than 24, less than 23, less than 22, less than 21, less than 20, less than 19, less than 18, less than 17, less than 16, less than 15, less than 14, less than 13, less than 12 or less than 11 carbon atoms.

28. A supramolecular material according to any of claims 10-27, wherein each of the at least one aliphatic subunits independently comprise 1-10 carbon atoms, such as, 2-9, 3-8, 4-7 or 5-6 carbon atoms.

29. A supramolecular material according to any of the claims 10-28, wherein each of the at least one aliphatic subunits independently is an alkyl or an alkenyl subunit.

30. A supramolecular material according to any of claim 12-29, wherein the hydrogen bonding group is selected from the group consisting of a urea functional group, a urethane, a carbonyl group, an amide, a carbamate, a carbonate, an ester and an ether.

31. A supramolecular material according to any of the preceding claims, wherein compound (b) comprises a formula selected from the group consisting of:

i) 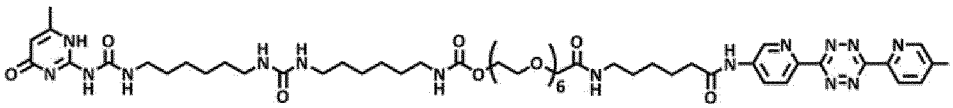

ii) 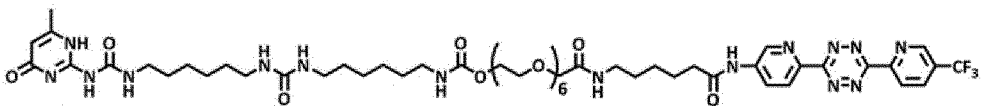

iii) 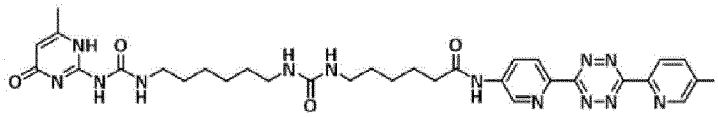

iv) 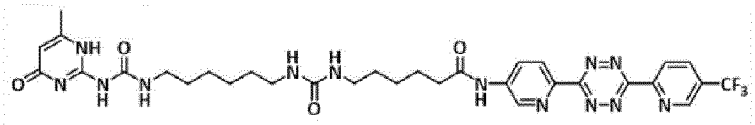

v) 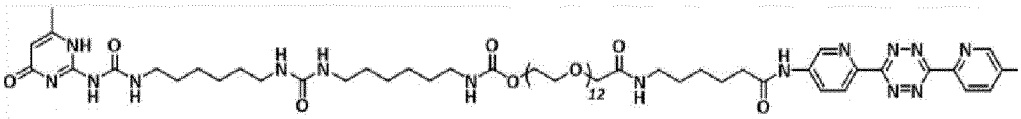

and vi)

32. 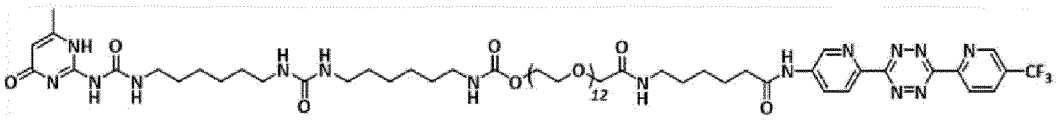

A supramolecular material according to any of the preceding claims, wherein the supramolecular material is a solid or semi-solid.

33. A supramolecular material according to any of the preceding claims, wherein compound (b) is present in an amount of from about 0.5 mol% to about 30 mol%, such as from about 1 mol% to about 25 mol%, from about 1.5 mol% to about 10 mol%, from about 2 to about 9 mol%, from about 2.5 to about 8 mol%,

from about 3 to about 7 mol%, from about 3.5 to about 6.5 mol%, from about 4 to about 6 mol% or at about 5 mol% of the supramolecular material.

34. A supramolecular material according to any of the preceding claims, wherein O1 of compound (b) is covalently linked to an O2 in a compound (c), wherein compound (c) comprises an O2 and a functionalizing group F.

35. A supramolecular material according to claim 34, wherein compound (c) has the formula O2-L(c)-F, wherein L(c) is a direct bond or a linker.

36. A supramolecular material according to claim 35, wherein L(c) is a linker comprising at least one aliphatic subunit and/or a polymer P(c).

37. A supramolecular material according to 36, wherein P(c) is a hydrophilic polymer.

38. A supramolecular material according to any of claims 36 and 37, wherein P(c) is a polyester or a polyether.

39. A supramolecular material according to any of claims 36-38, wherein P(c) is an oligoethylene glycol (OEG) or a polyethylene glycol (PEG).

40. A supramolecular material according to any of claims 36-39, wherein P(c) comprises from about 1 to about 20 repeating units, such as from about 1 to about 8, from about 2 to about 7, from about 3 to about 5, such as 4 repeating units.

41. A supramolecular material according to any of claims 36-40, wherein each of the at least one aliphatic subunits independently comprise less than 26 carbon atoms, such as less than 25, less than 24, less than 23, less than 22, less than 21, less than 20, less than 19, less than 18, less than 17, less than 16, less than 15, less than 14, less than 13, less than 12 or less than 11 carbon atoms.

42. A supramolecular material according to any of claims 36-41, wherein each of the at least one aliphatic subunits independently comprise 1-10 carbon atoms, such as, 2-9, 3-8, 4-7 or 5-6 carbon atoms.

43. A supramolecular material according to any of the claims 36-42, wherein each of the at least one aliphatic subunits independently is an alkyl or an alkenyl subunit.

44. A supramolecular material according to any of claims 35-43, wherein linker L(c) further comprises at least one hydrogen bonding group.

45. A supramolecular material according to claim 44, wherein the hydrogen bonding group is selected from the group consisting of a urea functional group, a urethane, a carbonyl group, an amide, a carbamate, a carbonate, an ester and an ether.

46. A supramolecular material according to any of claims 34-45, wherein the functionalizing group F is selected from the group consisting of imaging agents, therapeutical agents, bioactive molecules, proteins, peptides and antifouling agents.

47. A supramolecular material according to any of claims 34-46, wherein F is present on the surface of the supramolecular material in a surface:bulk ratio of at least 60:40, such as 65:35, 70:30, 75:25, 80:20, 85:15, 90:10, 95:5, 96:4, 97:3, 98:2 or 99:1.

48. Method for the preparation of a supramolecular material as defined in any of claims 1-47, the method comprising the steps of,

1. Mixing the compounds (a) and (b) in a solvent to obtain a polymer solution, and
2. Subjecting the polymer solution obtained in step 1) to any of the following steps:
    a) Evaporating at least 70% (v/v) of the solvent off from the polymer solution obtained in step 1) to obtain a supramolecular material, or
    b) Decreasing the pH in the polymer solution obtained in step 1) to obtain a hydrogel supramolecular material.

49. Method according to claim 48 for the preparation of a supramolecular material as defined in any of claims 34-47, the method further comprising a post-functionalizing step 3:

3. subjecting the supramolecular material obtained in any of steps 2a) or 2b) to a reaction with the compound (c) to obtain the covalent bond between O1 and O2.

50. Method according to claim 49, wherein O1 and O2 are selected such that the reaction in step 3 is selected from the group consisting of:
- Copper(I)-Catalyzed Azide-Alkyne Cycloaddition (CuAAC);
- Strain-promoted Azide-Alkyne Cycloaddition (SPAAC);
- Strain-promoted Alkyne-Nitrone Cycloaddition (SPANC);
- Staudinger ligation;
- Native chemical ligation; and
- Oxime ligation.

51. A method according to any of claims 49 and 50, wherein O1 and O2 are selected such that the reaction in step 3 is an inverse electron demand Diels-Alder (iEDDA) cycloaddition reaction.

52. A method according to any of claims 49-51, wherein the reaction in step 3 takes place in an aqueous solution.

53. A method according to any of claims 49-52, wherein step 3 is performed in less than 2 hours, such as less than 1.5 hour, less than 1 hour, less than 20 minutes, less than 10 minutes or less than 5 minutes.

54. A method according to any of claims 49-53, wherein the reaction in step 3 takes place at pH 6-8, such as 6.5-7.5 or at about 7.

55. Method according to any of claims 49-54, wherein
- O1 is a tetrazine;
- O2 is a *trans*-cyclooctene; and
- The reaction in step 3 is performed in an aqueous solution at pH 6-8 for less than 0.5 hours, such as less than 20 minutes, less than 10 minutes or less than 5 minutes.

56. A supramolecular material obtained by the process defined in any of claims 48-55.

57. A compound (b) as defined in any of claims 1-17 and 27-31.

58. A compound (b) according to claim 57, wherein compound (b) comprises a formula selected from the group consisting of:

i) 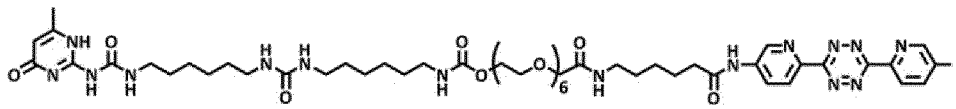

ii) 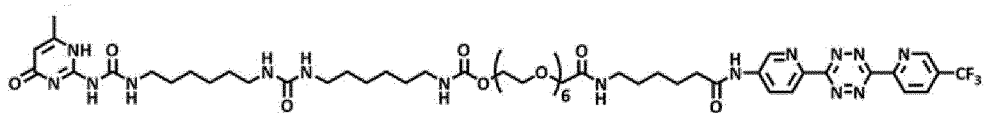

iii) 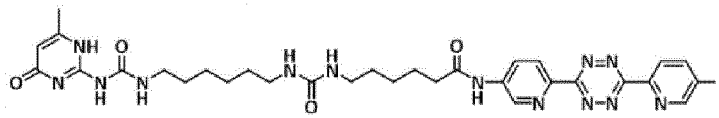

iv) 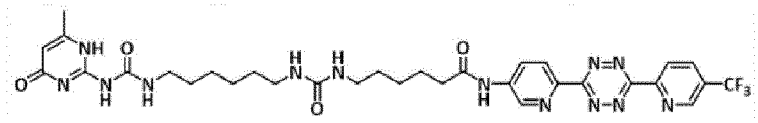

v) 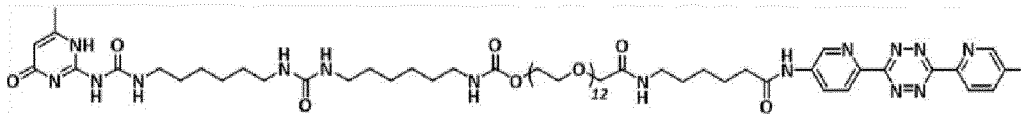

and vi)

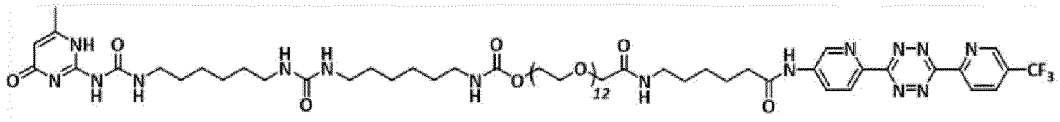

59. A biomaterial comprising a supramolecular material as defined in any of claims 1-47 and 56.

60. Use of a supramolecular material as defined in any of claims 1-47 and 56 as a biomaterial.

61. A supramolecular material as defined in any of claims 1-47 and 56, or a biomaterial as defined in claim 59, for use in regenerative medicine.

62. Use of a supramolecular material as defined in any of claims 1-47 and 56, or a biomaterial as defined in claim 59, in regenerative medicine.

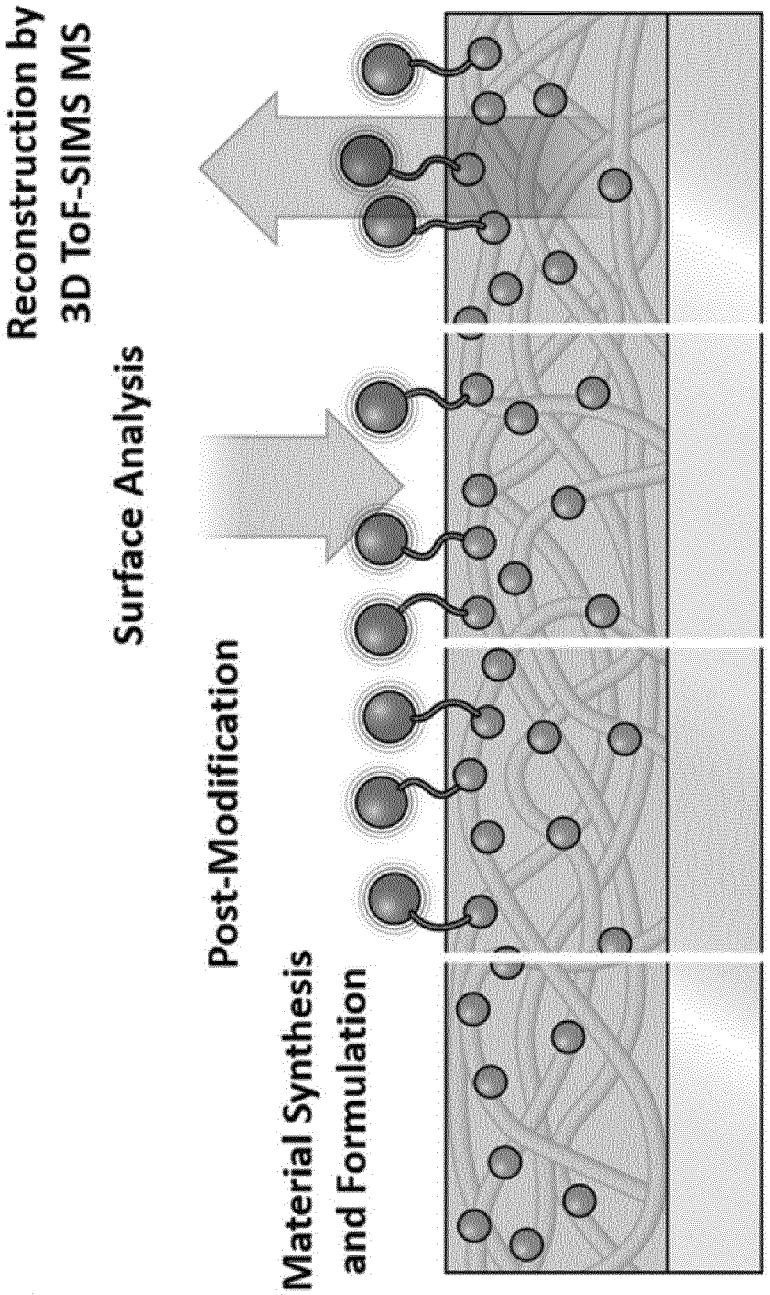
Reconstruction by
3D ToF-SIMS MS
Surface Analysis
Post-Modification
Material Synthesis
and Formulation

Fig. 1a

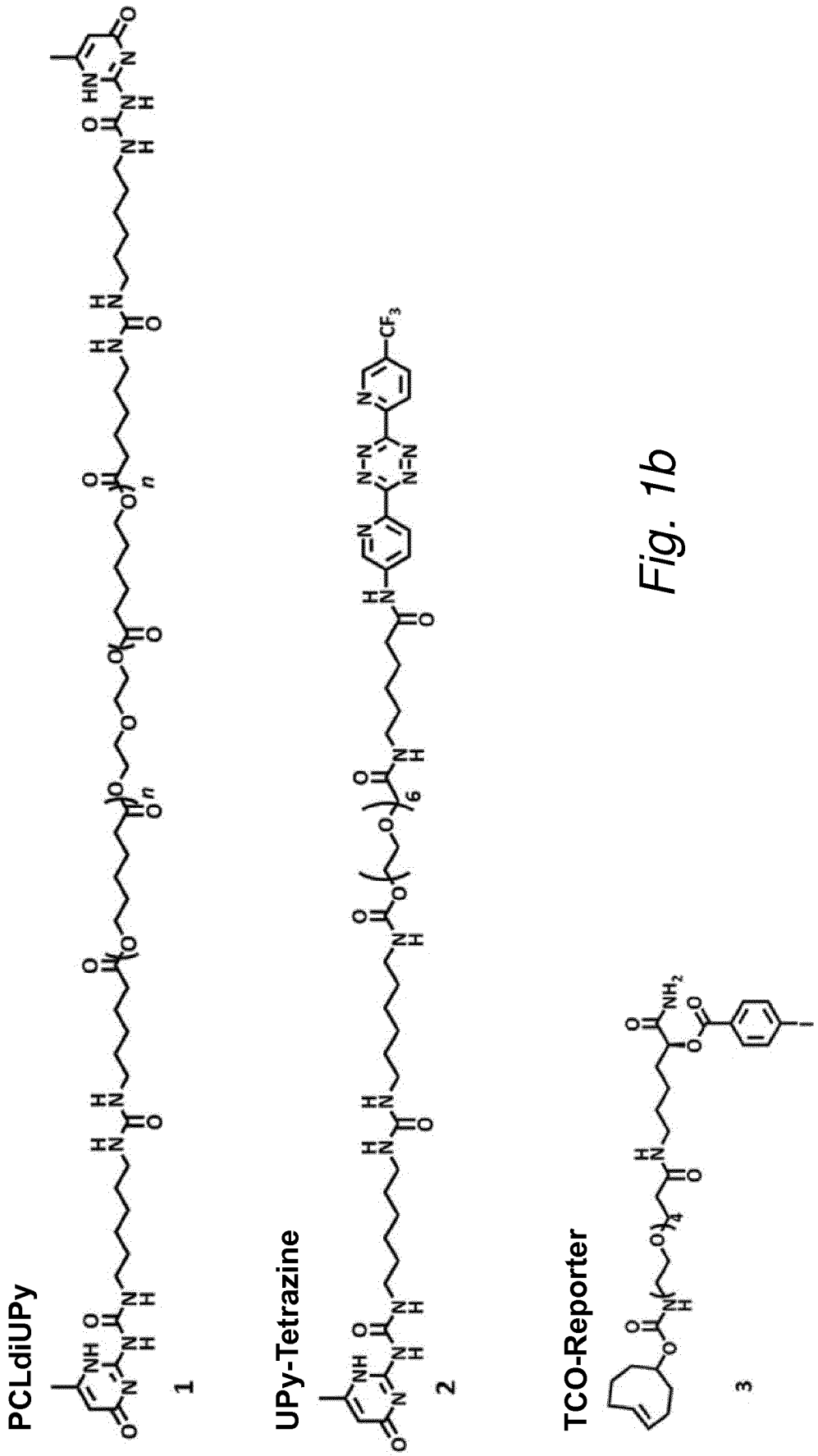

Fig. 1b

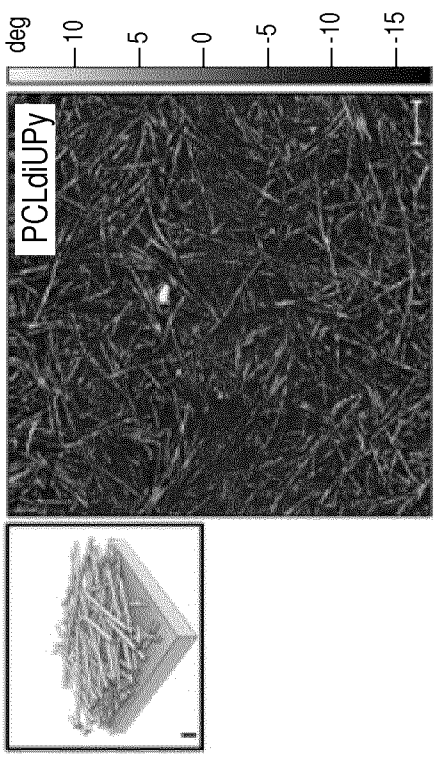
deg
10
5
0
-5
-10
-15
PCLdiUPy

Fig. 1c

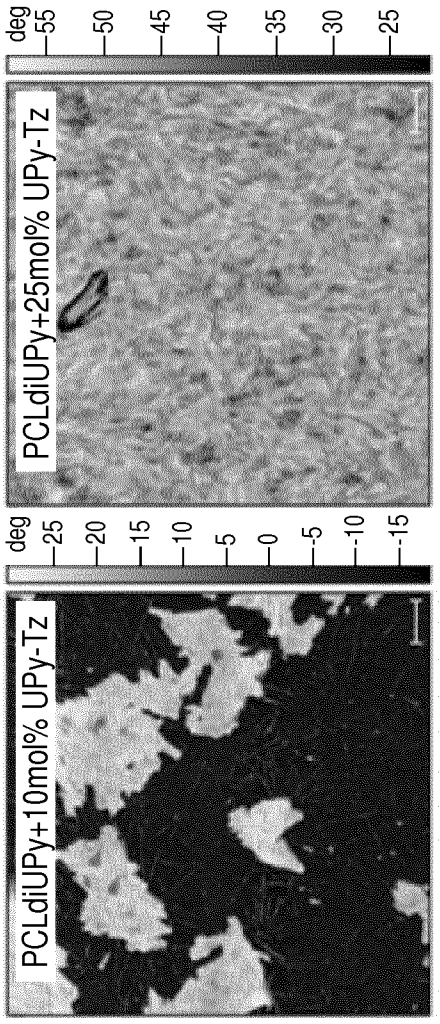
deg
55
50
45
40
35
30
25
PCLdiUPy+25mol% UPy-Tz
deg
25
20
15
10
5
0
-5
-10
-15
PCLdiUPy+10mol% UPy-Tz

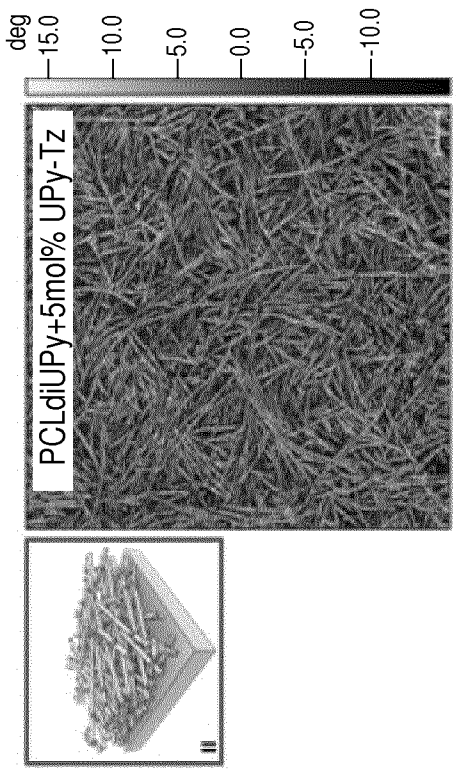
deg
15.0
10.0
5.0
0.0
-5.0
-10.0
PCLdiUPy+5mol% UPy-Tz

Fig. 1d

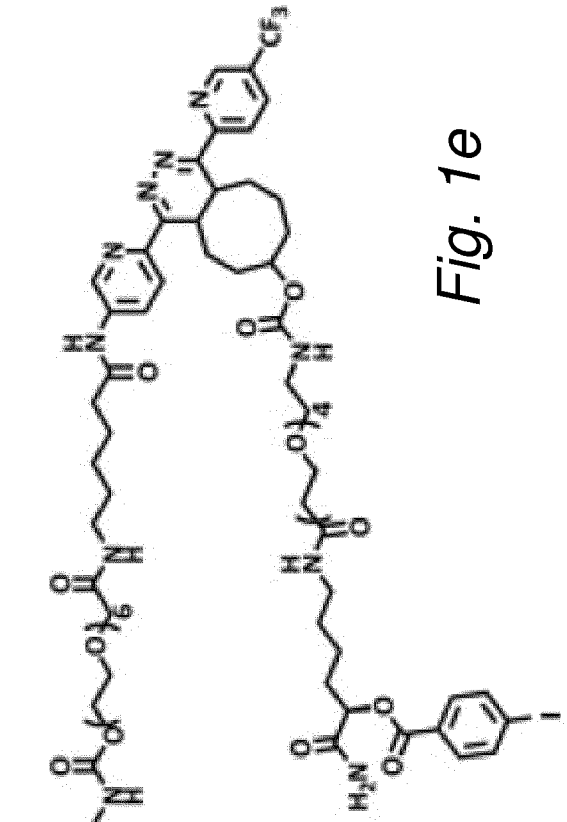

Fig. 1e

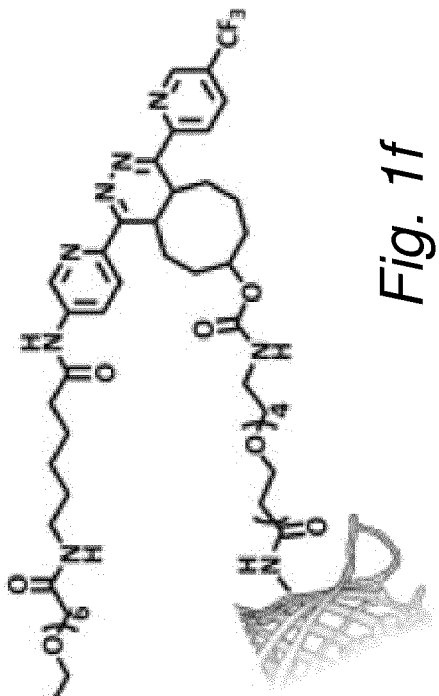

Fig. 1f

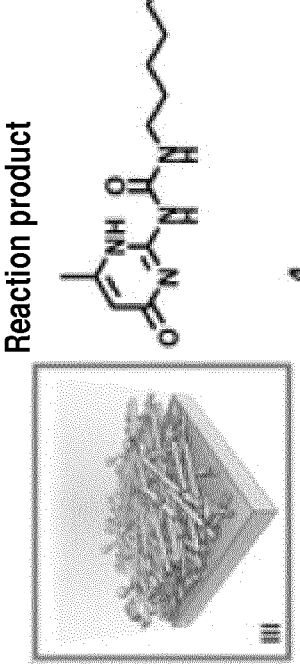

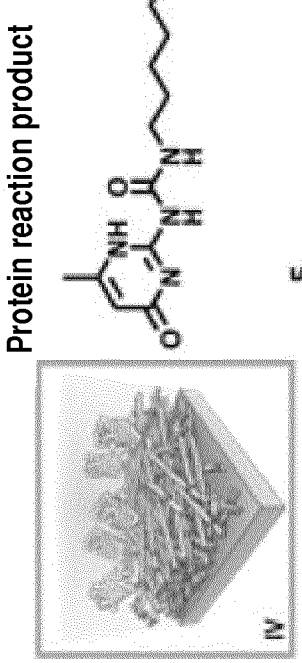

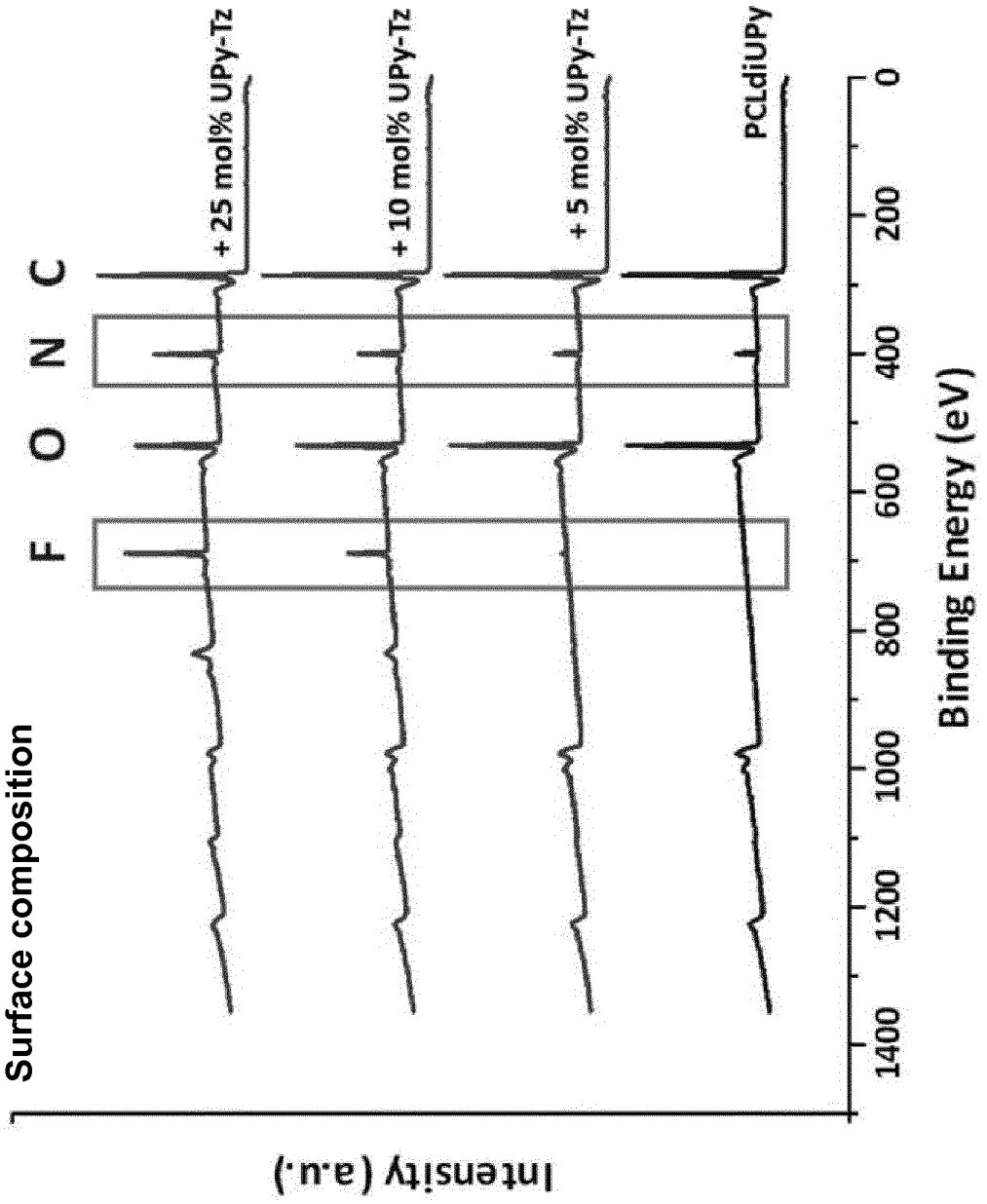
Surface composition
F O N C
+ 25 mol% UPy-Tz
+ 10 mol% UPy-Tz
+ 5 mol% UPy-Tz
PCLdiUPy
Intensity (a.u.)
1400 1200 1000 800 600 400 200 0
Binding Energy (eV)

Fig. 2a

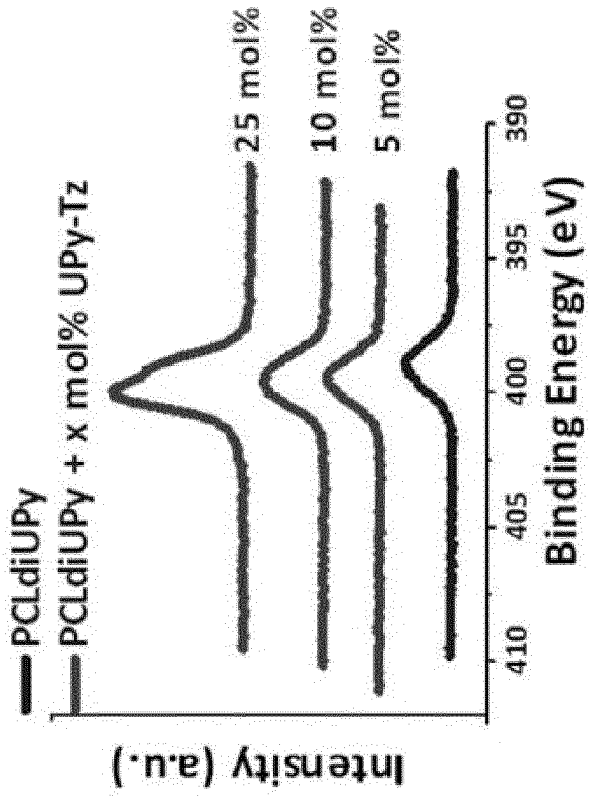
PCLdiUPy
PCLdiUPy + x mol% UPy-Tz
25 mol%
10 mol%
5 mol%
Intensity (a.u.)
Binding Energy (eV)
410
405
400
395
390

Fig. 2c

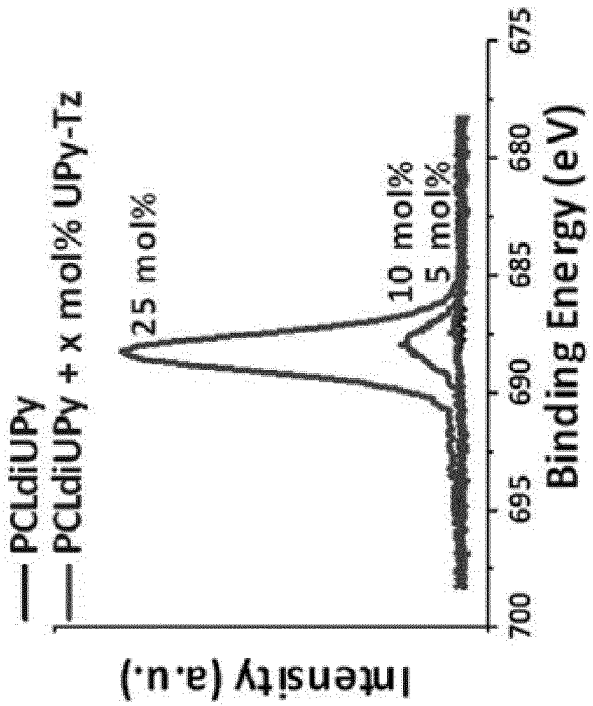
PCLdiUPy
PCLdiUPy + x mol% UPy-Tz
25 mol%
10 mol%
5 mol%
Intensity (a.u.)
Binding Energy (eV)
700
695
690
685
680
675

Fig. 2b

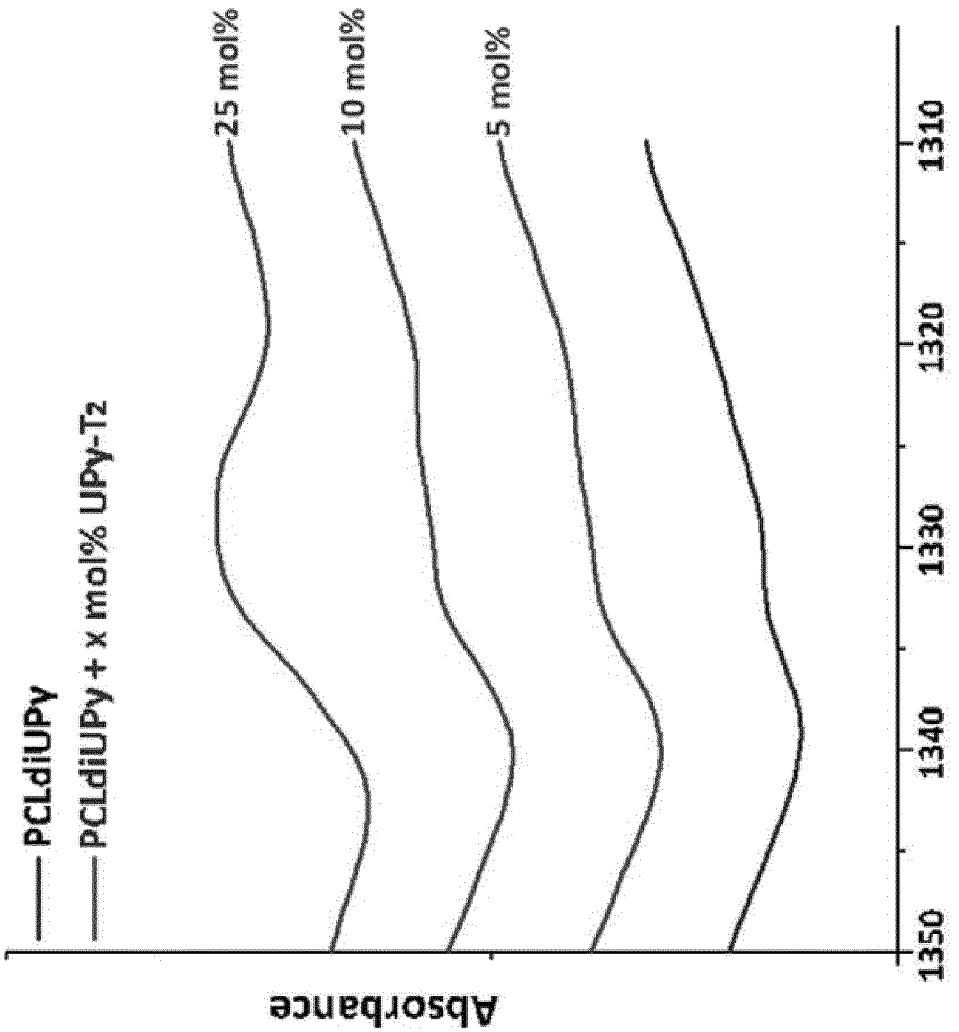
PCLdiUPy
PCLdiUPy + x mol% UPy-T2
25 mol%
10 mol%
5 mol%
Absorbance
1350
1340
1330
1320
1310
Wavelength (cm-1)

Fig. 2d

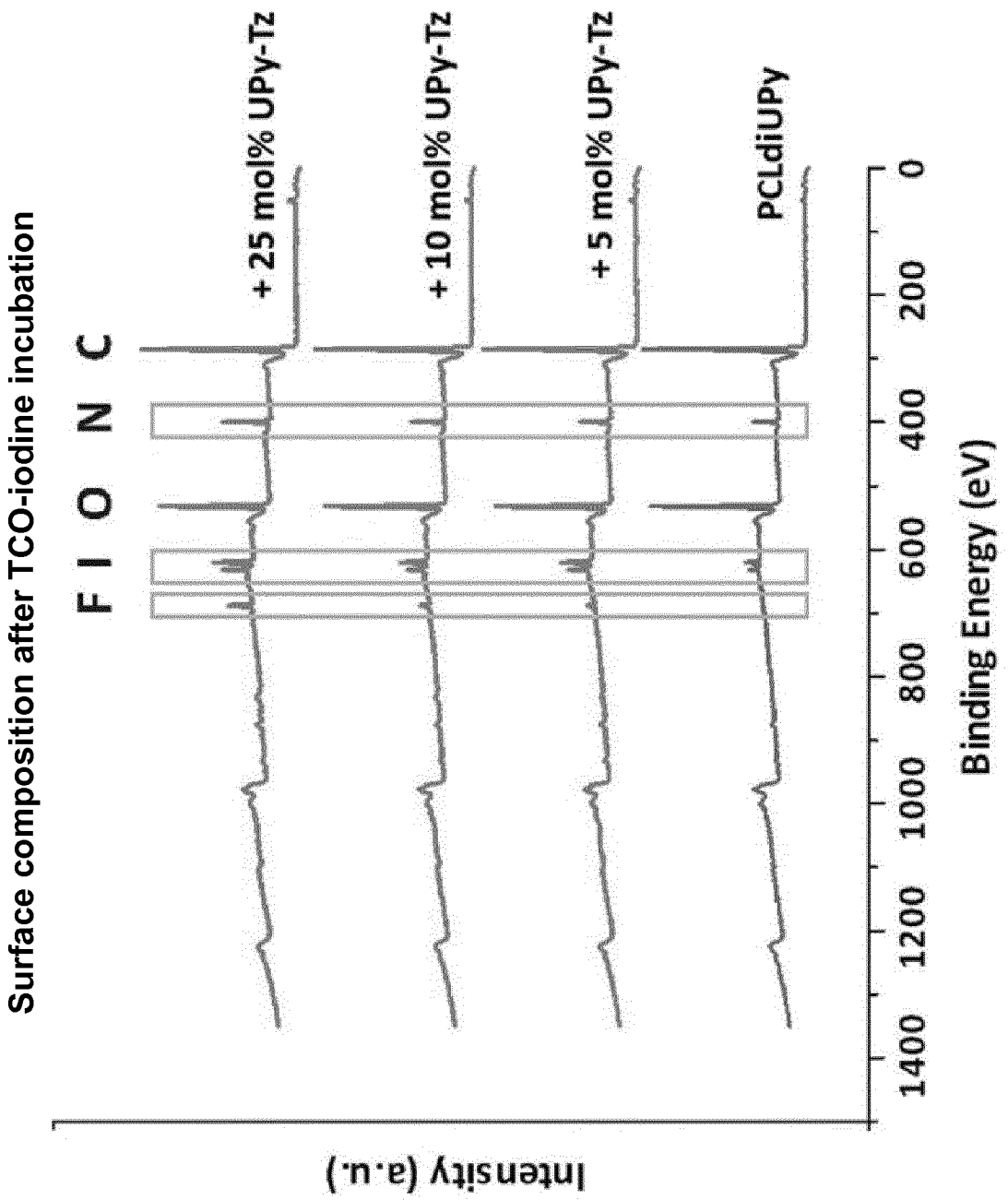
Surface composition after TCO-iodine incubation
F I O N C
+ 25 mol% UPy-Tz
+ 10 mol% UPy-Tz
+ 5 mol% UPy-Tz
PCLdiUPy
Intensity (a.u.)
1400 1200 1000 800 600 400 200 0
Binding Energy (eV)

Fig. 3a

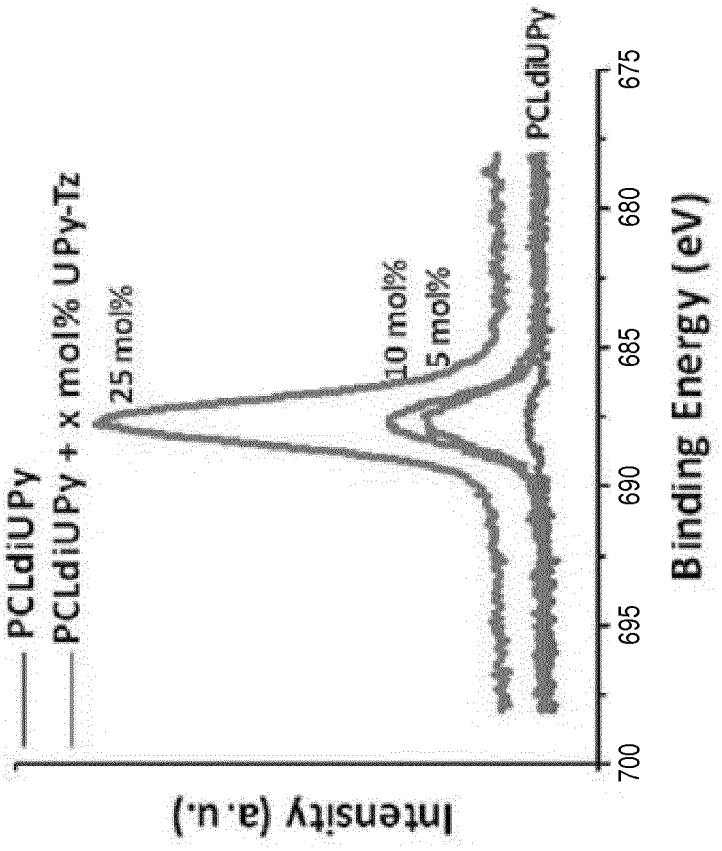
PCLdiUPy
PCLdiUPy + x mol% UPy-Tz
25 mol%
10 mol%
5 mol%
PCLdiUPy
Intensity (a.u.)
Binding Energy (eV)
700
695
690
685
680
675

Fig. 3c

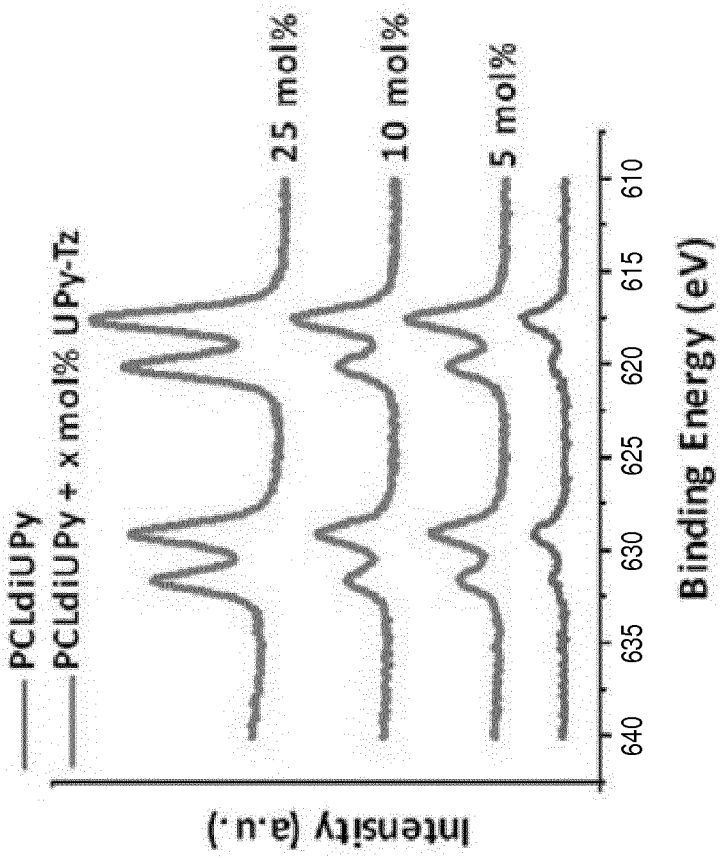
PCLdiUPy
PCLdiUPy + x mol% UPy-Tz
25 mol%
10 mol%
5 mol%
Intensity (a.u.)
Binding Energy (eV)
640
635
630
625
620
615
610

Fig. 3b

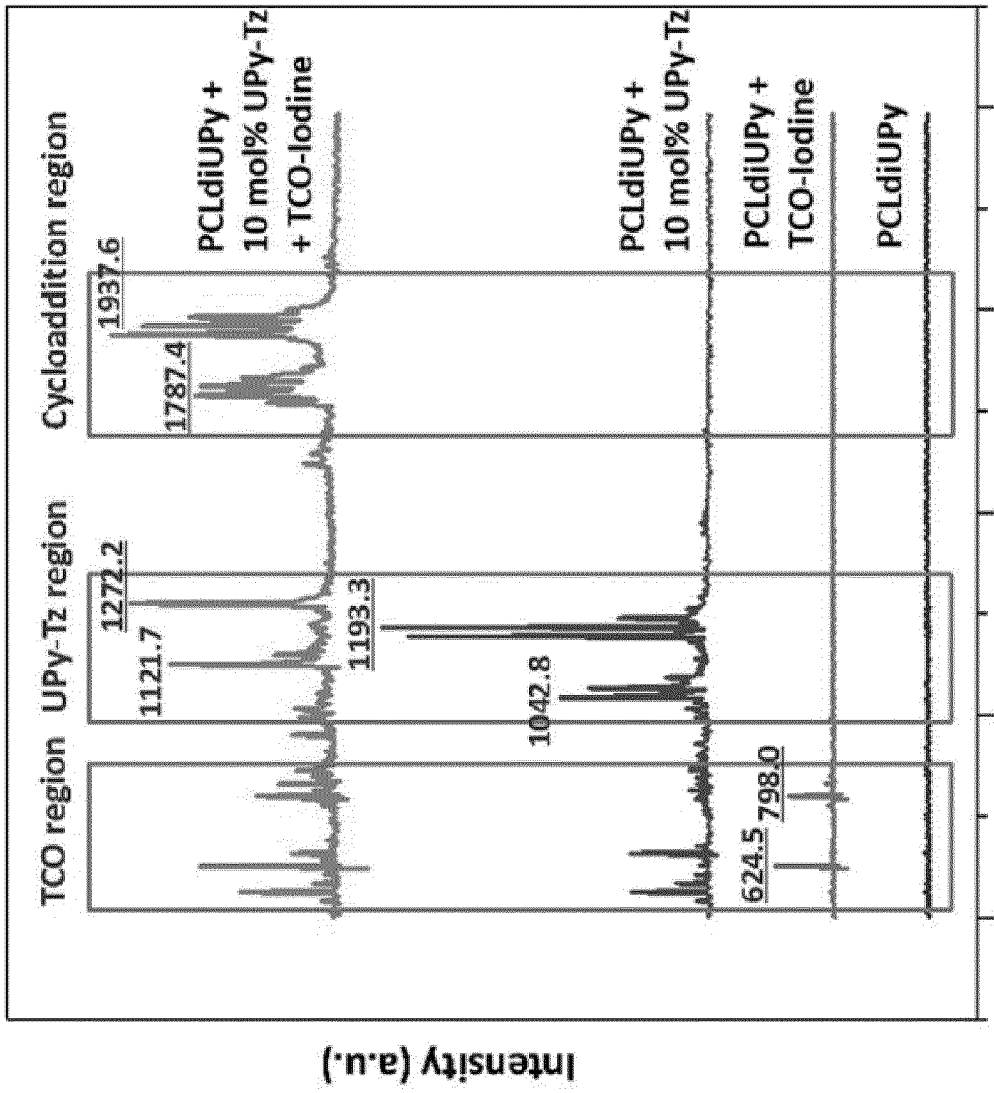
TCO region
UPy-Tz region
Cycloaddition region
PCLdiUPy +
10 mol% UPy-Tz
+ TCO-Iodine
PCLdiUPy +
10 mol% UPy-Tz
PCLdiUPy +
TCO-Iodine
PCLdiUPy
1937.6
1787.4
1272.2
1121.7
1193.3
1042.8
624.5
798.0
500
1000
1500
2000
2500
m/z
Intensity (a.u.)

Fig. 3d

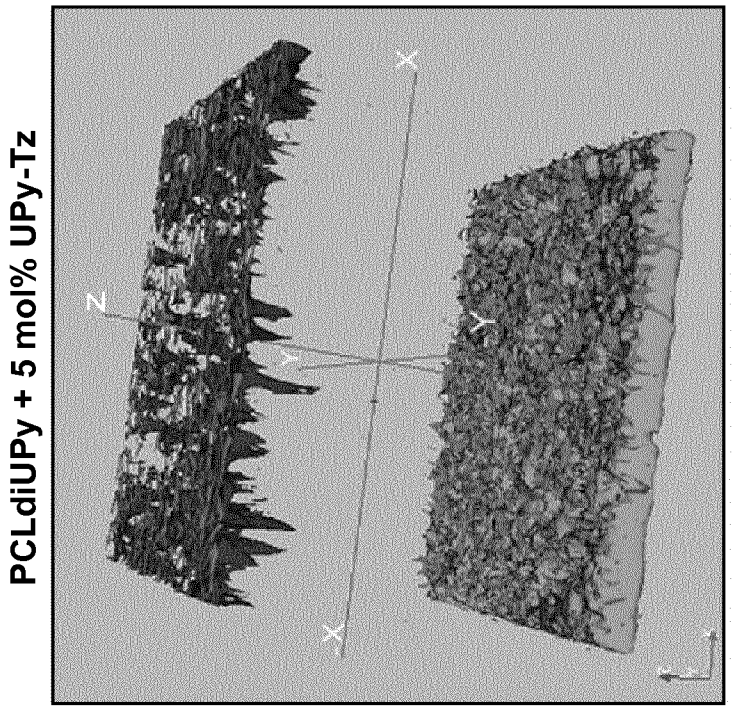

Fig. 4b

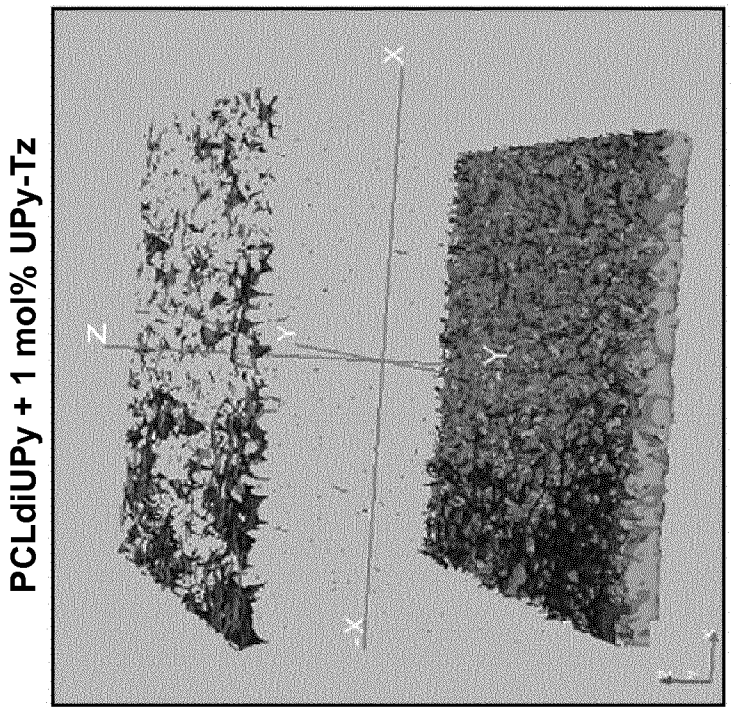

Fig. 4a

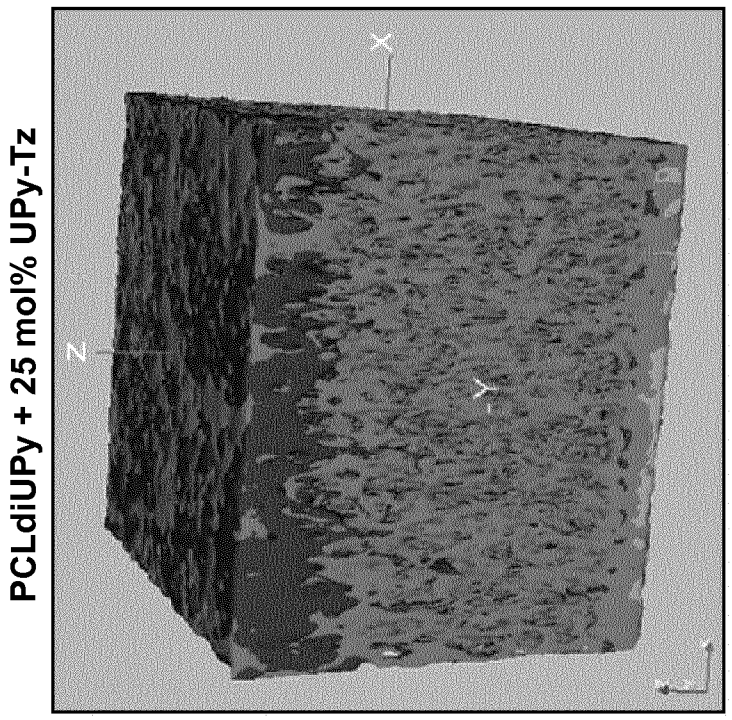

Fig. 4d

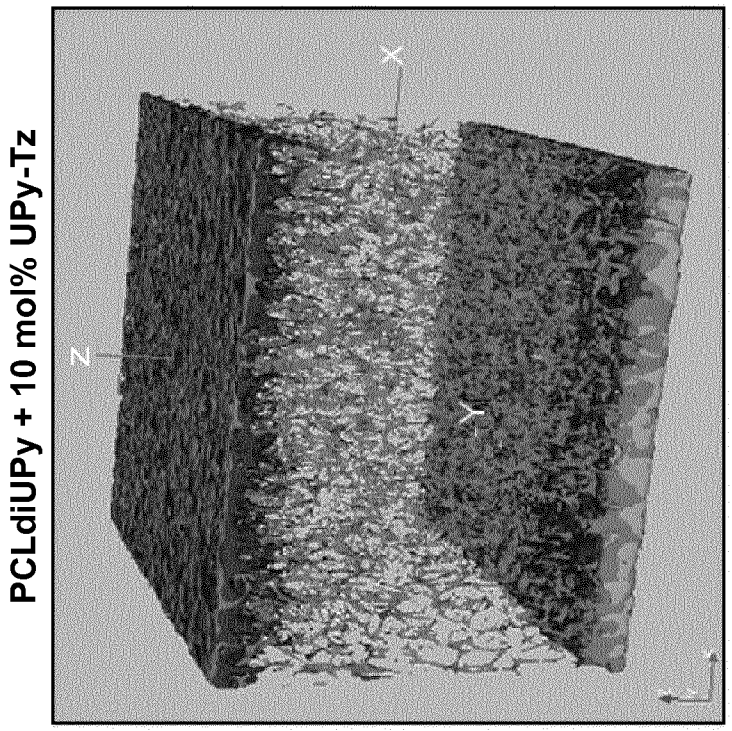

Fig. 4c

PCLdiUPy + 5 mol% UPy-Tz

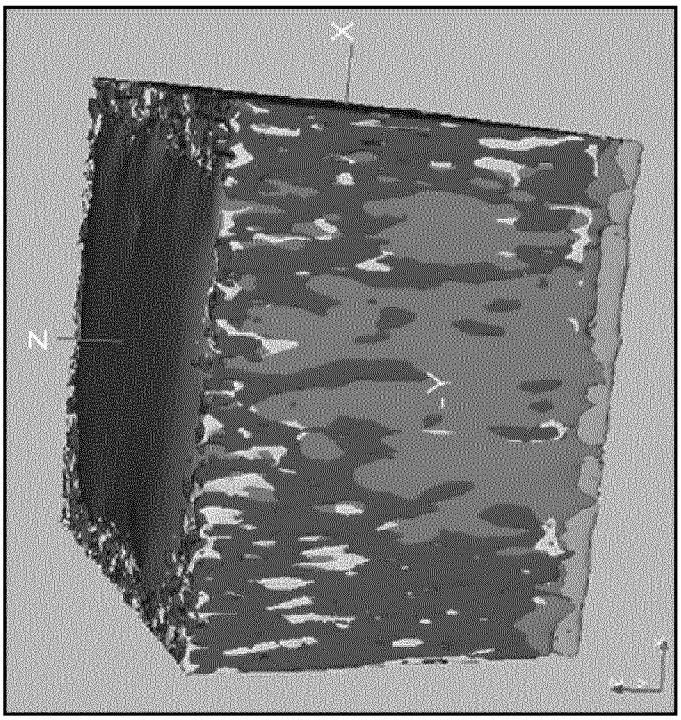

Fig. 4f

PCLdiUPy + 1 mol% UPy-Tz

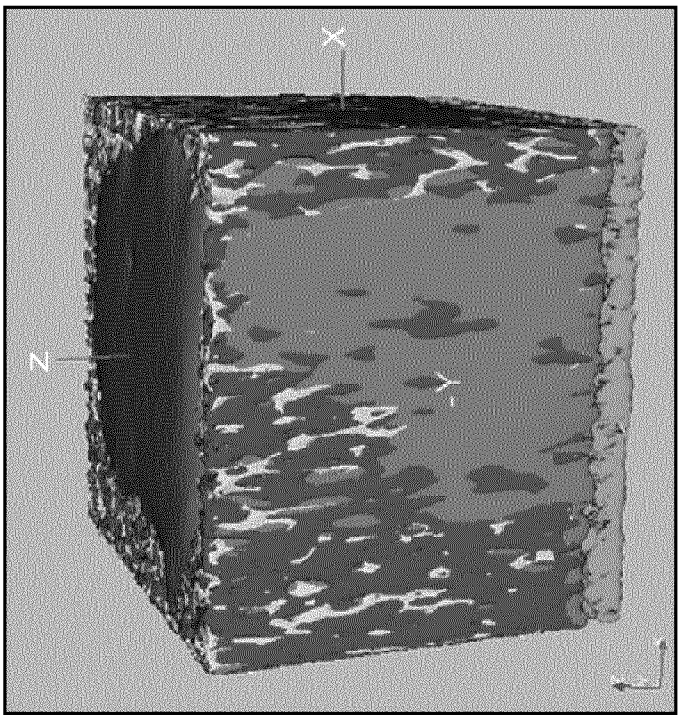

Fig. 4e

PCLdiUPy + 25 mol% UPy-Tz

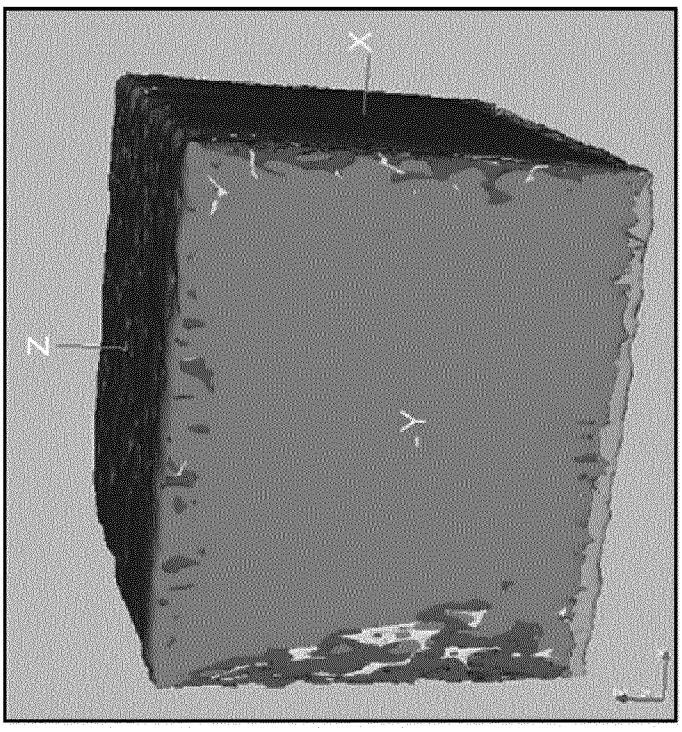

Fig. 4h

PCLdiUPy + 10 mol% UPy-Tz

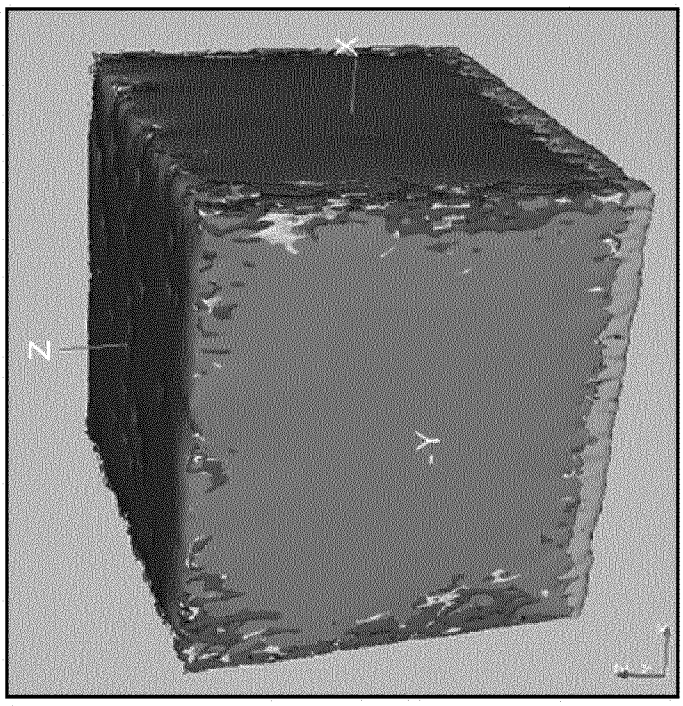

Fig. 4g

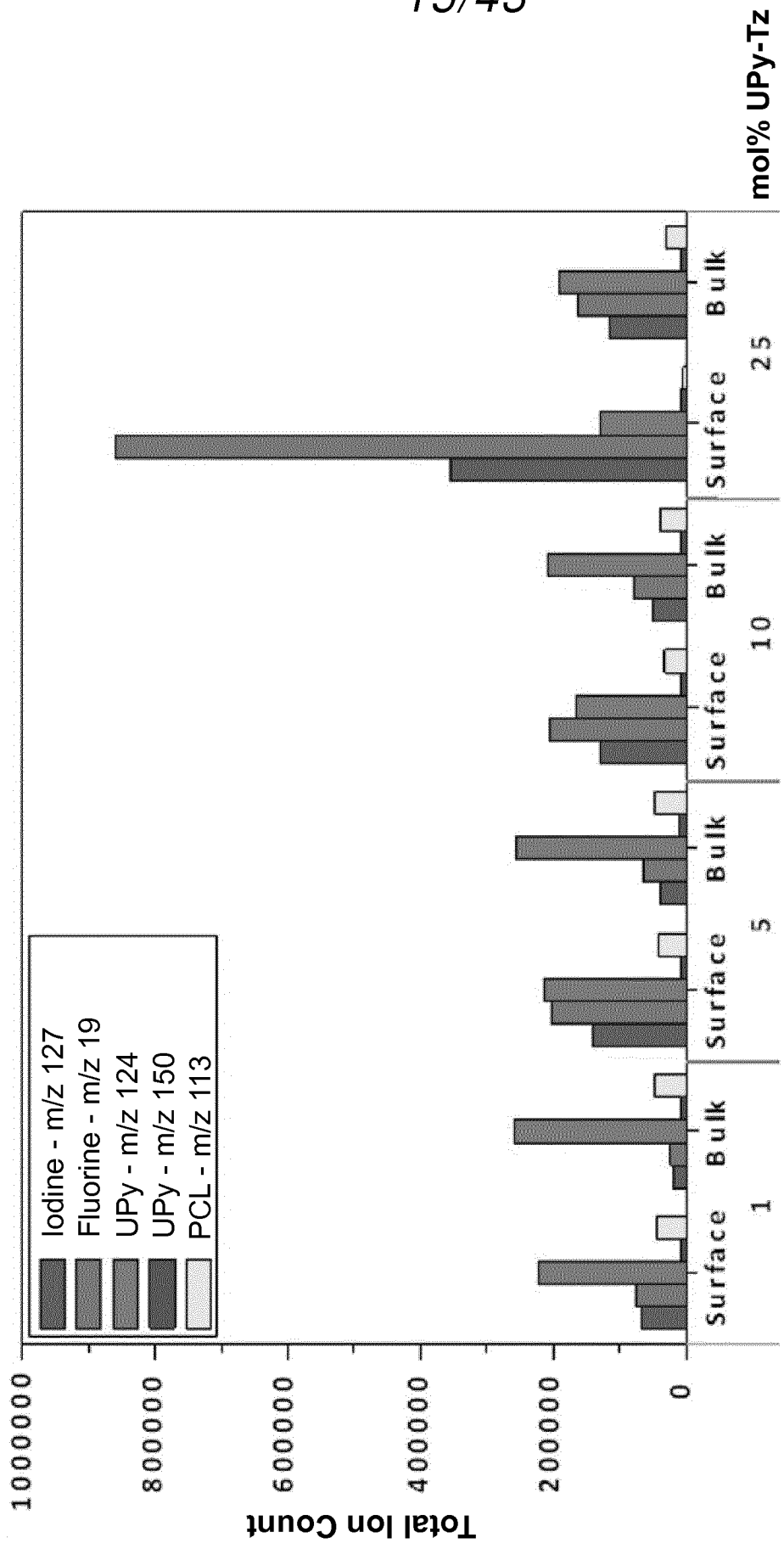
Total Ion Count
1000000
800000
600000
400000
200000
0
Iodine - m/z 127
Fluorine - m/z 19
UPy - m/z 124
UPy - m/z 150
PCL - m/z 113
Surface
Bulk
Surface
Bulk
Surface
Bulk
Surface
Bulk
1
5
10
25
mol% UPy-Tz
Material Formulation

Fig. 4i

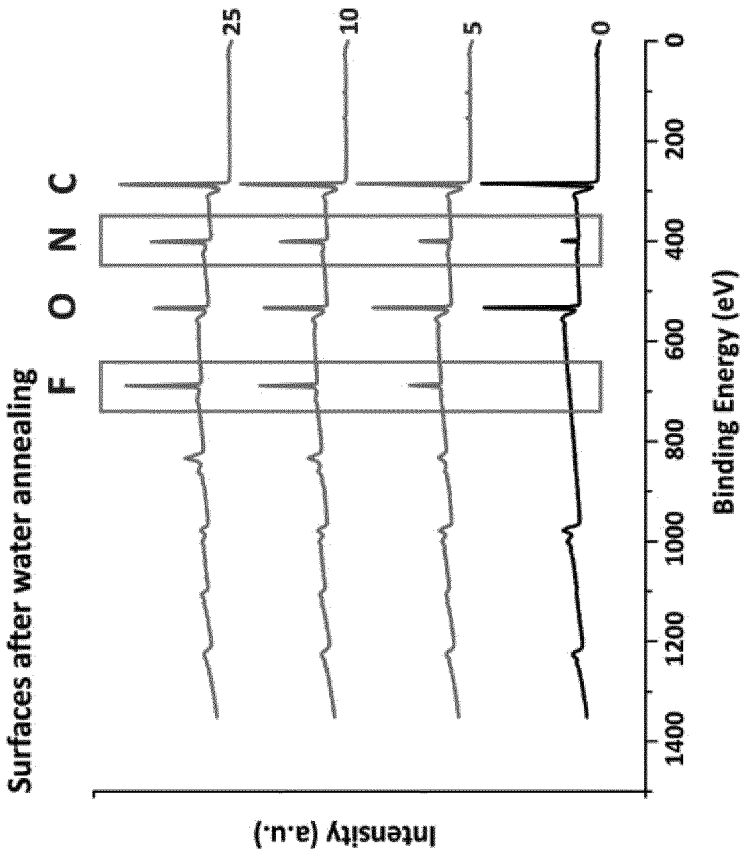

Fig. 5a

Air dried	Surface Composition (%)					Ratio
Surface	C	O	N	F		F:C
PCLdiUPy	74.0	21.3	4.75	-		-
PCLdiUPy + 5 mol% UPy-Tz	73.5	20.9	5.14	0.49		0.007
PCLdiUPy + 10 mol% UPy-Tz	69.2	16.9	8.92	4.07		0.06
PCLdiUPy + 25 mol% UPy-Tz	63.9	14.0	12.9	7.43		0.12

Water Annealing	Surface Composition (%)					Ratio
Surface	C	O	N	F		F:C
PCLdiUPy	73.8	21.4	4.82	-		-
PCLdiUPy + 5 mol% UPy-Tz	68.3	17.0	9.15	4.36		0.06
PCLdiUPy + 10 mol% UPy-Tz	63.5	14.3	12.9	7.54		0.12
PCLdiUPy + 25 mol% UPy-Tz	60.1	11.3	16.2	9.65		0.16

Fig. 5b

Tilt angle (°)	0	15	30	45	60	75
F:C ratio	0.13	0.12	0.13	0.15	0.18	0.22

Fig. 5d

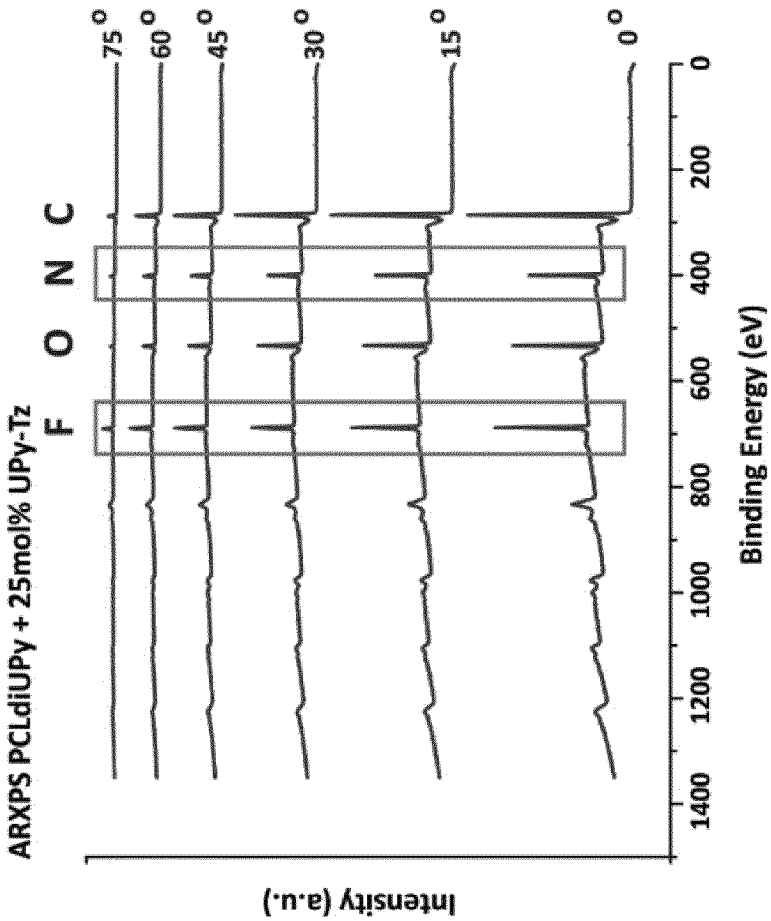

Fig. 5c

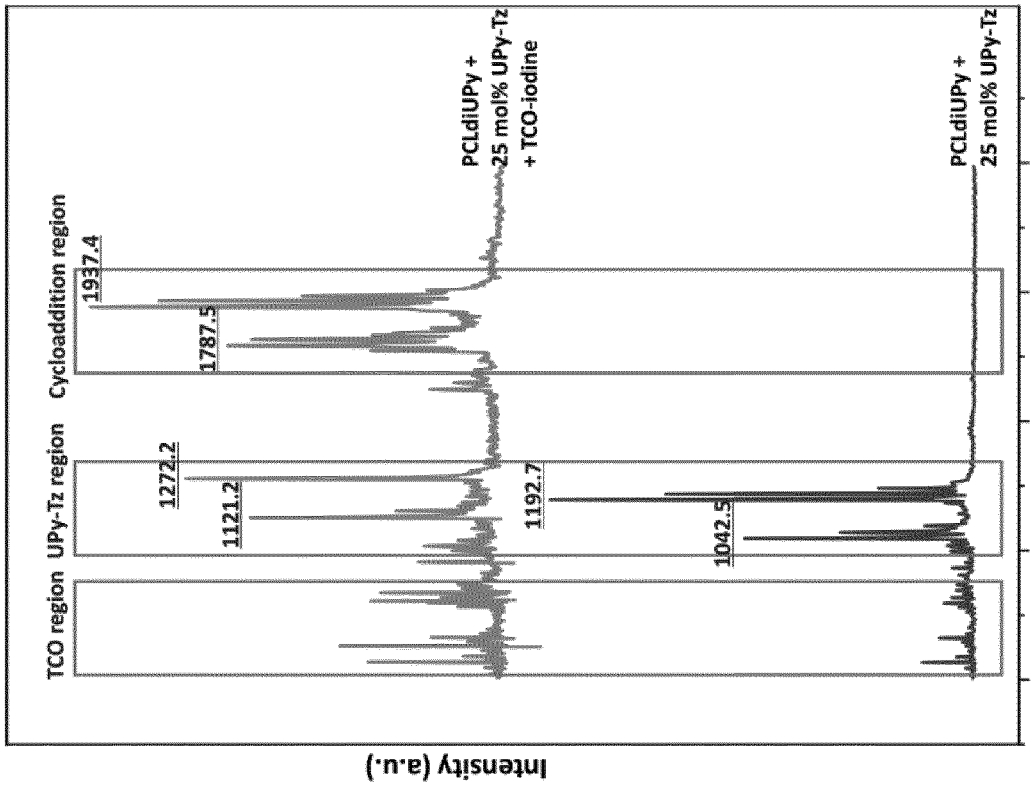
TCO region
UPy-Tz region
Cycloaddition region
1272.2
1121.2
1937.4
1787.5
1192.7
1042.5
PCLdiUPy +
25 mol% UPy-Tz
+ TCO-iodine
PCLdiUPy +
25 mol% UPy-Tz
500
1000
1500
2000
2500
m/z
Intensity (a.u.)

Fig. 6b

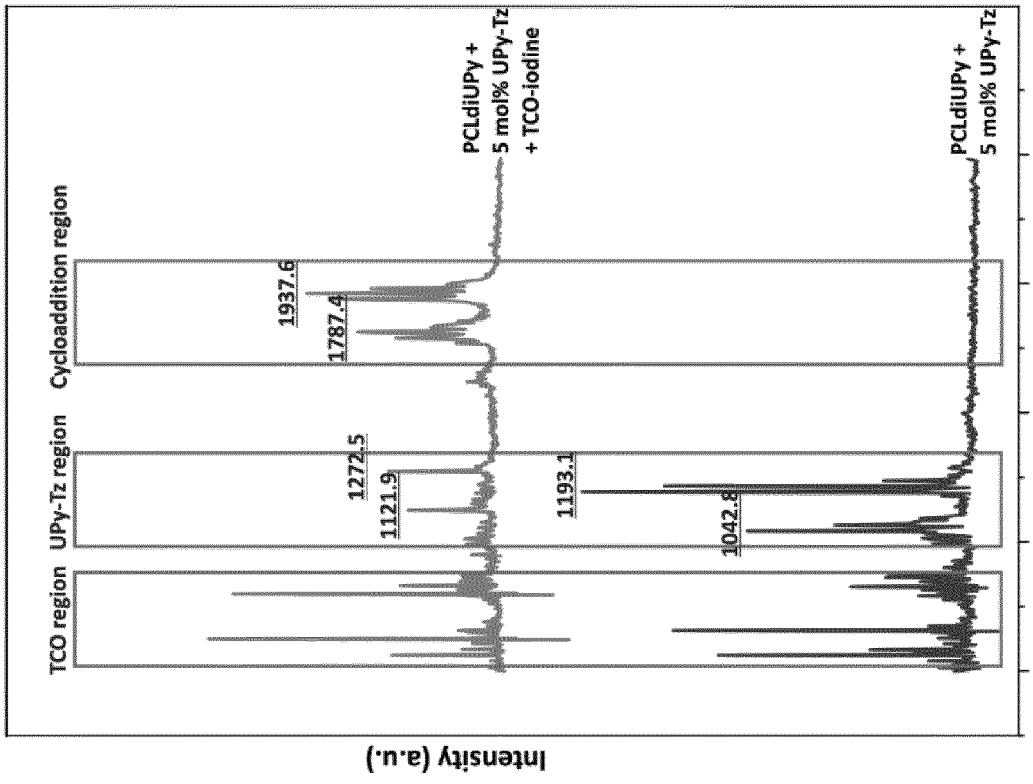
TCO region
UPy-Tz region
Cycloaddition region
1272.5
1121.9
1937.6
1787.4
1193.1
1042.8
PCLdiUPy +
5 mol% UPy-Tz
+ TCO-iodine
PCLdiUPy +
5 mol% UPy-Tz
500
1000
1500
2000
2500
m/z
Intensity (a.u.)

Fig. 6a

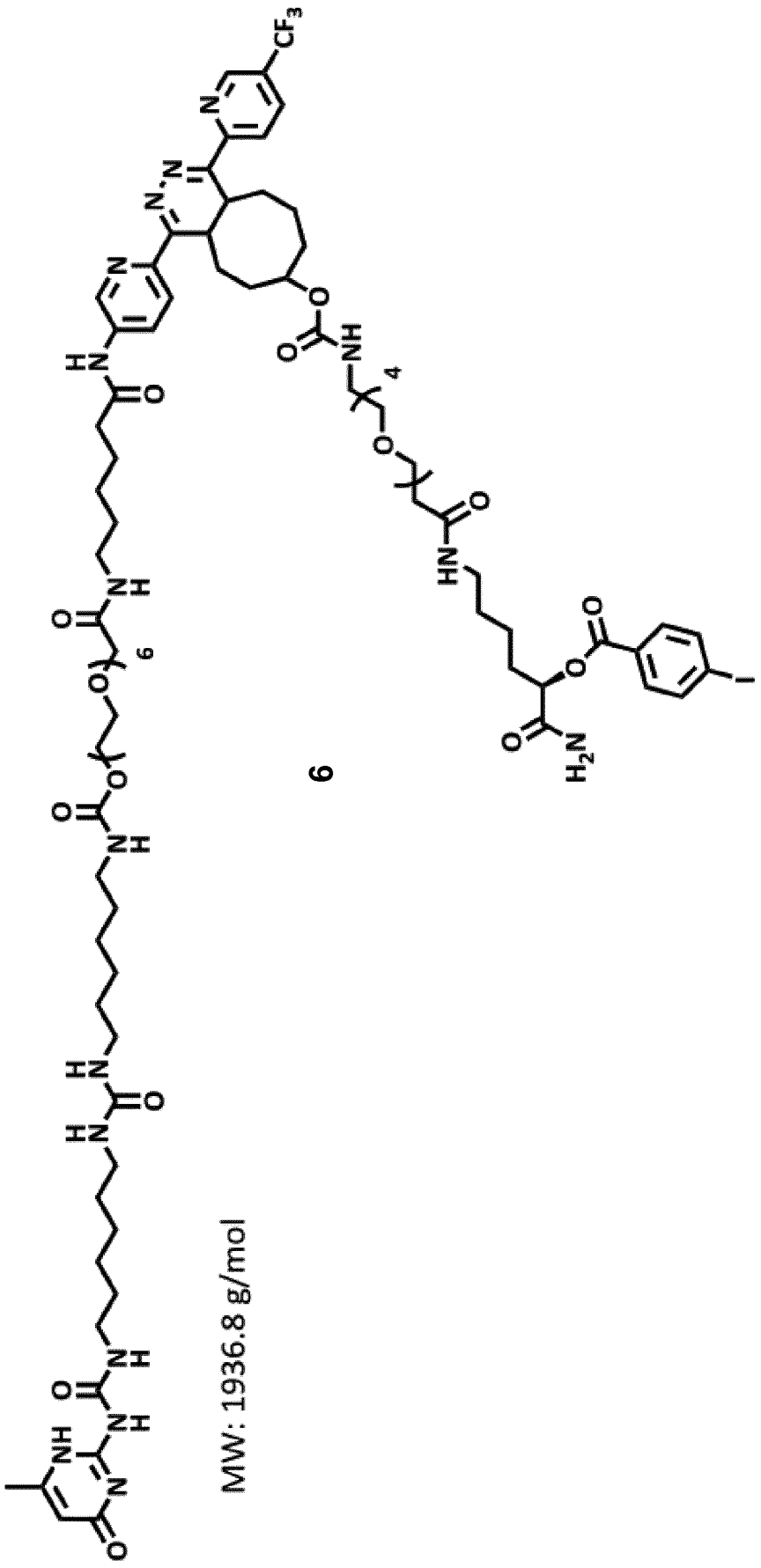

6

MW: 1936.8 g/mol

Fig. 6c

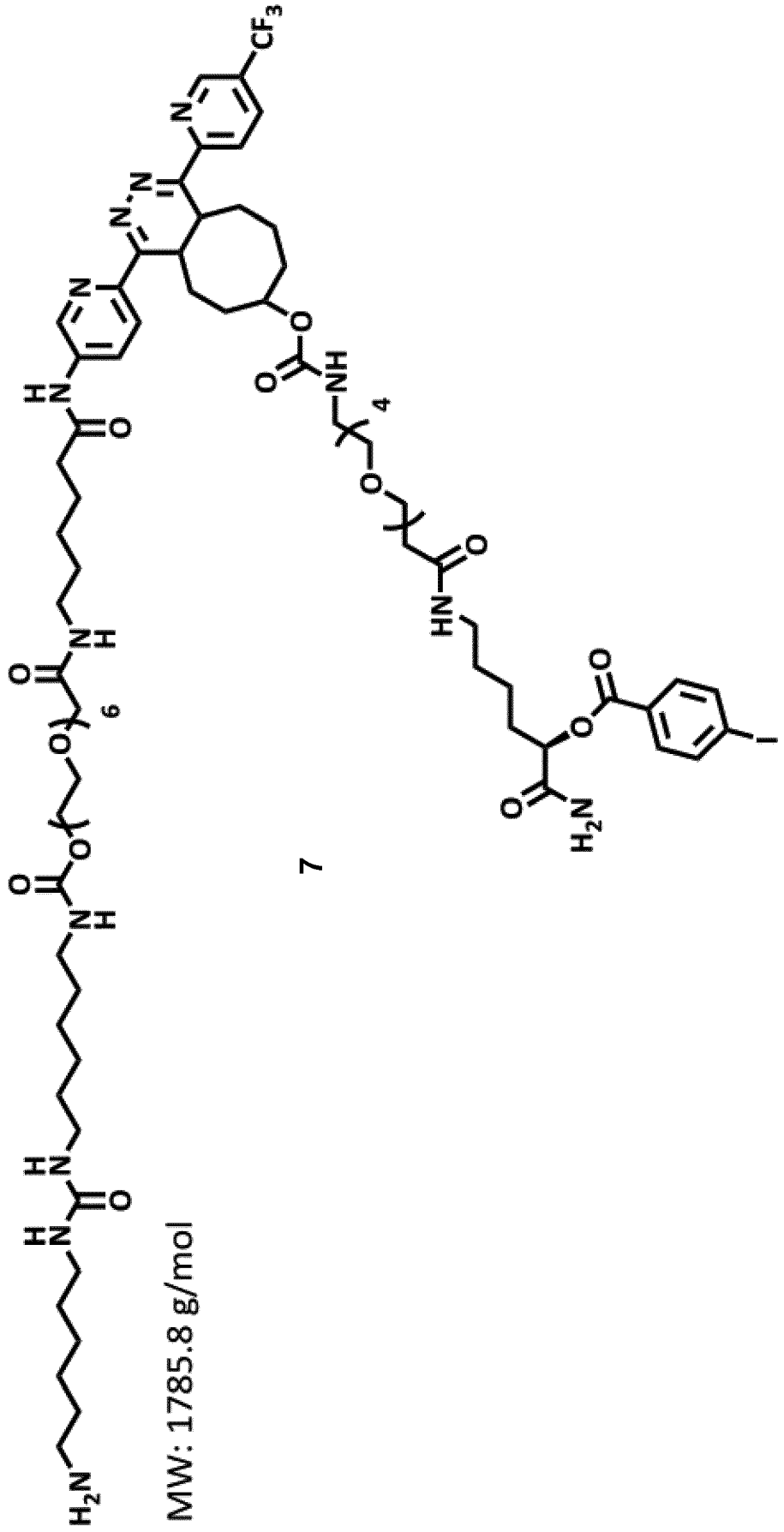

7

MW: 1785.8 g/mol

Fig. 6d

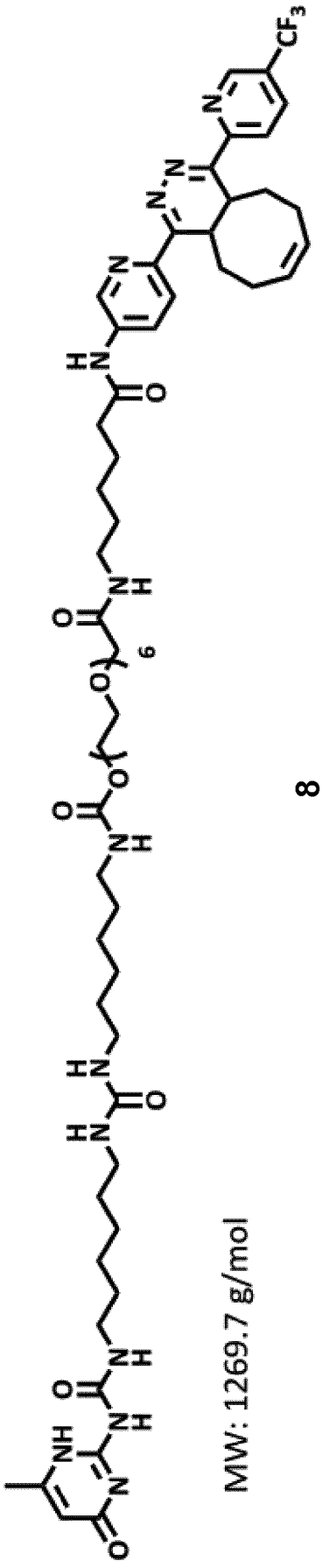

8

MW: 1269.7 g/mol

Fig. 6e

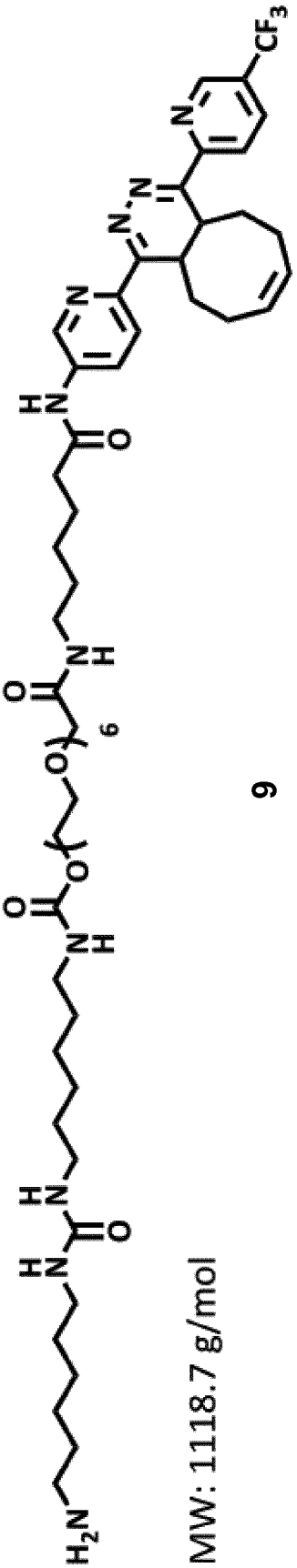

9

MW: 1118.7 g/mol

Fig. 6f

surface	water contact angle (°)		
	drop cast	TCO-model	TCO-eYFP
PCLdiUPy	68.4 ± 1.1	63.4 ± 5.0	77.5 ± 2.0
PCLdiUPy + 5 mol% UPy-Tz	72.2 ± 2.5	68.0 ± 4.0	80.3 ± 3.3
PCLdiUPy + 10 mol% UPy-Tz	79.5 ± 1.0	69.3 ± 1.3	82.2 ± 6.2
PCLdiUPy + 25 mol% UPy-Tz	84.4 ± 1.2	75.8 ± 1.1	84.0 ± 7.4

Fig. 7

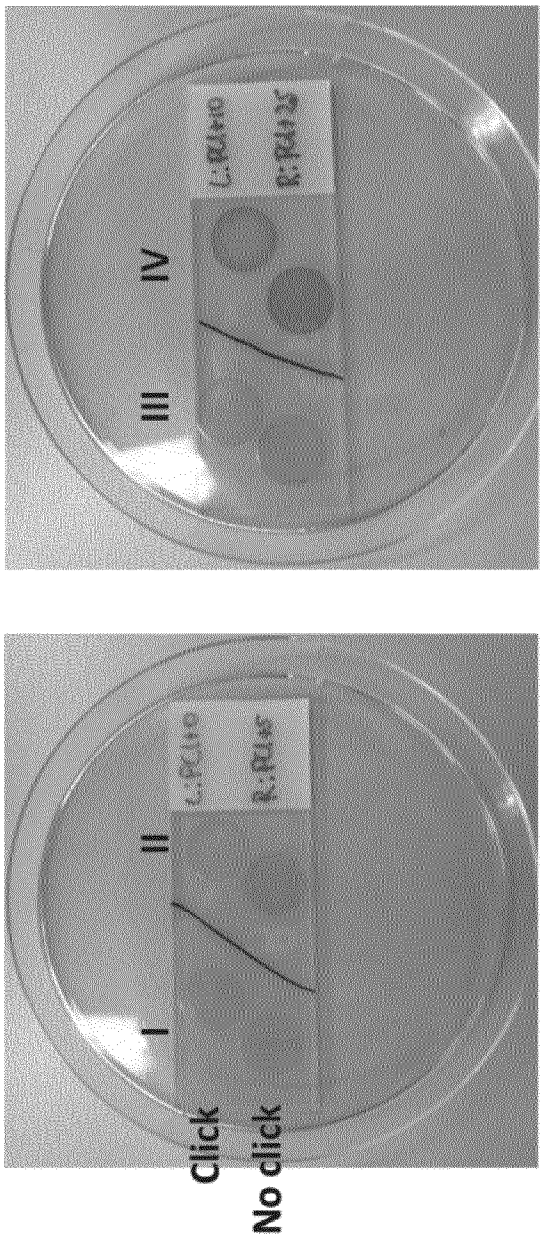

Fig. 8a

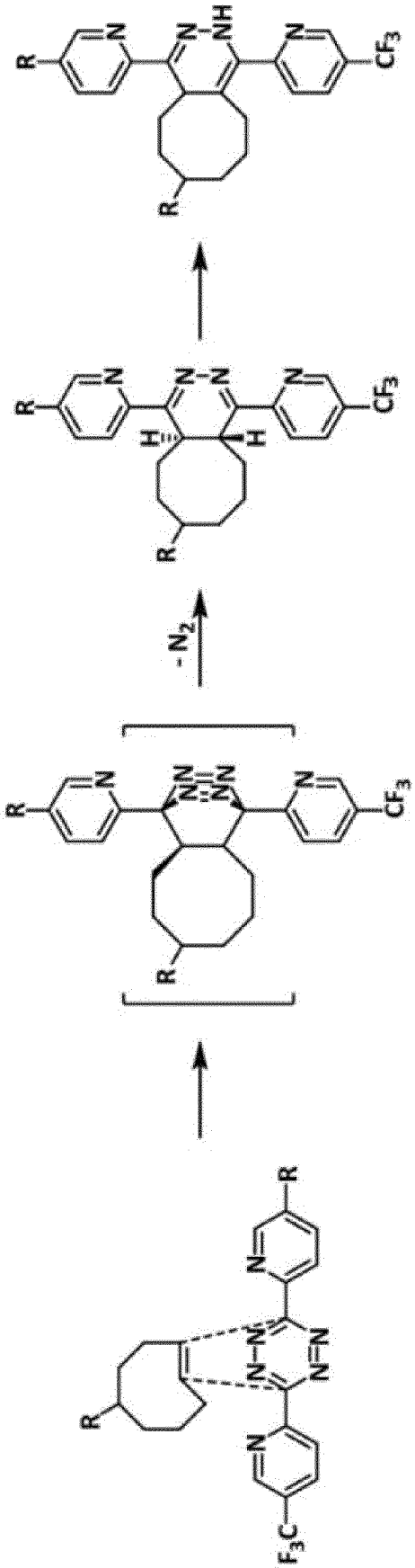

Fig. 8b

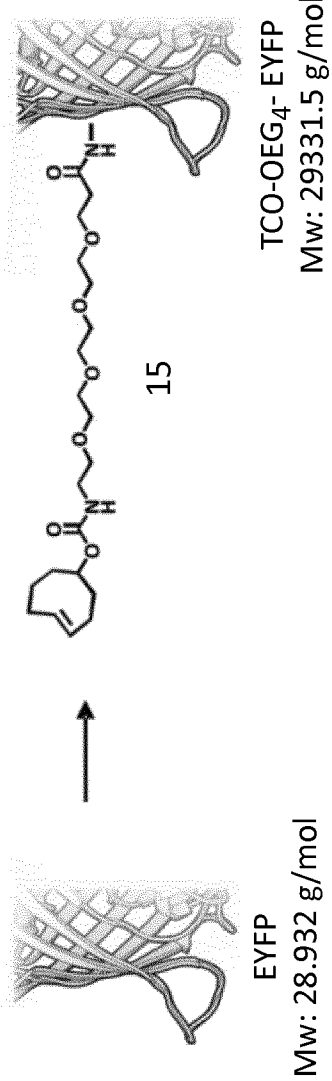
14
TCO-OEG4-NHS ester
Mw: 514.57 g/mol
+
EYFP
Mw: 28.932 g/mol
15
TCO-OEG4- EYFP
Mw: 29331.5 g/mol

Fig. 9a

TIC Chromatogram
Intensity (%)
Time (min)
m/z spectrum
Intensity (%)
m/z
Mass spectrum
Intensity (%)
Mass (Da)
29331.5
1x
29731
2x
30130
3x
30530
4x
30929.5
5x
28932
0x

Fig. 9b

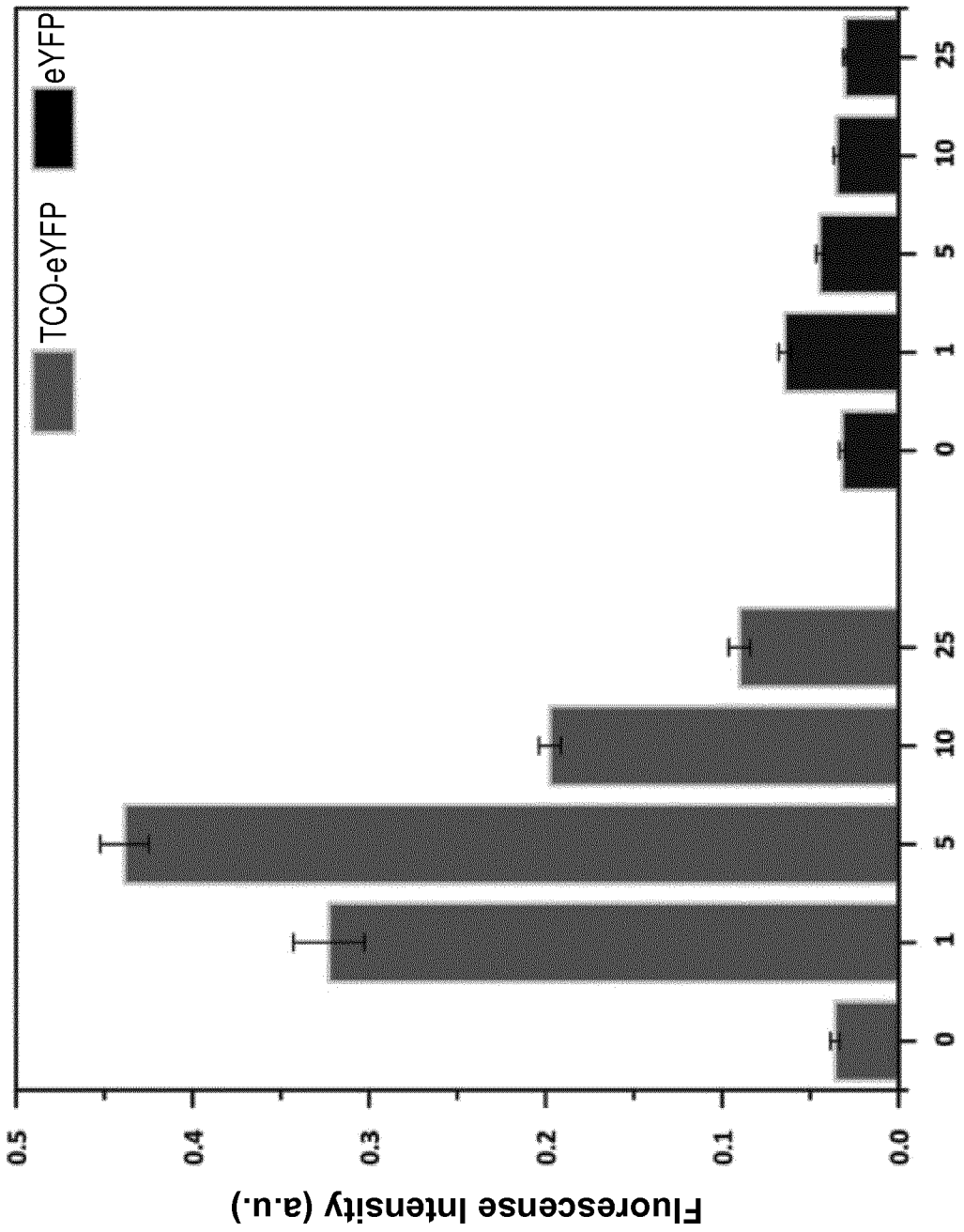
TCO-eYFP
eYFP
Fluorescense Intensity (a.u.)
0.0
0.1
0.2
0.3
0.4
0.5
0
1
5
10
25
0
1
5
10
25
Surface Composition

Fig. 10

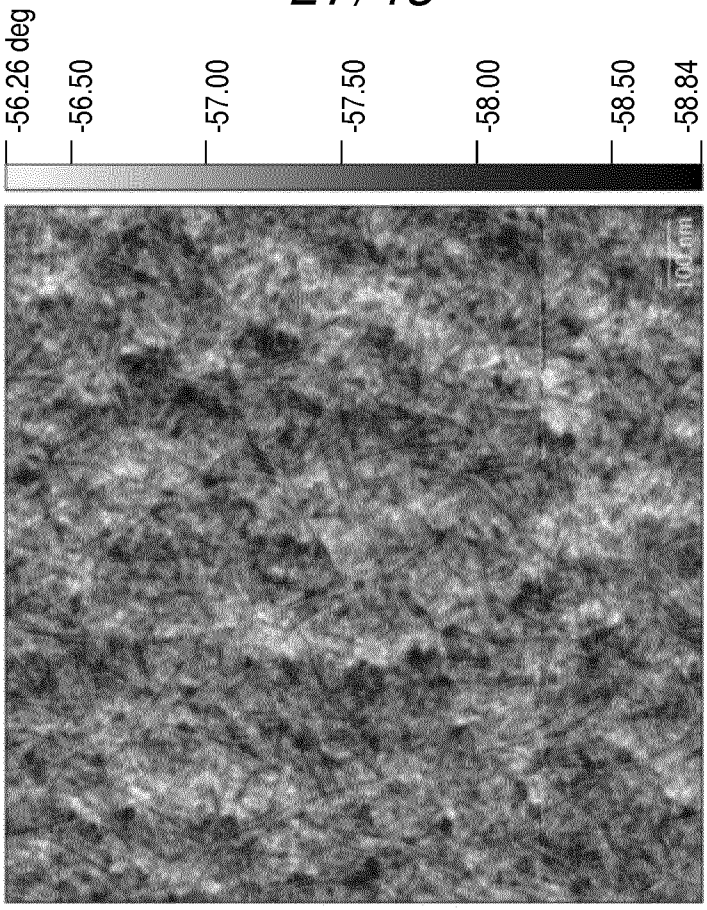

Fig. 11b

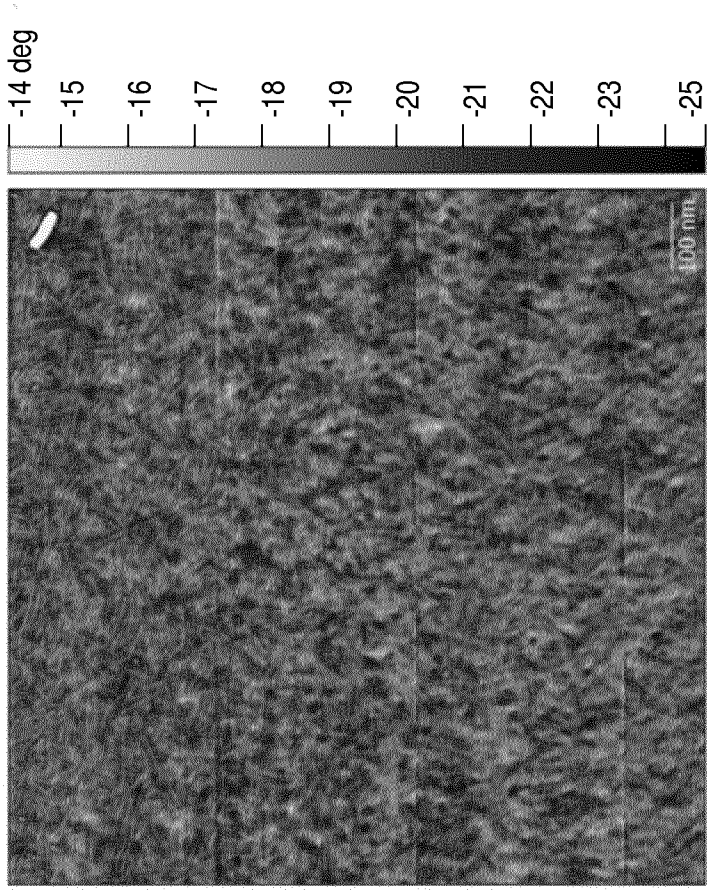

Fig. 11a

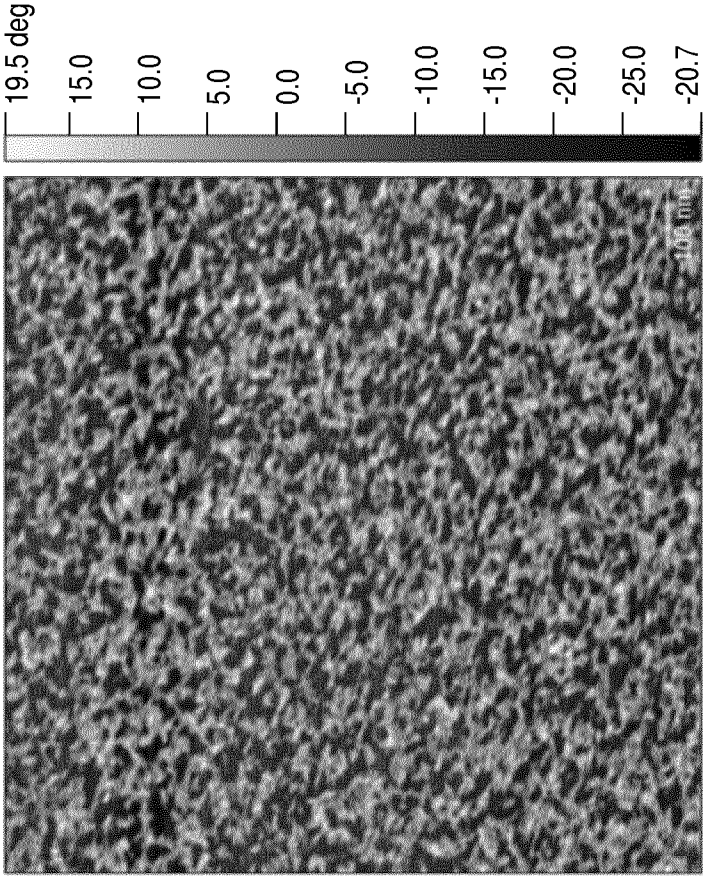

Fig. 11d

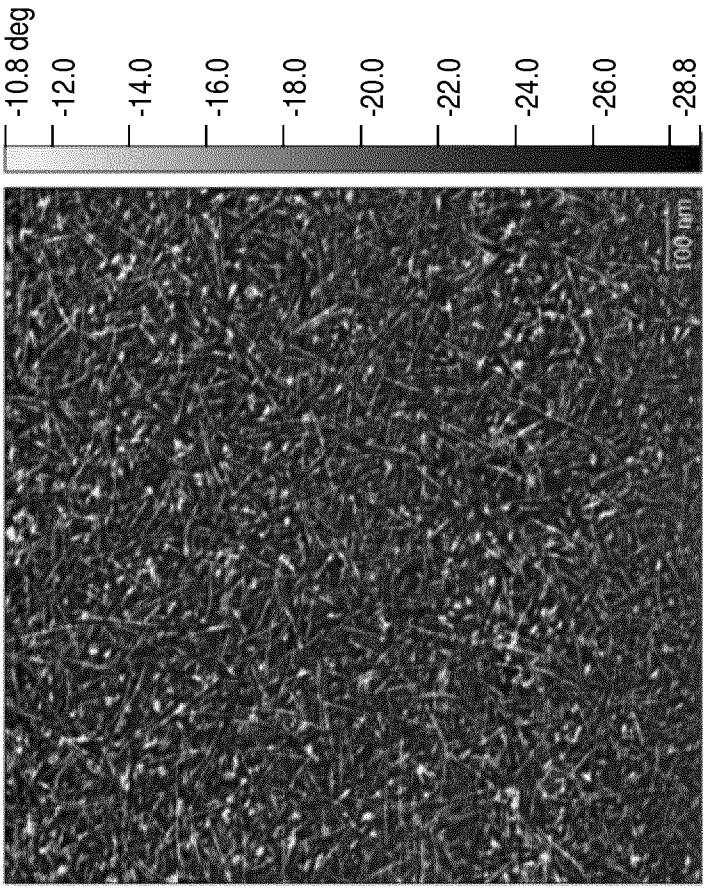

Fig. 11c

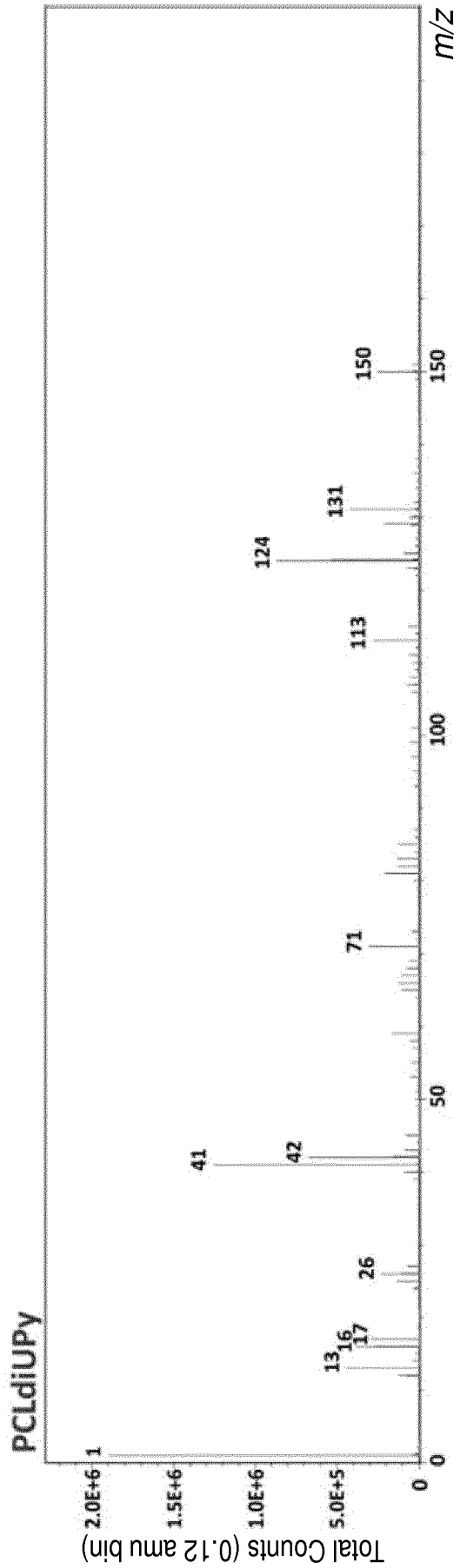

Fig. 12a

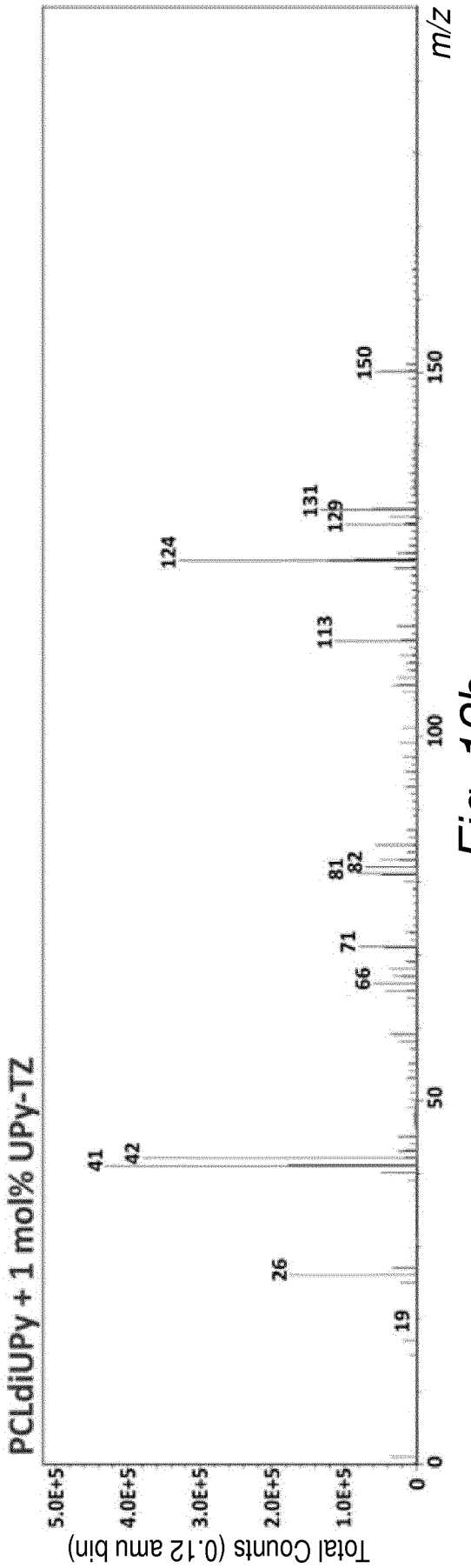

Fig. 12b

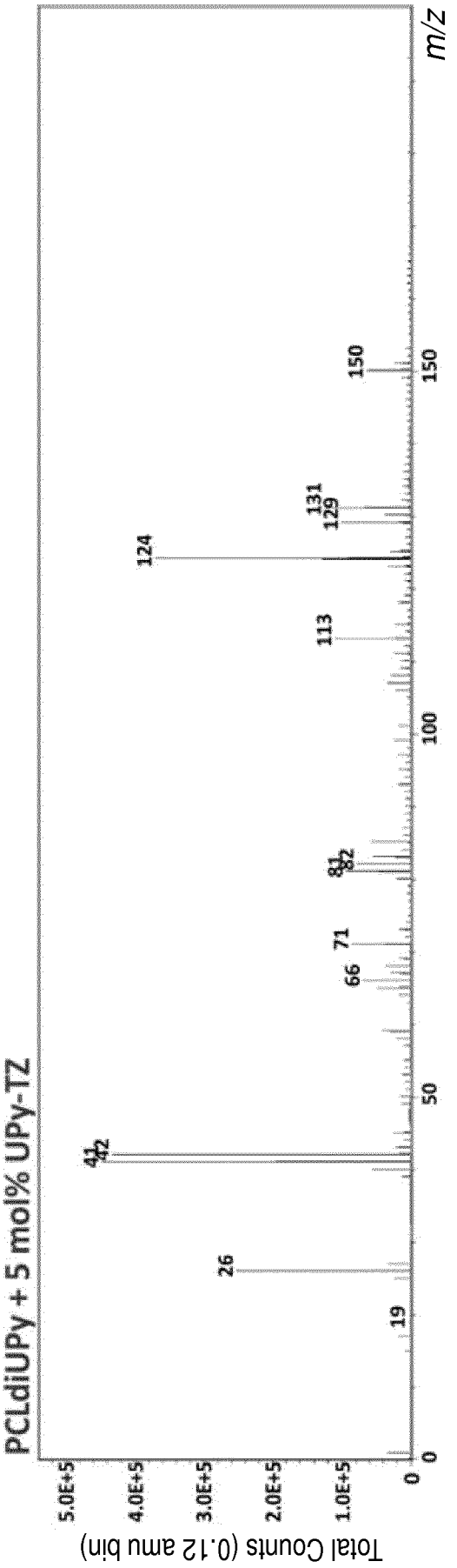

Fig. 12c

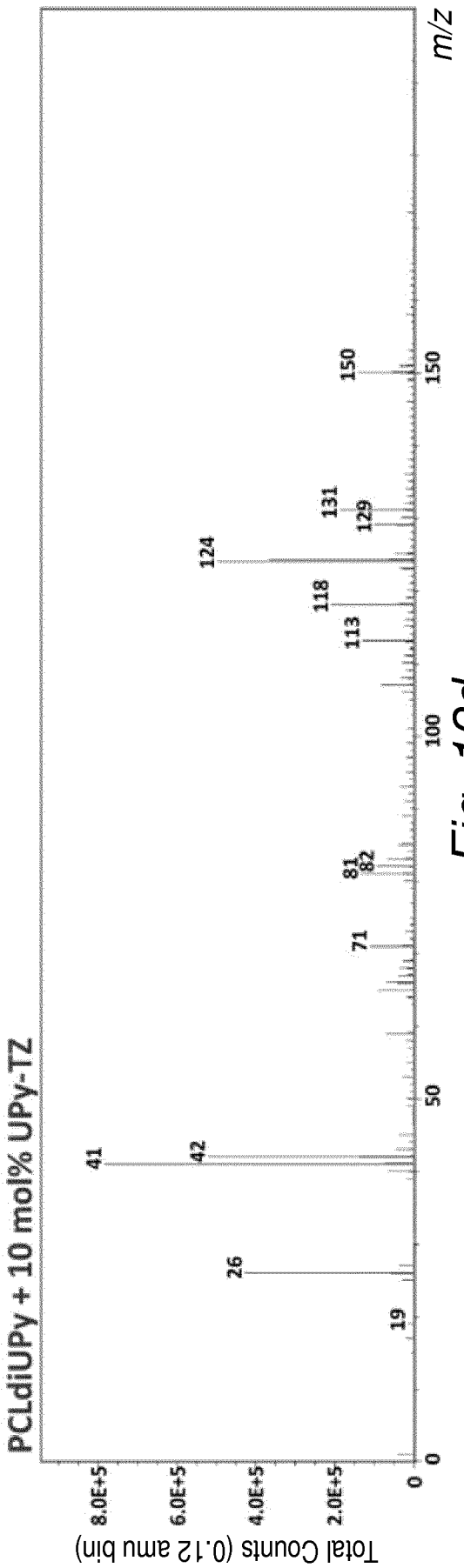

Fig. 12d

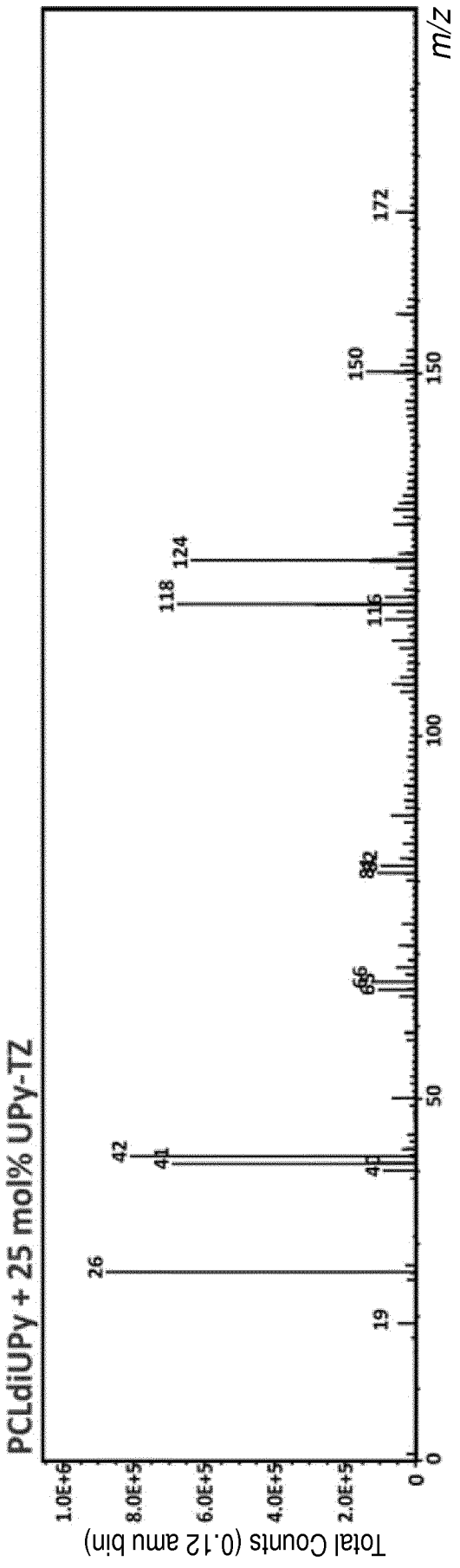
PCLdiUPy + 25 mol% UPy-TZ
Total Counts (0.12 amu bin)
1.0E+6
8.0E+5
6.0E+5
4.0E+5
2.0E+5
0
m/z
0
50
100
150
150
172
124
118
116
82
82
66
65
42
41
40
26
19

Fig. 12e

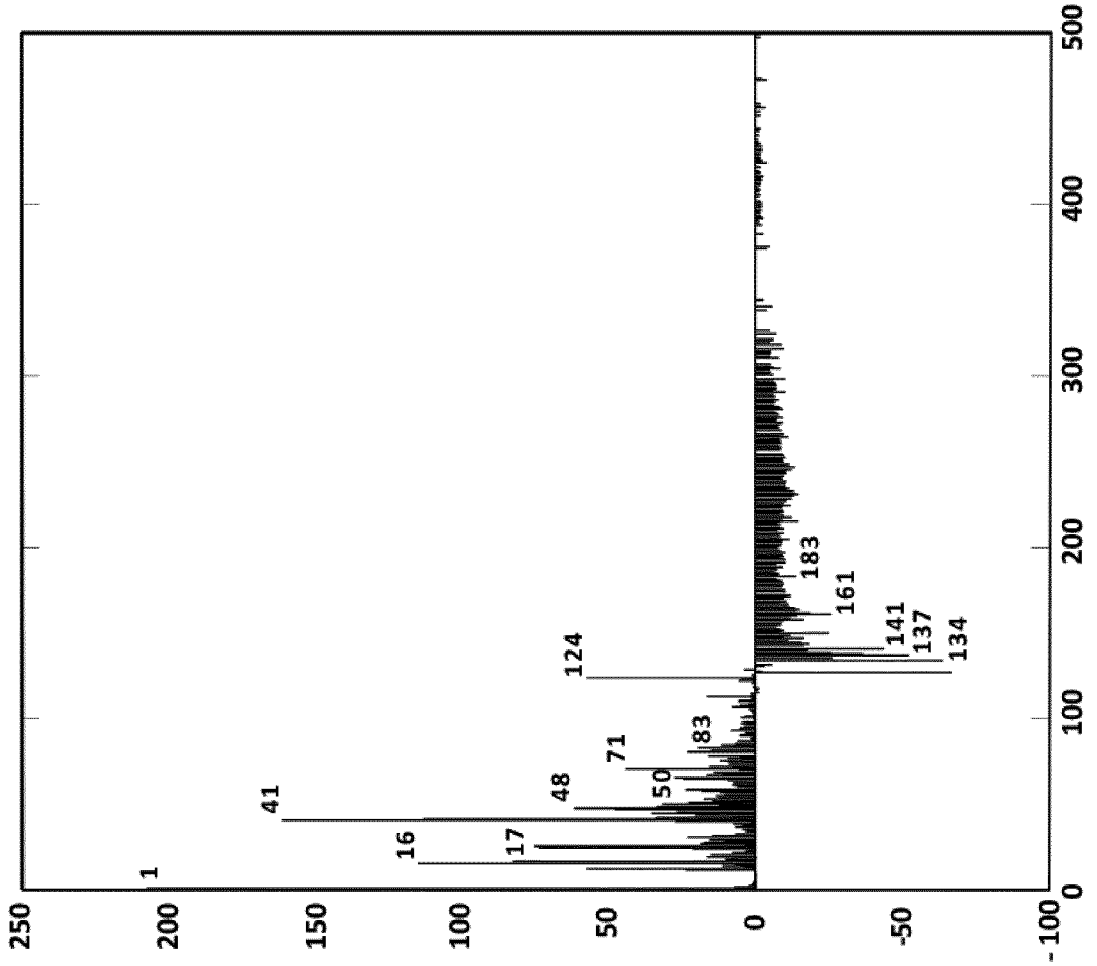

Fig. 13c

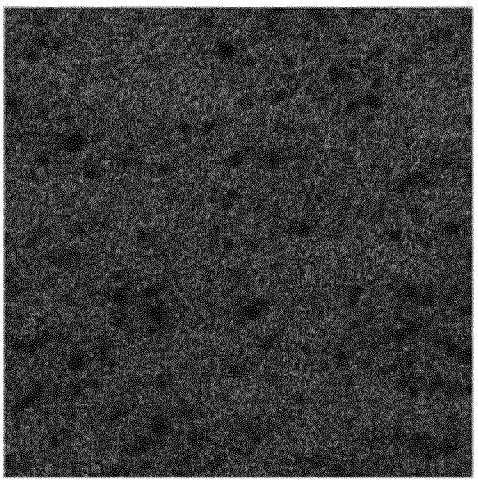

Fig. 13a

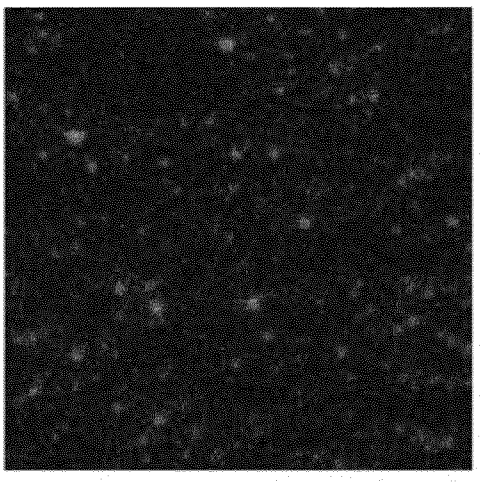

Fig. 13b

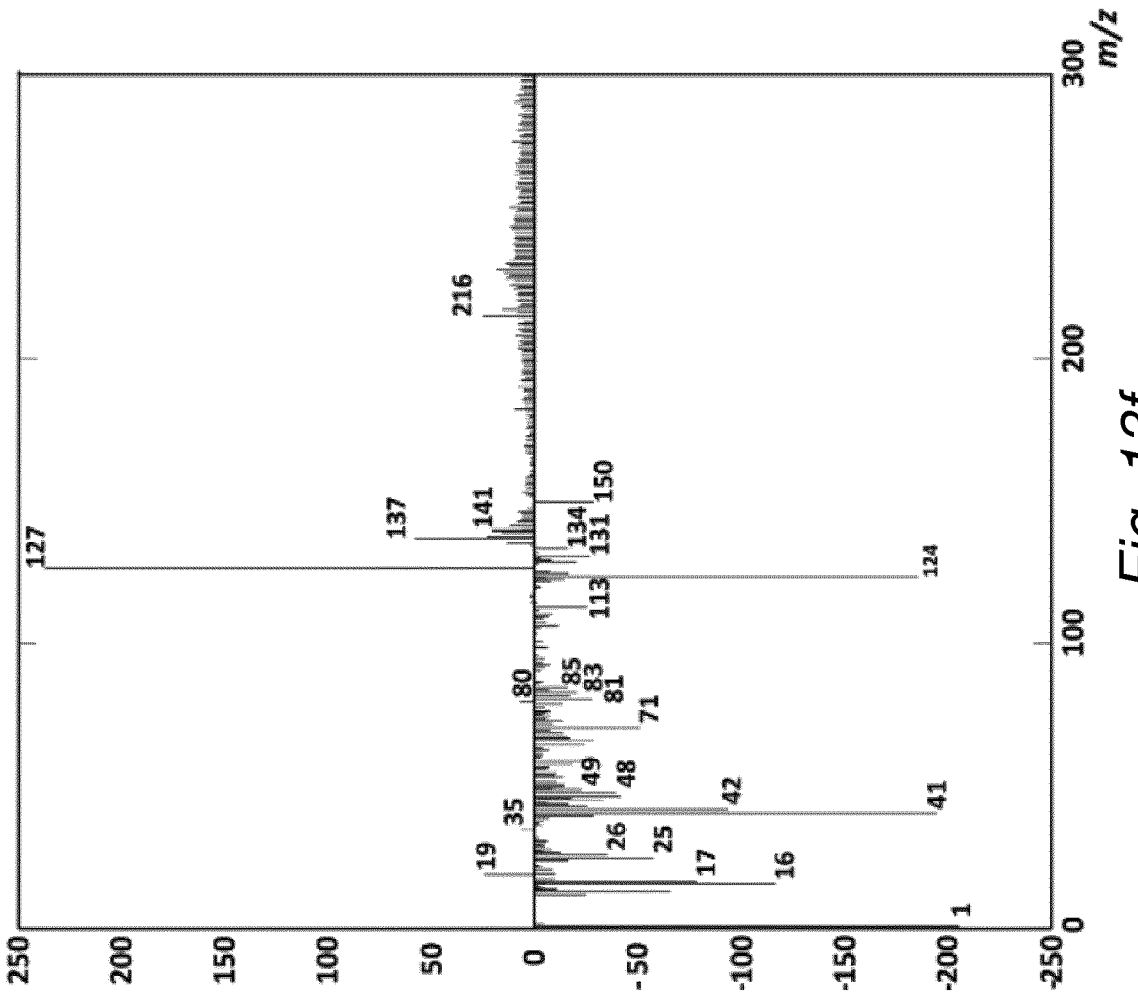

Fig. 13f

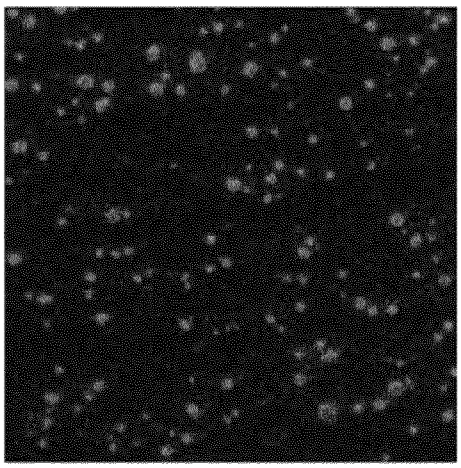

Fig. 13d

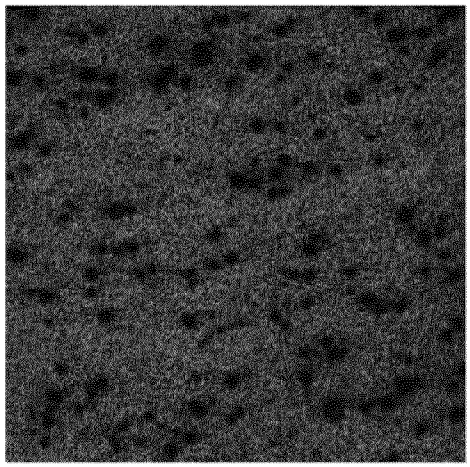

Fig. 13e

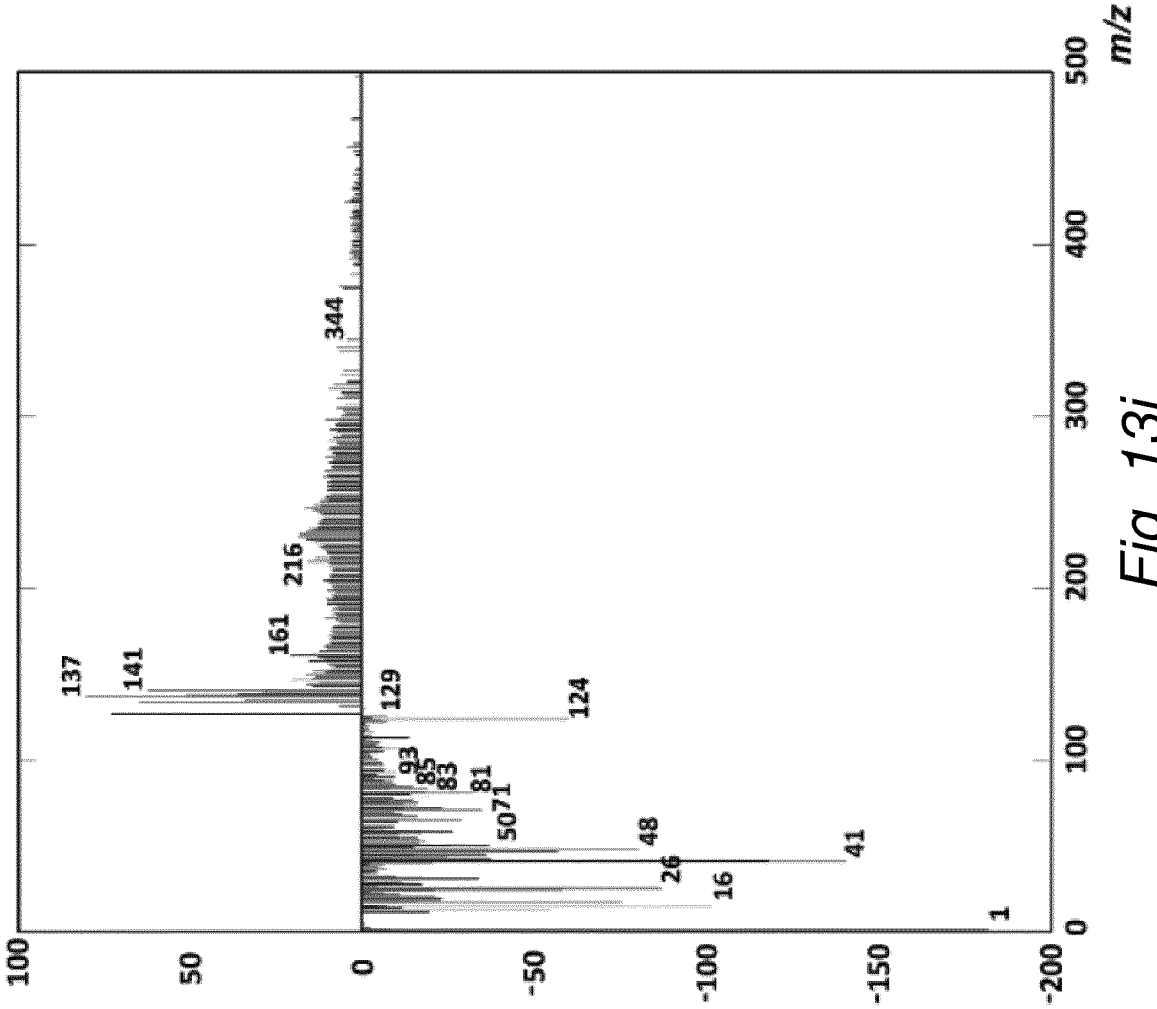

Fig. 13i

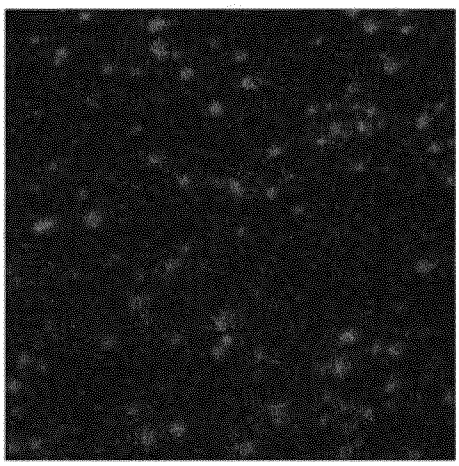

Fig. 13g

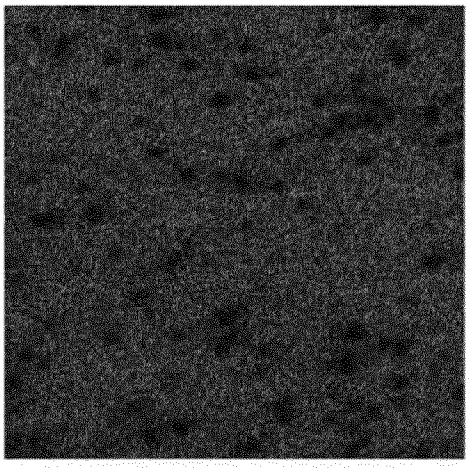

Fig. 13h

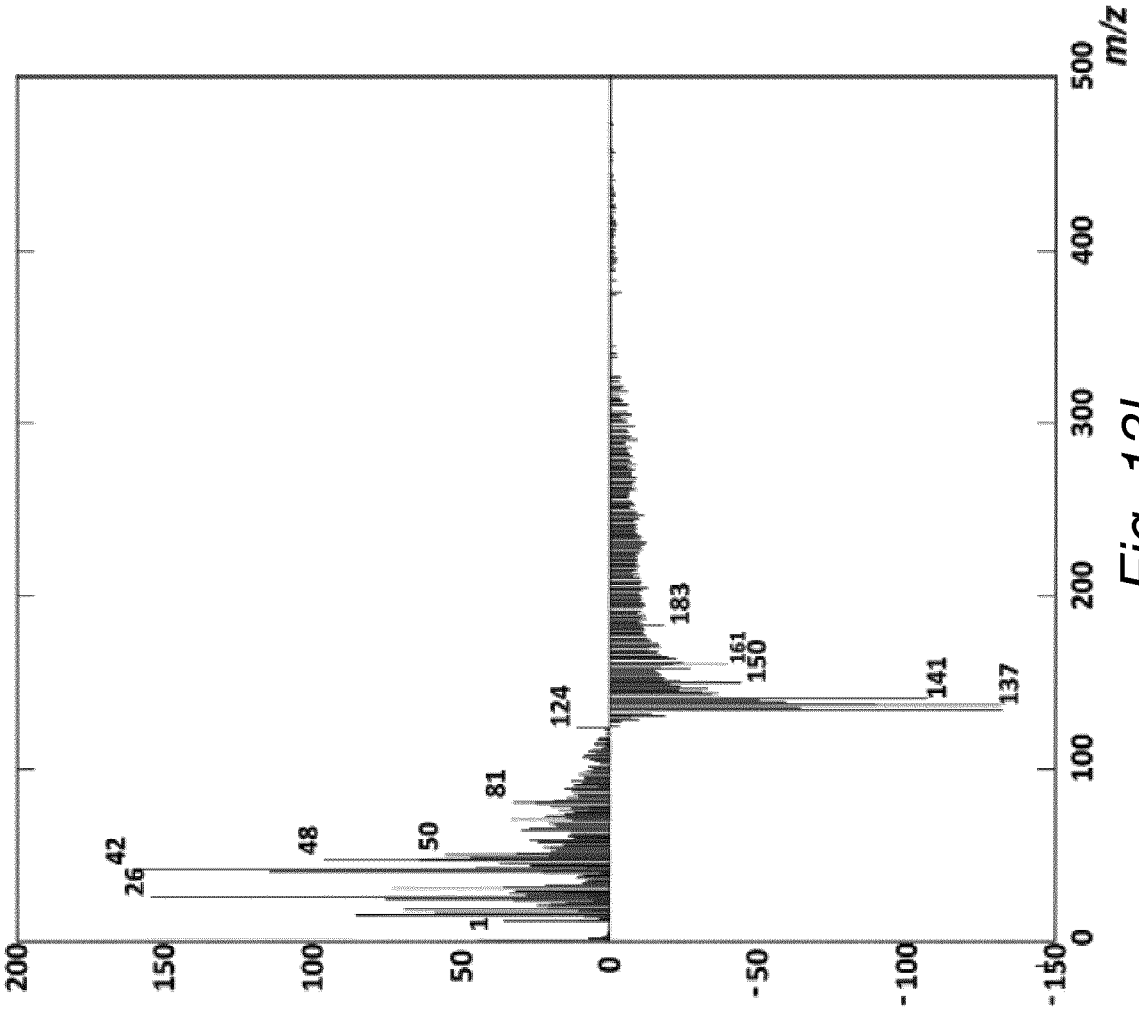

Fig. 13l

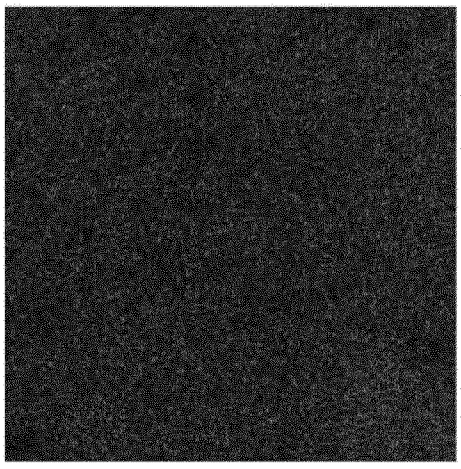

Fig. 13j

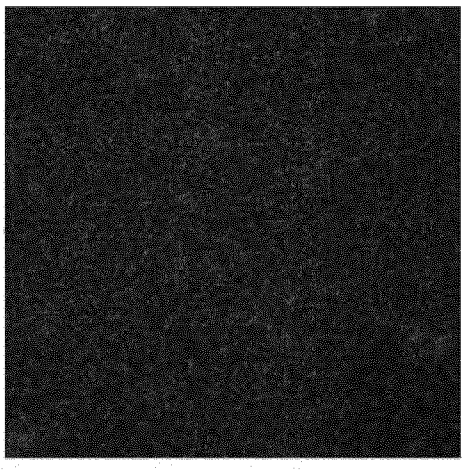

Fig. 13k

Fig. 14

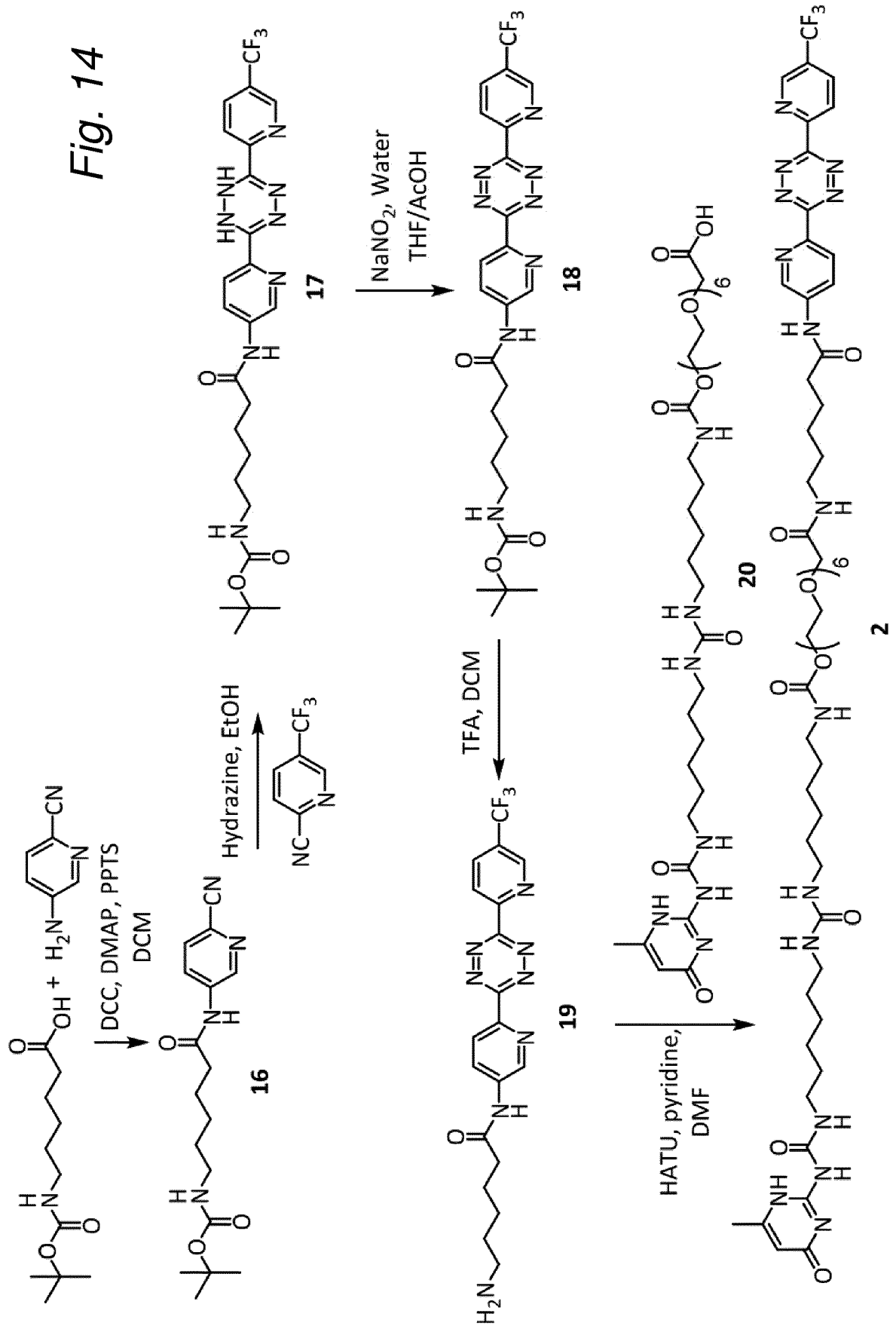
DCC, DMAP, PPTS
DCM
16
Hydrazine, EtOH
17
NaNO2, Water
THF/AcOH
18
TFA, DCM
19
HATU, pyridine,
DMF
20
2

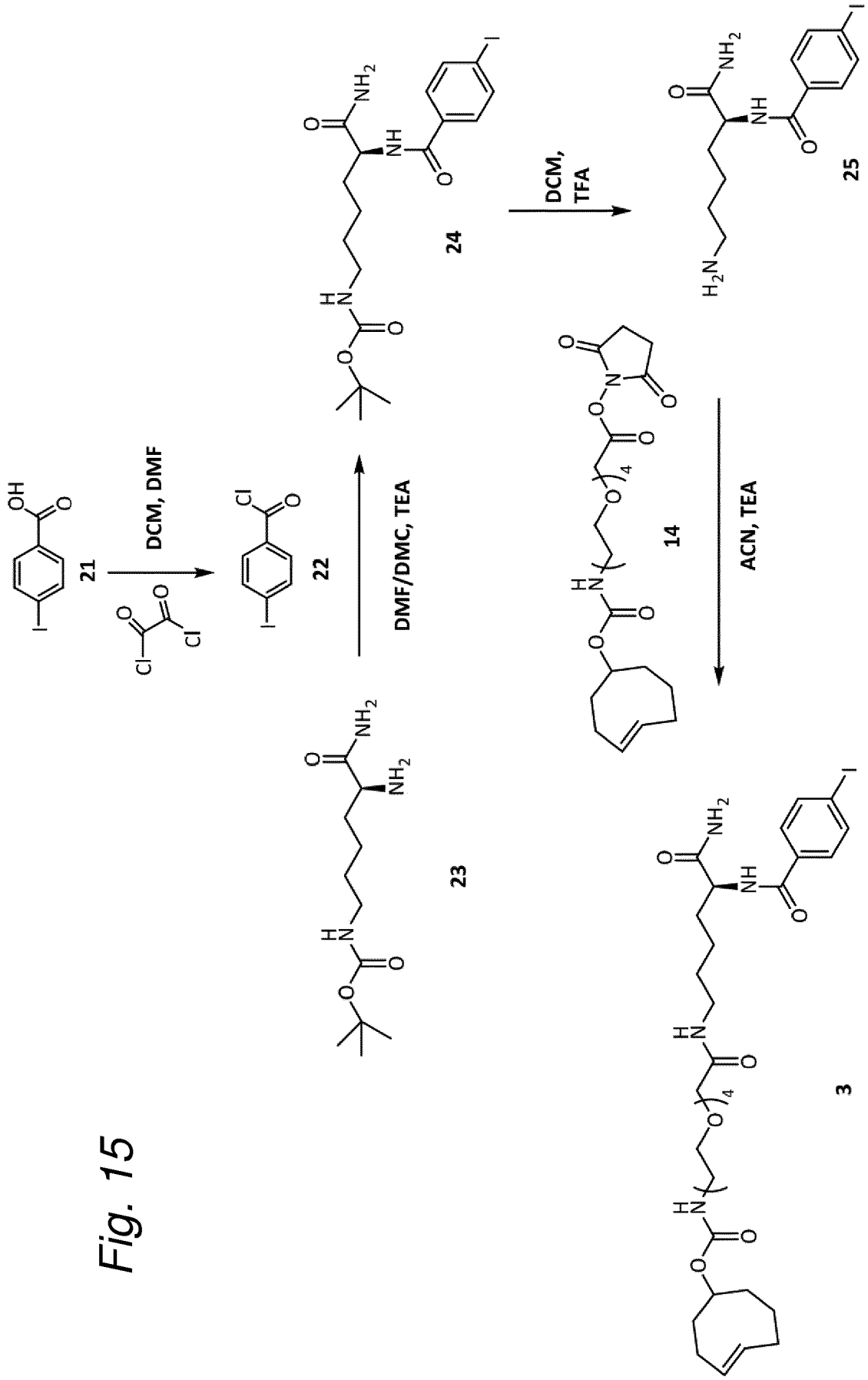

Fig. 15

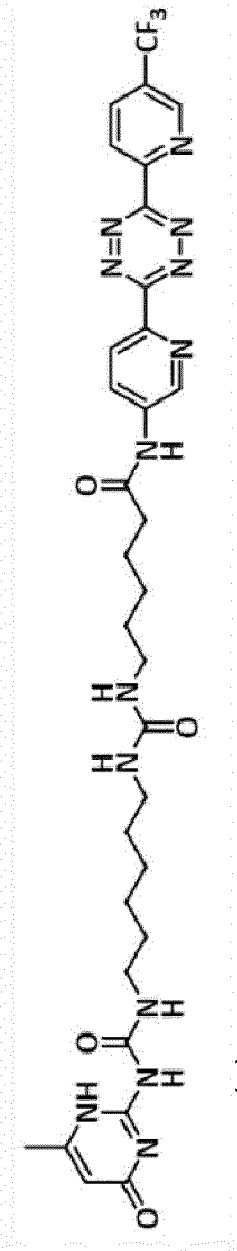

(a)

Fig. 16a

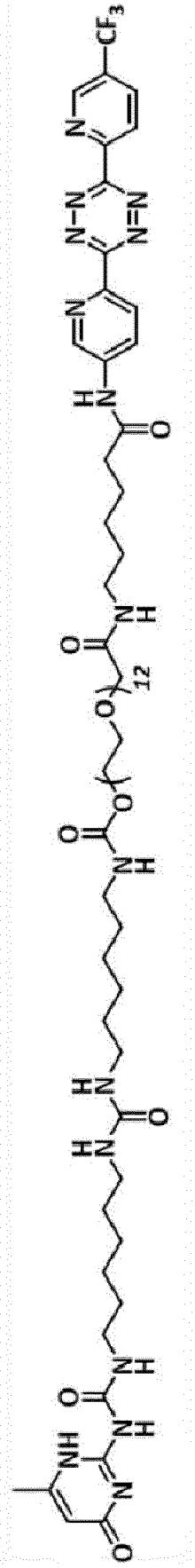

(b)

Fig. 16b

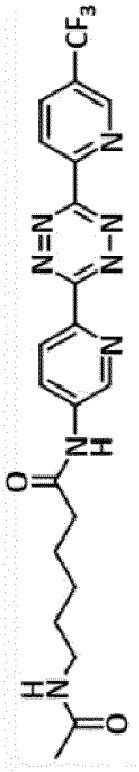

(c)

Fig. 16c

Mono-functional-PEG-BCN

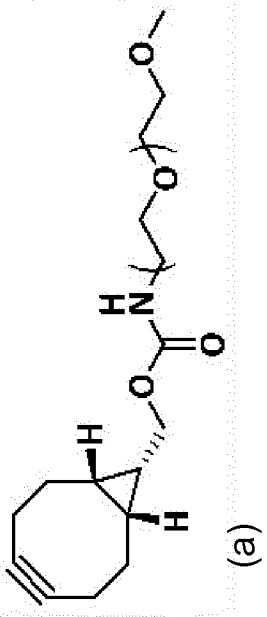

(a)

Fig. 17a

Bi-functional-PEG-BCN

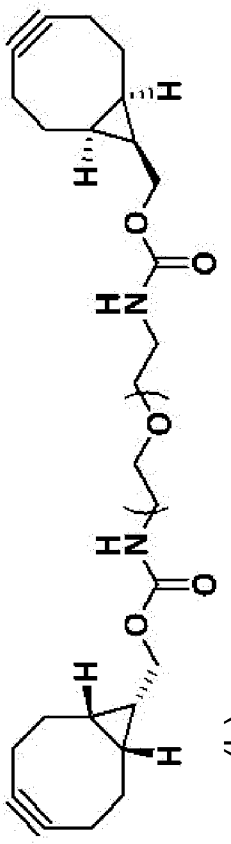

(b)

Fig. 17b

Star-PEG-BCN

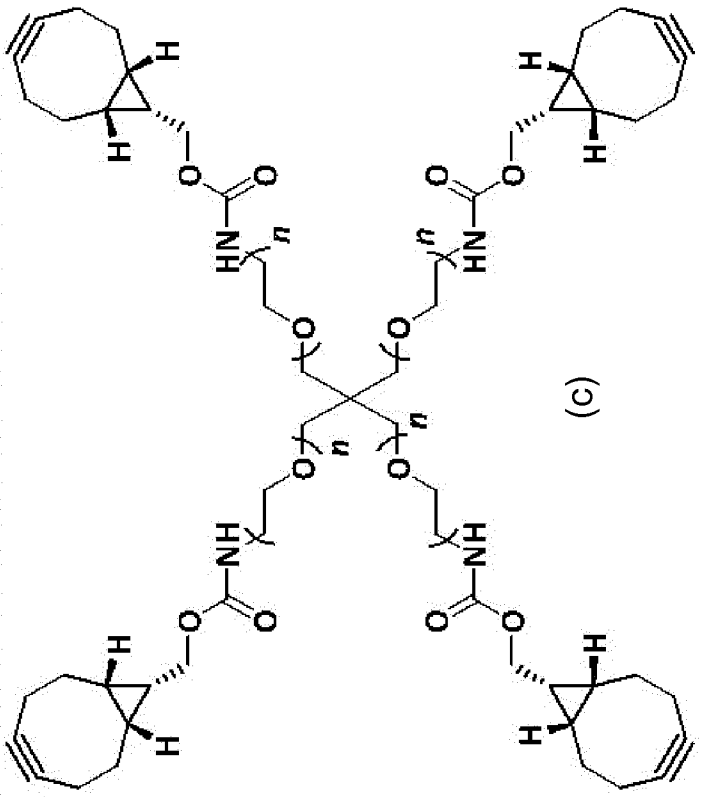

(c)

Fig. 17c

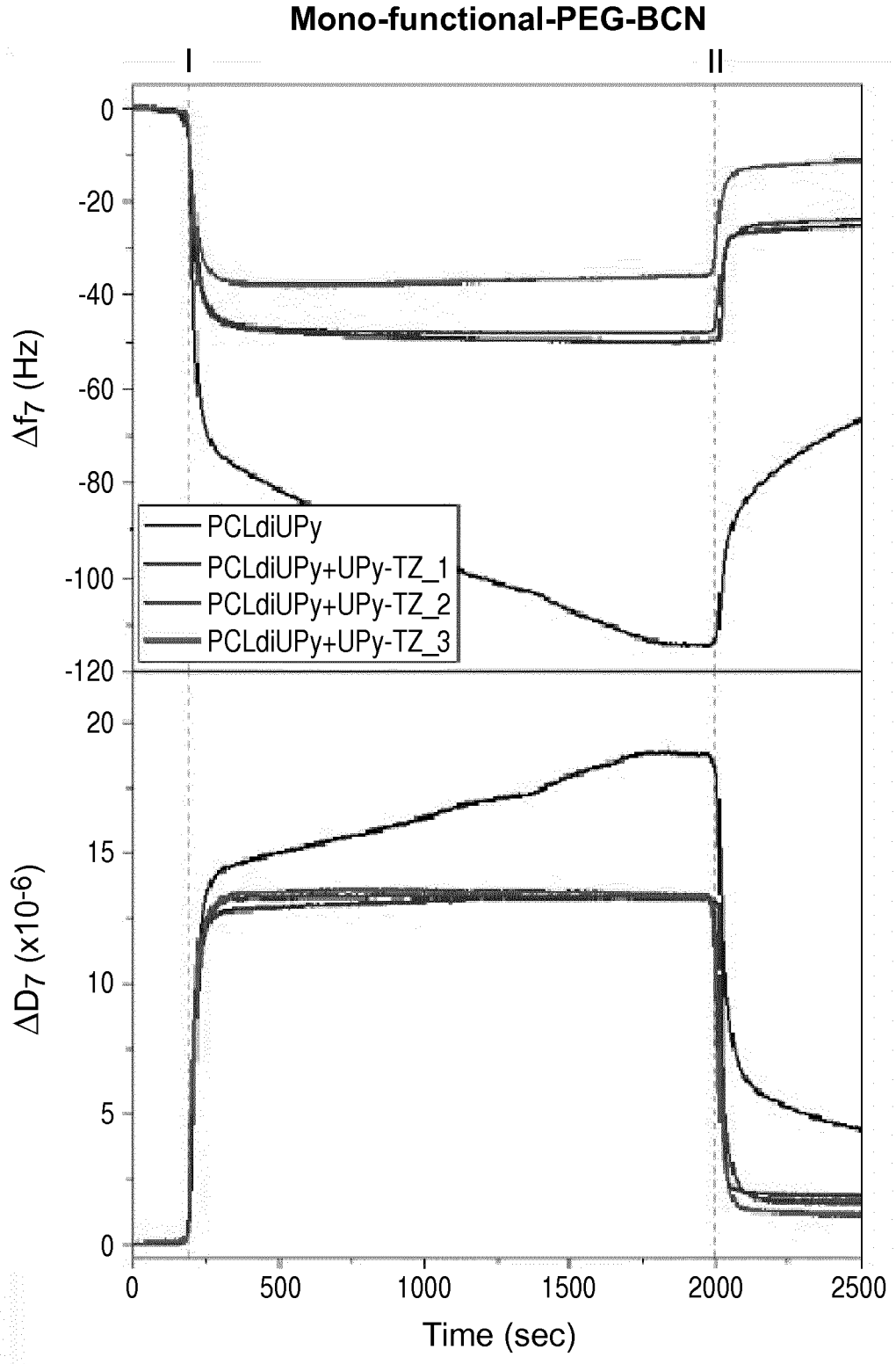
Mono-functional-PEG-BCN
I
II
0
-20
-40
-60
-80
-100
-120
Δf7 (Hz)
PCLdiUPy
PCLdiUPy+UPy-TZ_1
PCLdiUPy+UPy-TZ_2
PCLdiUPy+UPy-TZ_3
20
15
10
5
0
ΔD7 (x10-6)
0
500
1000
1500
2000
2500
Time (sec)

Fig. 18a

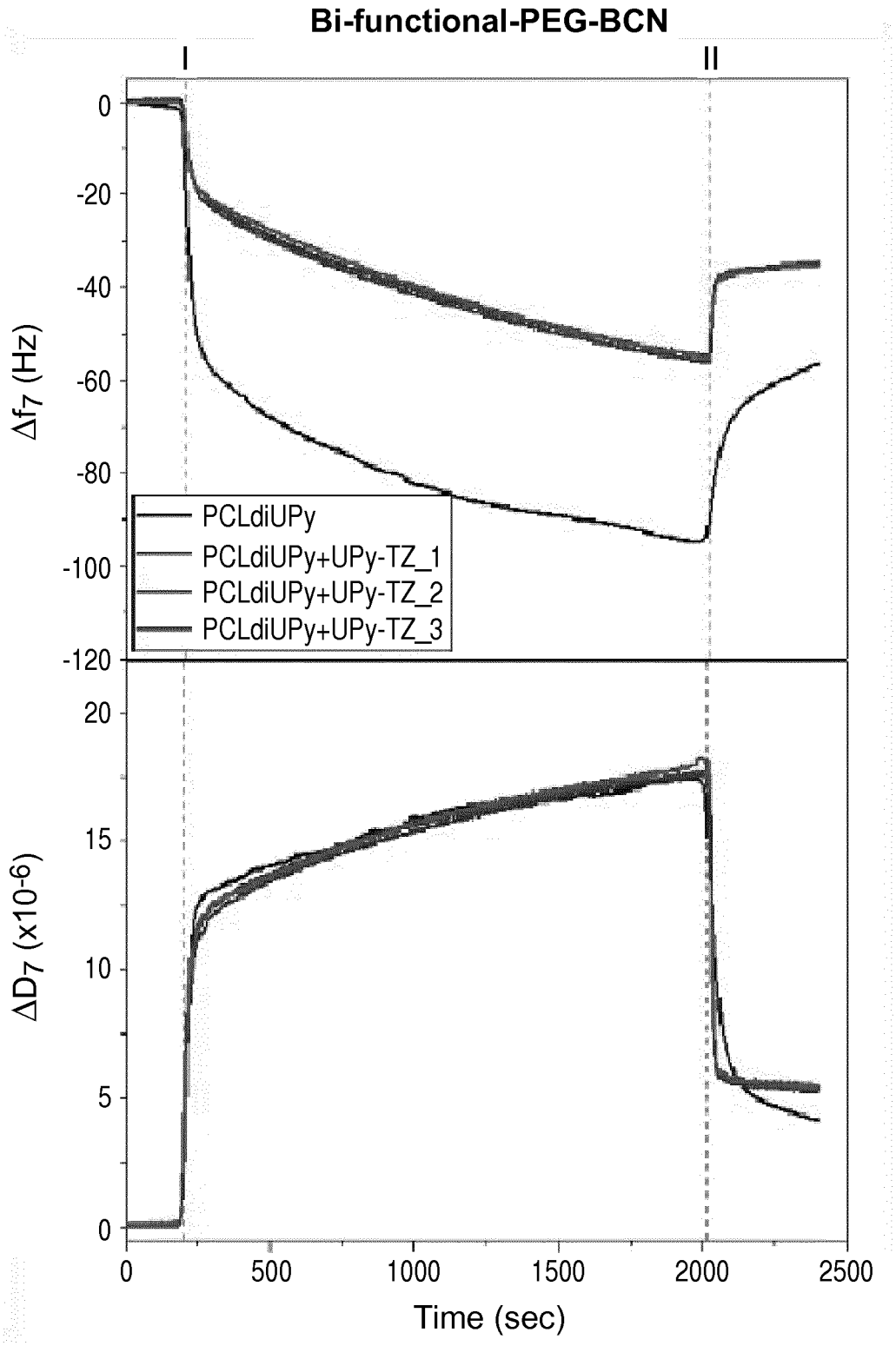
Bi-functional-PEG-BCN
I
II
0
-20
-40
-60
-80
-100
-120
Δf7 (Hz)
PCLdiUPy
PCLdiUPy+UPy-TZ_1
PCLdiUPy+UPy-TZ_2
PCLdiUPy+UPy-TZ_3
20
15
10
5
0
ΔD7 (x10-6)
0
500
1000
1500
2000
2500
Time (sec)

Fig. 18b

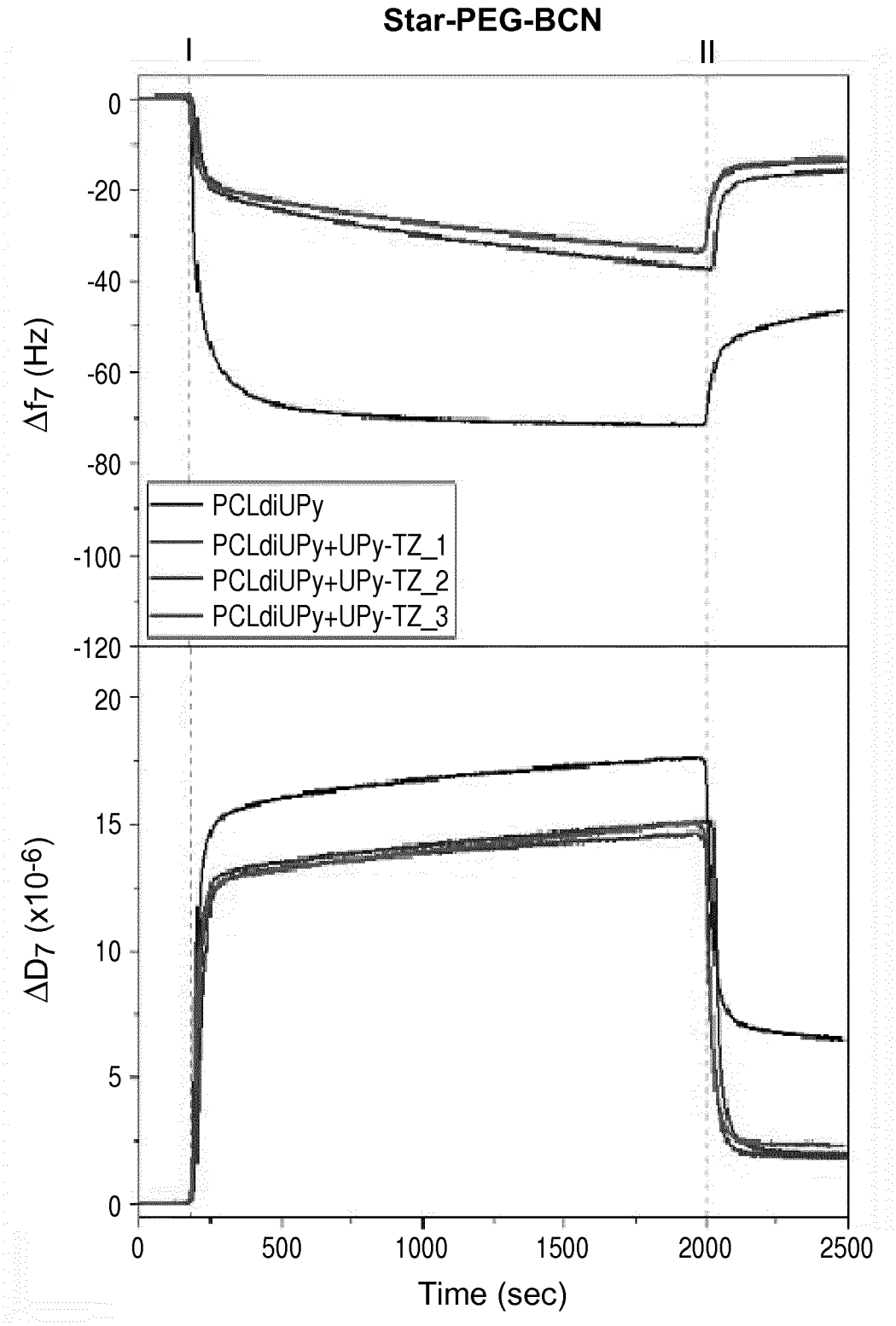
Star-PEG-BCN
I
II
0
-20
-40
-60
-80
-100
-120
Δf7 (Hz)
PCLdiUPy
PCLdiUPy+UPy-TZ_1
PCLdiUPy+UPy-TZ_2
PCLdiUPy+UPy-TZ_3
20
15
10
5
0
ΔD7 (x10-6)
0
500
1000
1500
2000
2500
Time (sec)

Fig. 18c

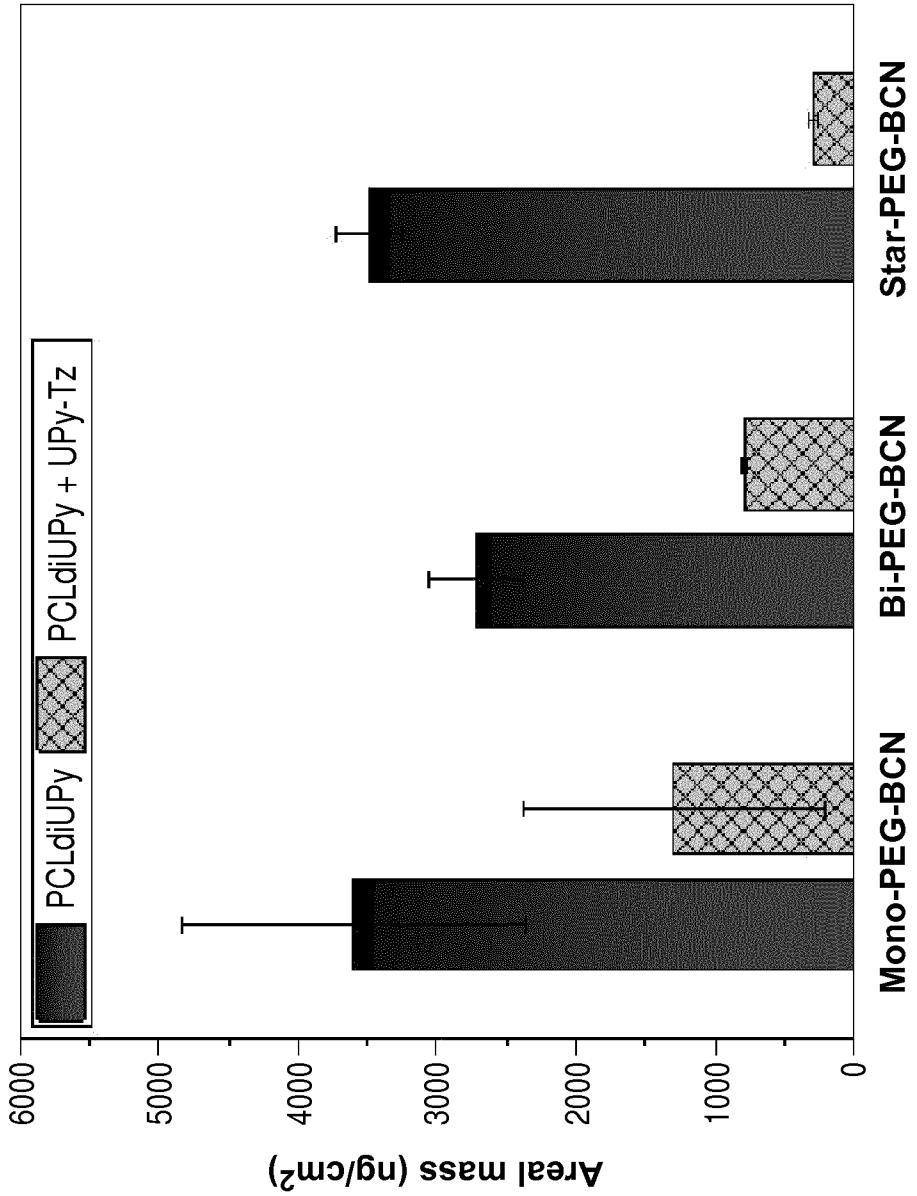
PCLdiUPy
PCLdiUPy + UPy-Tz
Areal mass (ng/cm²)
0
1000
2000
3000
4000
5000
6000
Mono-PEG-BCN
Bi-PEG-BCN
Star-PEG-BCN
Surface composition

Fig. 18d

INTERNATIONAL SEARCH REPORT

International application No
PCT/EP2017/061593

A. CLASSIFICATION OF SUBJECT MATTER
INV. A61K47/60 A61K47/59
ADD.

According to International Patent Classification (IPC) or to both national classification and IPC

B. FIELDS SEARCHED

Minimum documentation searched (classification system followed by classification symbols)
A61K

Documentation searched other than minimum documentation to the extent that such documents are included in the fields searched

Electronic data base consulted during the international search (name of data base and, where practicable, search terms used)
EPO-Internal, WPI Data, EMBASE, BIOSIS

C. DOCUMENTS CONSIDERED TO BE RELEVANT

Category*	Citation of document, with indication, where appropriate, of the relevant passages	Relevant to claim No.
X	ROXANNE E. KIELTYKA ET AL: "Modular synthesis of supramolecular ureidopyrimidinone-peptide conjugates using an oxime ligation strategy", CHEMICAL COMMUNICATIONS, vol. 48, no. 10, 1 January 2012 (2012-01-01), pages 1452-1454, XP055175144, ISSN: 1359-7345, DOI: 10.1039/C1CC14728E	1,2, 6-30, 33-47, 59-62
Y	page 1453; figures 1, 2	1-62

-/--

[X] Further documents are listed in the continuation of Box C.

[X] See patent family annex.

* Special categories of cited documents :

"A" document defining the general state of the art which is not considered to be of particular relevance

"E" earlier application or patent but published on or after the international filing date

"L" document which may throw doubts on priority claim(s) or which is cited to establish the publication date of another citation or other special reason (as specified)

"O" document referring to an oral disclosure, use, exhibition or other means

"P" document published prior to the international filing date but later than the priority date claimed

"T" later document published after the international filing date or priority date and not in conflict with the application but cited to understand the principle or theory underlying the invention

"X" document of particular relevance; the claimed invention cannot be considered novel or cannot be considered to involve an inventive step when the document is taken alone

"Y" document of particular relevance; the claimed invention cannot be considered to involve an inventive step when the document is combined with one or more other such documents, such combination being obvious to a person skilled in the art

"&" document member of the same patent family

Date of the actual completion of the international search	Date of mailing of the international search report
24 August 2017	31/08/2017

Name and mailing address of the ISA/	Authorized officer
European Patent Office, P.B. 5818 Patentlaan 2 NL - 2280 HV Rijswijk Tel. (+31-70) 340-2040, Fax: (+31-70) 340-3016	Langer, Miren

6

Form PCT/ISA/210 (second sheet) (April 2005)

C(Continuation). DOCUMENTS CONSIDERED TO BE RELEVANT

Category*	Citation of document, with indication, where appropriate, of the relevant passages	Relevant to claim No.
X	MUYLAERT DIMITRI E P ET AL: "Early in-situ cellularization of a supramolecular vascular graft is modified by synthetic stromal cell-derived factor-1[alpha] derived peptides", BIOMATERIALS, vol. 76, 23 October 2015 (2015-10-23), pages 187-195, XP029317310, ISSN: 0142-9612, DOI: 10.1016/J.BIOMATERIALS.2015.10.052 page 189; figure 1	1,7-15, 17-30, 45,46, 59-62
X	BJÖRNE B. MOLLET ET AL: "A modular approach to easily processable supramolecular bilayered scaffolds with tailorable properties", JOURNAL OF MATERIALS CHEMISTRY B, vol. 2, no. 17, 1 January 2014 (2014-01-01), pages 2483-2493, XP055175156, ISSN: 2050-750X, DOI: 10.1039/C3TB21516D page 2485; figure 1	1,7-30, 33-47, 59-62
Y	CRAIG S. MCKAY ET AL: "Click Chemistry in Complex Mixtures: Bioorthogonal Bioconjugation", CHEMISTRY AND BIOLOGY., vol. 21, no. 9, 1 September 2014 (2014-09-01), pages 1075-1101, XP055398778, GB ISSN: 1074-5521, DOI: 10.1016/j.chembiol.2014.09.002 the whole document page 1090, column 2, paragraph 1	1-62
Y	WO 2012/168392 A1 (UNIV EINDHOVEN TECH [NL]; GUO MINGYU [NL]; WYSS HANS MARKUS [NL]; DANK) 13 December 2012 (2012-12-13) claim 1	1-62
A	PATRICIA Y. W. DANKERS ET AL: "Convenient Solid-Phase Synthesis of Ureido-Pyrimidinone Modified Peptides", EUROPEAN JOURNAL OF ORGANIC CHEMISTRY, vol. 2007, no. 22, 1 August 2007 (2007-08-01), pages 3622-3632, XP055398729, DE ISSN: 1434-193X, DOI: 10.1002/ejoc.200700191	1-62

-/--

6

INTERNATIONAL SEARCH REPORT

International application No
PCT/EP2017/061593

C(Continuation). DOCUMENTS CONSIDERED TO BE RELEVANT

Category*	Citation of document, with indication, where appropriate, of the relevant passages	Relevant to claim No.
A	ROXANNE E. KIELTYKA ET AL: "Mesoscale Modulation of Supramolecular Ureidopyrimidinone-Based Poly(ethylene glycol) Transient Networks in Water", JOURNAL OF THE AMERICAN CHEMICAL SOCIETY, vol. 135, no. 30, 31 July 2013 (2013-07-31), pages 11159-11164, XP055161854, ISSN: 0002-7863, DOI: 10.1021/ja403745w ----	1-62
A	ISJA DE FEIJTER ET AL: "Solid-Phase-Based Synthesis of Ureidopyrimidinone-Peptide Conjugates- for Supramolecular Biomaterials", SYNLETT, vol. 26, no. 19, 17 November 2015 (2015-11-17), pages 2707-2713, XP055398681, DE ISSN: 0936-5214, DOI: 10.1055/s-0035-1560520 ----	1-62
A	OLIVER ROLING ET AL: "Surface patterning with natural and synthetic polymers via an inverse electron demand Diels-Alder reaction employing microcontact chemistry", ORGANIC & BIOMOLECULAR CHEMISTRY, vol. 12, no. 39, 1 January 2014 (2014-01-01), pages 7828-7835, XP055398727, GB ISSN: 1477-0520, DOI: 10.1039/C4OB01379D the whole document ----	1-62
X,P	OLGA J. G. M. GOOR ET AL: "Efficient Functionalization of Additives at Supramolecular Material Surfaces", ADVANCED MATERIALS, vol. 29, no. 5, 1 February 2017 (2017-02-01), page 1604652, XP055398684, DE ISSN: 0935-9648, DOI: 10.1002/adma.201604652 page 1604652; figure 1 ----	1-62

6

INTERNATIONAL SEARCH REPORT

Information on patent family members

International application No
PCT/EP2017/061593

Patent document cited in search report	Publication date	Patent family member(s)	Publication date
WO 2012168392 A1	13-12-2012	NONE	